AD_____

AWARD NUMBER: DAMD17-03-1-0671

TITLE: The Role of Protein Elongation Factor eEF1A2 in Breast Cancer

PRINCIPAL INVESTIGATOR: Jonathan M. Lee, Ph.D.

CONTRACTING ORGANIZATION: Hamilton Regional Cancer Centre
                           Hamilton Ontario Canada L8V 5C2

REPORT DATE: September 2006

TYPE OF REPORT: Final

PREPARED FOR: U.S. Army Medical Research and Materiel Command
               Fort Detrick, Maryland 21702-5012

DISTRIBUTION STATEMENT: Approved for Public Release;
                        Distribution Unlimited

The views, opinions and/or findings contained in this report are those of the author(s) and should not be construed as an official Department of the Army position, policy or decision unless so designated by other documentation.

REPORT DOCUMENTATION PAGE

Form Approved
OMB No. 0704-0188

Public reporting burden for this collection of information is estimated to average 1 hour per response, including the time for reviewing instructions, searching existing data sources, gathering and maintaining the data needed, and completing and reviewing this collection of information. Send comments regarding this burden estimate or any other aspect of this collection of information, including suggestions for reducing this burden to Department of Defense, Washington Headquarters Services, Directorate for Information Operations and Reports (0704-0188), 1215 Jefferson Davis Highway, Suite 1204, Arlington, VA 22202-4302. Respondents should be aware that notwithstanding any other provision of law, no person shall be subject to any penalty for failing to comply with a collection of information if it does not display a currently valid OMB control number. **PLEASE DO NOT RETURN YOUR FORM TO THE ABOVE ADDRESS.**

1. REPORT DATE *(DD-MM-YYYY)*	2. REPORT TYPE	3. DATES COVERED *(From - To)*
01-09-2006	Final	15 Aug 2003 – 14 Aug 2006

4. TITLE AND SUBTITLE	5a. CONTRACT NUMBER
The Role of Protein Elongation Factor eEF1A2 in Breast Cancer	**5b. GRANT NUMBER** DAMD17-03-1-0671
	5c. PROGRAM ELEMENT NUMBER

6. AUTHOR(S)	5d. PROJECT NUMBER
Jonathan M. Lee, Ph.D.	**5e. TASK NUMBER**
E-Mail: jlee@uottawa.ca	**5f. WORK UNIT NUMBER**

7. PERFORMING ORGANIZATION NAME(S) AND ADDRESS(ES)	8. PERFORMING ORGANIZATION REPORT NUMBER
Hamilton Regional Cancer Centre Hamilton Ontario Canada L8V 5C2	

9. SPONSORING / MONITORING AGENCY NAME(S) AND ADDRESS(ES)	10. SPONSOR/MONITOR'S ACRONYM(S)
U.S. Army Medical Research and Materiel Command Fort Detrick, Maryland 21702-5012	
	11. SPONSOR/MONITOR'S REPORT NUMBER(S)

12. DISTRIBUTION / AVAILABILITY STATEMENT
Approved for Public Release; Distribution Unlimited

13. SUPPLEMENTARY NOTES

14. ABSTRACT

The overall goal of the project is to explore the role of protein elongation factor eEF1A2 in breast tumour development and to determine whether eEF1A2 is a useful breast cancer prognostic factor. eEF1A2 is one of two members of the eEF1A family of proteins (eEF1A1 and eEF1A2) that bind amino-acylated tRNA and facilitate their recruitment to the ribosome during protein translation elongation. We have identified eEF1A2 as a novel breast cancer oncogene. Supporting this idea are our observations that: a) eEF1A2 expression is increased in approximately 50% of human breast tumours; b) eEF1A2 protein expression is a prognostic marker for breast cancer survival; c) eEF1A2 enhances the growth rate of malignant breast cells; d) eEF1A2 inhibits anoikis; e) eEF1A1 activates the Akt/PKB serine/threonine kinase; e) siRNA that inactivate eEF1A2 and inhibit the in vitro growth of breast cell lines; and f) eEF1A2 expression causes rearrangement of the actin cytoskeleton. Taken together, our observations indicate that eEF1A2 is likely to play a causal role in the development of breast cancer and that it is a likely target for breast cancer therapy.

15. SUBJECT TERMS
No subject terms provided.

16. SECURITY CLASSIFICATION OF:			17. LIMITATION OF ABSTRACT	18. NUMBER OF PAGES	19a. NAME OF RESPONSIBLE PERSON USAMRMC
a. REPORT U	**b. ABSTRACT** U	**c. THIS PAGE** U	UU	94	**19b. TELEPHONE NUMBER** *(include area code)*

Standard Form 298 (Rev. 8-98)
Prescribed by ANSI Std. Z39.18

Table of Contents

Introduction
The overall goal of the project is to explore the role of protein elongation factor eEF1A2 in breast tumour development and to determine whether eEF1A2 is a useful breast cancer prognostic factor. Elongation factor eEF1A2 is one of two members of the eEF1A family of proteins (eEF1A1 and eEF1A2) that bind amino-acylated tRNA and facilitate their recruitment to the ribosome during protein translation elongation[1]. eEF1A proteins have other functions and can also induce actin [2] and tubulin [3] cytoskeleton rearrangements. Inactivation of the mouse eEF1A2 homolog, *Eef1a2*, leads to immunodeficiency and neural/muscular defects and death by 30 days of age [4, 5]. We had previously identified eEF1A2 as an ovarian cancer oncogene that could transform human and mouse cells[6], but its role in breast cancer was unknown. We also proposed to test the idea that eEF1A2 could modulate sensitivity to cisplatin and taxol and whether eEF1A2-inactivation could be used as a treatment for breast cancer. In addition, we hoped to understand the mechanism by which eEF1A2 regulates cell and oncogenesis.

We have made progress in the following areas:
1. The prognostic significance of eEF1A2 in breast cancer.
2. The ability of eEF1A2 to enhance the growth properties of malignant breast cells.
3. Generation of eEF1A2 transgenic mice.
4. The role of eEF1A2 in regulating the cytotoxicity of anti-cancer agents.
5. eEF1A2 inactivation as an anti-cancer treatment.
6. Modulation of cell adhesion and migration by eEF1A2.

Specific Aim 1. The prognostic significance of eEF1A2 in breast cancer.
Progress. We analyzed 69 primary breast tumours for eEF1A2 mRNA expression and divided them into eEF1A2 positive and negative groups (Fig 1a). eEF1A2 mRNA expression does not correlate with tumour size (Fig 1b), or ER or HER-2 status (not shown). To complement the eEF1A2 gene and mRNA studies, we have derived an rabbit polyclonal antibody that is reactive against eEF1A2 in Western blots of whole cell lysates from breast cells that express eEF1A2 (Fig 2a and b). This antibody recognizes eEF1A2 in paraffin embedded cells and we used this antibody to determine the prognostic significance of eEF1A2 in breast cancer. To this end, we measured eEF1A2 protein expression in a sample of 438 primary breast tumours annotated with 20-year survival data. We find that high levels of eEF1A2 protein are detected in 60% of primary breast tumours independent of HER-2 protein expression, tumour size, lymph node status, and estrogen receptor (ER) expression. Importantly, we find that high eEF1A2 is a significant predictor of outcome. Women whose tumour has high eEF1A2 protein expression have a significantly increased probability of 20-year survival compared to those women whose tumour does not express substantial eEF1A2 (Figure 3). In addition, eEF1A2 protein expression predicts increased survival probability in those breast cancer patients whose tumour is HER-2 negative or who do not have lymph node involvement (not shown). A paper detailing these findings is in press (Kulkarni et al. 2006. *Breast Cancer Research and Treatment*).

Specific Aim 2 eEF1A2 enhances growth of human malignant breast cell lines and activates Akt.

Progress. We have analyzed eEF1A2 in a panel of breast cancer cell lines and identified lines that highly express eEF1A2 and those that do not (Fig. 4a). We have made variants of MCF10AT and BT549 cell lines that highly express eEF1A2 (Fig 4b). eEF1A2 expression increases the *in vitro* growth rates of both cell lines (Fig 4c). Importantly, we have found that eEF1A2 is an activator of the Akt kinase as measured by an eEF1A2-dependent increase in phosphorylation on Akt residues 308 and 473 (Fig 4d). The involvement of eEF1A2 in increasing Akt phosphorylation suggests a plausible mechanism by which eEF1A2 could enhance oncogenesis. A paper containing our observation that eEF1A2 is a novel Akt activator is in press in Oncogene (Amiri et al. *Oncogene*).

Specific Aim 3. eEF1A2 transgenic mice.

Progress. We have derived three independent lines of mice that express eEF1A2 under the control of the MMTV promoter. Expression of transgenic eEF1A2 in the two highest expressing lines are shown in figure 5a. 6-8 month old virgin mice from these two lines show some evidence of nodal hyperplasia and increased ductal branching in their duct network (Fig 5b). The oldest of these mice is 20 months of age, but no spontaneous breast tumours have been observed in virgin mice. At the moment we are making multiparous eEF1A2 mice, but none have currently developed spontaneous breast tumours.

Specific Aim 4 eEF1A2 and sensitivity to taxol and cisplatin.

Progress. We have found no difference in sensitivity to cisplatin and taxol between eEF1A2 expressing cells and parental and vector controls (nor shown). Moreover, si-RNA mediated inactivation of eEF1A2 in MCF7, a breast tumour line that has high endogenous eEF1A2 levels, has no effect on sensitivity to either agent (not shown).

Specific Aim 5. eEF1A2-inactivating agents.

Progress. We have derived two siRNA and two phospho-orthioated antisense that reduce eEF1A2 mRNA and protein. Transient delivery of these siRNA into MCF7 reduce *in vitro* growth rate and sensitize them to anoikis (not shown). This suggests that eEF1A2 could be a suitable target for anti-cancer therapy.

Other Progress

eEF1A2 regulates cellular adhesion and migration. We have found that eEF1A2 regulates actin cytoskeleton rearrangement and *in vitro* migration. BT549 cells that stable express eEF1A2 have more filopodia-like structures than control cell lines (Fig 6a). This alteration in actin structure correlates with an increased ability of eEF1A2 to migrate and invade *in vitro* (Fig 6b). Enhanced filopodia production, increased migration is dependent on both Akt and phosphatidyl-inositol-3' kinase (not shown). This suggests that eEF1A2 is a novel component of phospho-inositide signaling. A paper detailing these findings is in press in *Oncogene*.

eEF1A2 is a novel activator of phosphatidyl-inoistol 4-kinase beta.   We have found that purified recombinant eEF1A2 binds recombinant phosphatidyl-4-kinase III beta (PI4KIIIβ) (fig 7a) and increases its lipid kinase activity *in vitro* (fig 7b). eEF1A2 expression also increases the generation of phosphatidyl-inositol 4 phosphate (PI4P) in living cells (fig 7c). PI4P generation is an essential step in the generation of PI(3,4,5)P, a signaling intermediary crucial in Akt activation and other signaling cascades Our data suggests that eEF1A2 activates phosphatidyl-inositol signaling through PI4 kinases. A paper detailing this work is current under revision for *Journal of Biological Chemistry*.

List of Publications.
1. **J.M. Lee,** S. Dedhar, R. Kalluri, & E.W. Thompson. 2006. The Epithelial-Mesnechymal transition: New insights in signaling, development and disease. *Journal of Cell Biology*. 172: 973-981.
2. G. Kulkarni, , D.A. Turbin, A. Amiri, S. Jeganathan, M.A. Andrade-Navarro, T.D. Wu, D.G. Huntsman & **J.M. Lee.** 2006. Expression of protein elongation factor eEF1A2 predicts favorable outcome in breast cancer. (*in press, Breast Cancer Research & Treatment)*
3. A. Amiri, F. Noei, S. Jeganathan, G.Kulkarni & **J.M. Lee**. eEF1A2 activates Akt and actin remodeling and enhances cell invasion and migration. (*in press, Oncogene*)
4. S. Jeganathan & **J.M. Lee.** Binding of elongation factor eEF1A2 to Phosphatidylinositol-4 kinase beta stimulates lipid kinase activity and phosphatidyl-4 phosphate generation (*under revision, J. Biol. Chem*)

Key Research Accomplishments

- Determined that eEF1A2 expression is increased in approximately 30% of human breast tumours.
- Identified high eEF1A2 mRNA expression as a marker for breast tumour recurrence.
- Generated a rabbit polyclonal antibody that recognizes eEF1A2 protein.
- Determined that eEF1A2 can enhance the growth rate of malignant breast cells.
- Determined that eEF1A2 is an inhibitor of anoikis.
- Determined that eEF1A2 is a novel activator of the Akt/PKB serine/threonine kinase.
- Generated three independent lines of transgenic mice that expresses eEF1A2 in their mammary tissue.
- Generated siRNA that inactivate eEF1A2 and inhibit the in vitro growth of breast cell lines.
- Determined that eEF1A2 regulates the actin cytoskeleton.

Reportable Outcomes

- eEF1A2 expression is increased in approximately 50% of human breast tumours.
- An eEF1A2 rabbit polyclonal antibody has been derived
- eEF1A2 protein expression is a marker for breast tumour recurrence.
- eEF1A2 enhances the growth rate of malignant breast cells.
- eEF1A2 inhibits anoikis.
- eEF1A1 activates the Akt/PKB serine/threonine kinase.
- Three independent lines of eEF1A2 transgenic mice have been derived
- siRNA that inactivate eEF1A2 and inhibit the in vitro growth of breast cell lines have been created.
- eEF1A2 regulates filopodia and the actin cytoskeleton.

Conclusions

EEF1A2 has been identified as a novel breast cancer oncogene. Supporting this idea are our observations that:

- eEF1A2 expression is increased in approximately 50% of human breast tumours.
- eEF1A2 mRNA expression is a prognostic marker for breast tumour recurrence.
- eEF1A2 enhances the growth rate of malignant breast cells.
- eEF1A2 inhibits anoikis.
- eEF1A1 activates the Akt/PKB serine/threonine kinase.
- Three independent lines of eEF1A2 transgenic mice have been derived
- siRNA that inactivate eEF1A2 and inhibit the in vitro growth of breast cell lines have been created.
- eEF1A2 regulates the actin cytoskeleton.

Taken together, our observations indicate that eEF1A2 is likely to play a causal role in the development of breast cancer and that it is a likely target for breast cancer therapy.

References

1.	Hershey, J. W. (1991). Translational control in mammalian cells. *Annu Rev Biochem* **60,** 717-55.
2.	Condeelis, J. (1995). Elongation factor 1 alpha, translation and the cytoskeleton. *Trends Biochem Sci* **20,** 169-70.
3.	Shiina, N., Gotoh, Y., Kubomura, N., Iwamatsu, A., and Nishida, E. (1994). Microtubule severing by elongation factor 1 alpha. *Science* **266,** 282-5.
4.	Shultz, L. D., Sweet, H. O., Davisson, M. T., and Coman, D. R. (1982). 'Wasted', a new mutant of the mouse with abnormalities characteristic to ataxia telangiectasia. *Nature* **297,** 402-4.
5.	Chambers, D. M., Peters, J., and Abbott, C. M. (1998). The lethal mutation of the mouse wasted (wst) is a deletion that abolishes expression of a tissue-specific isoform of translation elongation factor 1alpha, encoded by the Eef1a2 gene. *Proc Natl Acad Sci U S A* **95,** 4463-8.
6.	Anand, N., Murthy, S., Amann, G., Wernick, M., Porter, L. A., Cukier, I. H., Collins, C., Gray, J. W., Diebold, J., Demetrick, D. J., and Lee, J. M. (2002). Protein elongation factor EEF1A2 is a putative oncogene in ovarian cancer. *Nat Genet* **31,** 301-5.
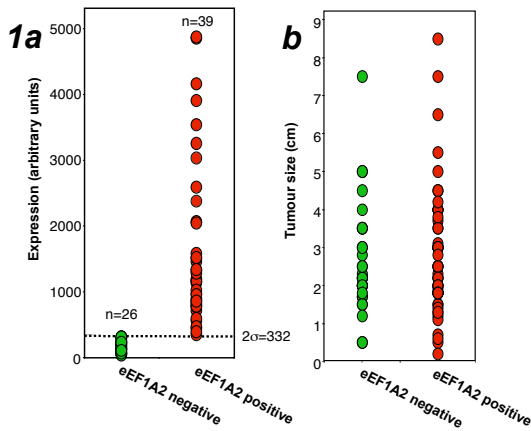
Appendix A. Figures.

Figure 1. eEF1A2 mRNA expression in human breast tumours (*a*) Value of eEF1A2 expression in eEF1A2 positive and negative breast tumours. The 2σ value above the negative expression is drawn and none of the tumours in the positive population is less than this value. (*b*) Tumour size in the eEF1A2 positive and negative populations.
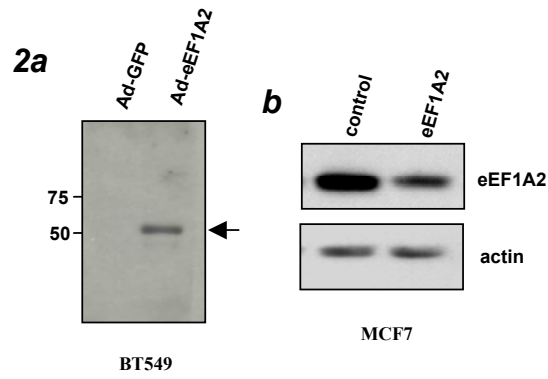

Figure 2. Derivation of an eEF1A2 antibody. (*a*) The eEF1A2 antiserum detects an ~50 kDa band, indicated by an arrow, in Western blots of BT549 cells infected with an eEF1A2 adenovirus but not in the GFP infected control. (*b*) A ~50kDa band is detected in MCF7 cells and the intensity of this band is reduced after transfection of an eEF1A2 siRNA. The control MCF7 has been transfected with a scrambled siRNA.
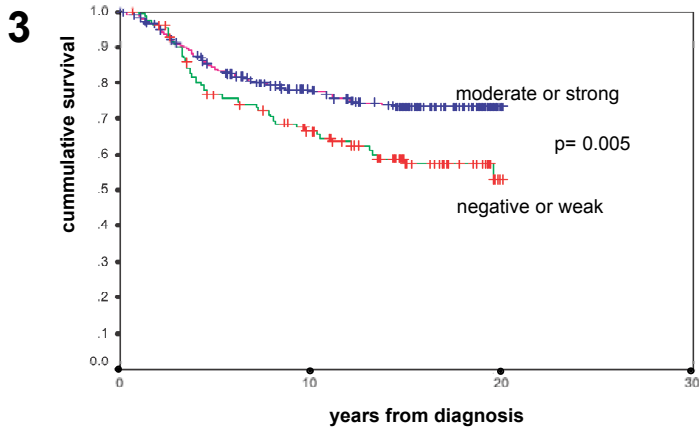
Figure 3. eEF1A2 expression is associated with increased 20-year survival probability. Disease-specific survival comparison for the patients with negative or weak expression of eEF1A2 compared to those with moderate to strong eEF1A2 expression. Cumulative survival probability is plotted as a function of years following diagnosis. The difference is significant at $p = 0.005$.
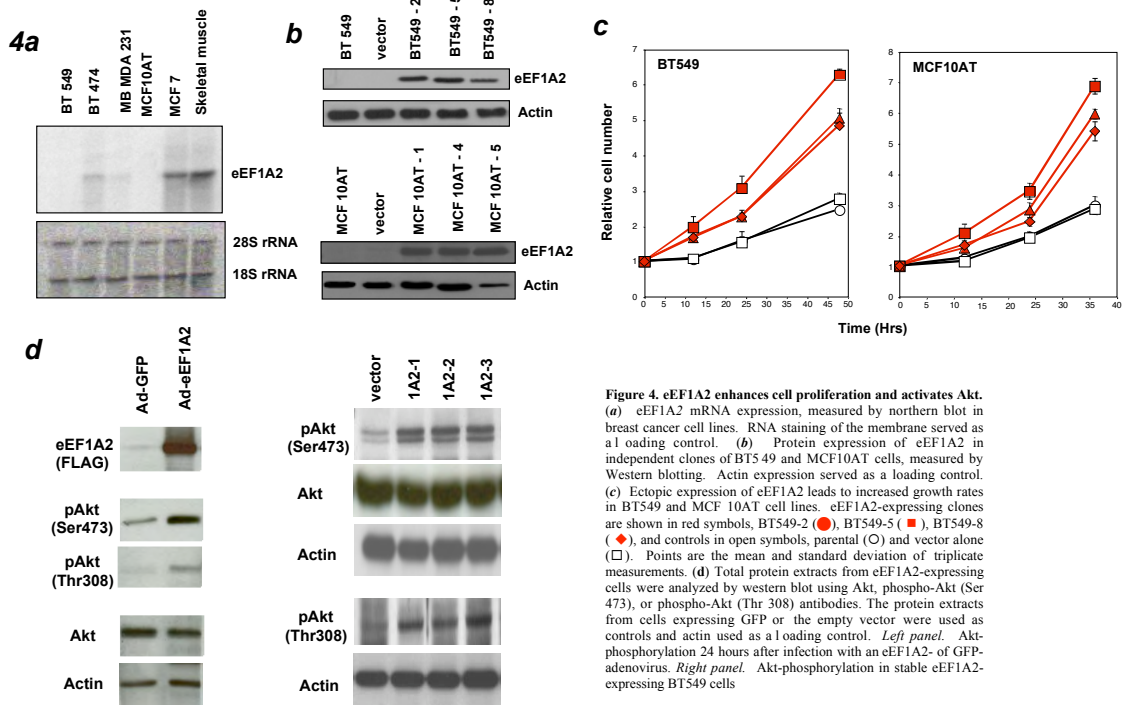

Figure 4. eEF1A2 enhances cell proliferation and activates Akt. (*a*) eEF1A2 mRNA expression, measured by northern blot in breast cancer cell lines. RNA staining of the membrane served as a loading control. (*b*) Protein expression of eEF1A2 in independent clones of BT549 and MCF10AT cells, measured by Western blotting. Actin expression served as a loading control. (*c*) Ectopic expression of eEF1A2 leads to increased growth rates in BT549 and MCF 10AT cell lines. eEF1A2-expressing clones are shown in red symbols, BT549-2 (●), BT549-5 (■), BT549-8 (◆), and controls in open symbols, parental (○) and vector alone (□). Points are the mean and standard deviation of triplicate measurements. (**d**) Total protein extracts from eEF1A2-expressing cells were analyzed by western blot using Akt, phospho-Akt (Ser 473), or phospho-Akt (Thr 308) antibodies. The protein extracts from cells expressing GFP or the empty vector were used as controls and actin as a loading control. *Left panel.* Akt-phosphorylation 24 hours after infection with an eEF1A2- of GFP-adenovirus. *Right panel.* Akt-phosphorylation in stable eEF1A2-expressing BT549 cells
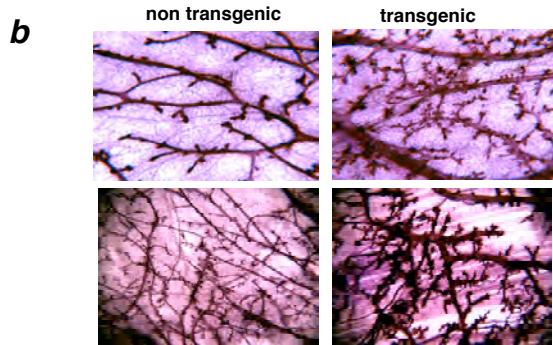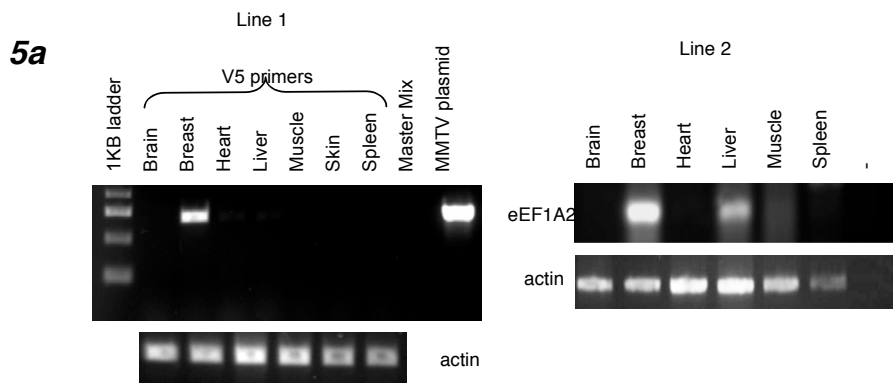
Page 12

5a

Line 1

Line 2

eEF1A2

actin

actin

b

non transgenic   transgenic

Line 1

Line 2

Figure 5.   Breast hyperplasia in MMTV-eEF1A2   mice.   (*a*) Transgene expression in two lines of eEF1A2/MMTV mice. RT-PCR was used to measure transgene expression in the indicated tissues. Actin serves as the loading control. (*b*) Transgenic mice have more nodes and increased branching relative to non-transgenic animals.
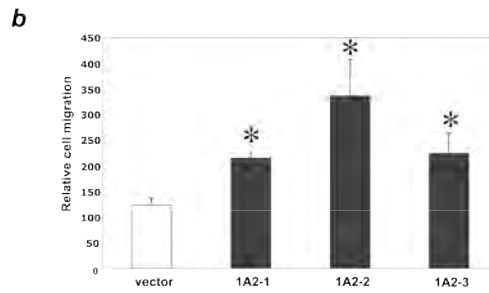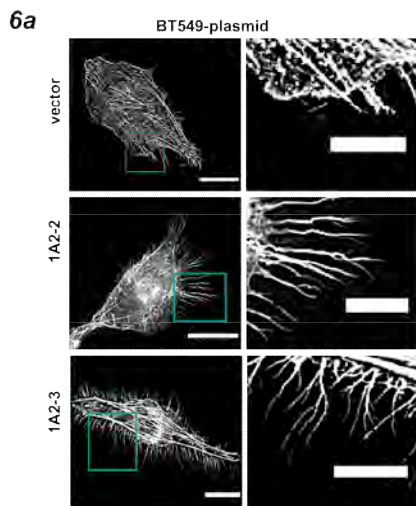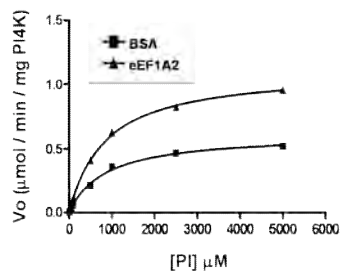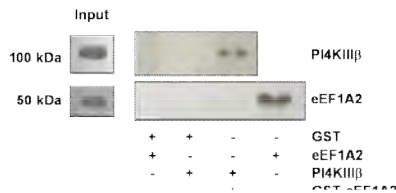
6a
BT549-plasmid

vector

1A2-2

1A2-3

b

Figure 6. eEF1A2 expression induces actin cytoskeletal rearrangement. (a) Fluorescence micrographs of eEF1A2-expressing and control BT549 cells stained with Alexa Fluor 546 phalloidin to examine actin filaments. The scale bar in each of the left panels is 30 uM in length. The right panel is a higher magnification of the blue box of the left picture. The scale bar in these images is 12 uM in length. (b) Transwell migration of control and eEF1A2 expressing cells is expressed as a percentage of vector only controls and is the mean and standard deviation of triplicate independent experiments. Enhanced migration is statistically significant (*p<0.05*, Students's t-test) and marked by an asterix.

Input

100 kDa   PI4KIIIβ

50 kDa   eEF1A2

GST	+	+	-	-
eEF1A2	+	-	-	+
PI4KIIIβ	-	+	+	-
GST-eEF1A2				

Page 13

Appendix B.

1. **J.M. Lee,** S. Dedhar, R. Kalluri, & E.W. Thompson. 2006. The Epithelial-Mesnechymal transition: New insights in signaling, development and disease. *Journal of Cell Biology.* 172: 973-981.
2. G. Kulkarni, , D.A. Turbin, A. Amiri, S. Jeganathan, M.A. Andrade-Navarro, T.D. Wu, D.G. Huntsman & **J.M. Lee.** 2006. Expression of protein elongation factor eEF1A2 predicts favorable outcome in breast cancer. (*in press, Breast Cancer Research & Treatment)*
3. A. Amiri, F. Noei, S. Jeganathan, G.Kulkarni & **J.M. Lee**. eEF1A2 activates Akt and actin remodeling and enhances cell invasion and migration. (*in press, Oncogene*)
4. S. Jeganathan & **J.M. Lee.** Binding of elongation factor eEF1A2 to Phosphatidylinositol-4 kinase beta stimulates lipid kinase activity and phosphatidyl-4 phosphate generation (*under revision, J. Biol. Chem*).

The epithelial–mesenchymal transition: new insights in signaling, development, and disease

Jonathan M. Lee,[1] Shoukat Dedhar,[2,3] Raghu Kalluri,[4,5,6] and Erik W. Thompson[7,8]

[1]Department of Biochemistry, Microbiology, and Immunology, University of Ottawa, Ottawa, Ontario K1N 6N5, Canada
[2]Department of Biochemistry, University of British Columbia, Vancouver, British Columbia V57 1L3, Canada
[3]British Columbia Cancer and Research Centre at the British Columbia Cancer Agency, Vancouver, British Columbia V57 1L3, Canada
[4]Department of Medicine, Center for Matrix Biology, Beth Israel Deaconess Medical Center and [5]Department of Biological Chemistry and Molecular Pharmacology, Harvard Medical School, Boston, MA 02215
[6]Harvard–Massachusetts Institute of Technology Division of Health Sciences and Technology, Cambridge, MA 02139
[7]Department of Surgery, University of Melbourne, St. Vincent's Hospital, Fitzroy, 3065, Australia
[8]St. Vincent's Institute of Medical Research, Fitzroy, 3065, Australia

The conversion of an epithelial cell to a mesenchymal cell is critical to metazoan embryogenesis and a defining structural feature of organ development. Current interest in this process, which is described as an epithelial–mesenchymal transition (EMT), stems from its developmental importance and its involvement in several adult pathologies. Interest and research in EMT are currently at a high level, as seen by the attendance at the recent EMT meeting in Vancouver, Canada (October 1–3, 2005). The meeting, which was hosted by The EMT International Association, was the second international EMT meeting, the first being held in Port Douglas, Queensland, Australia in October 2003. The EMT International Association was formed in 2002 to provide an international body for those interested in EMT and the reverse process, mesenchymal–epithelial transition, and, most importantly, to bring together those working on EMT in development, cancer, fibrosis, and pathology. These themes continued during the recent meeting in Vancouver.

Discussion at the Vancouver meeting spanned several areas of research, including signaling pathway activation of EMT and the transcription factors and gene targets involved. Also covered in detail was the basic cell biology of EMT and its role in cancer and fibrosis, as well as the identification of new markers to facilitate the observation of EMT in vivo. This is particularly important because the potential contribution of EMT during neoplasia is the subject of vigorous scientific debate (Tarin, D., E.W. Thompson, and D.F. Newgreen. 2005. *Cancer Res.* 65:5996–6000; Thompson, E.W., D.F. Newgreen, and D. Tarin. 2005. *Cancer Res.* 65:5991–5995).

Defining epithelial–mesenchymal transition (EMT)

Historically, epithelial and mesenchymal cells have been identified on the basis of their unique visual appearance and the morphology of the multicellular structures they create (Shook and Keller, 2003). A typical epithelium is a sheet of cells, often one cell thick, with individual epithelial cells abutting each other in a uniform array. Regularly spaced cell–cell junctions and adhesions between neighboring epithelial cells hold them tightly together and inhibit the movement of individual cells away from the epithelial monolayer. Internal adhesiveness allows an epithelial sheet to enclose a three-dimensional space and provide it with structural definition and mechanical rigidity. The epithelial sheet itself is polarized, meaning that the apical and basal surfaces are likely to be visually different, adhere to different substrates, or have different functions. Mesenchymal cells, on the other hand, generally exhibit neither regimented structure nor tight intracellular adhesion. Mesenchymal cells form structures that are irregular in shape and not uniform in composition or density. Adhesions between mesenchymal cells are less strong than in their epithelial counterparts, allowing for increased migratory capacity. Mesenchymal cells also have a more extended and elongated shape, relative to epithelial cells, and they possess front-to-back leading edge polarity. Unlike epithelia, the irregular structure of mesenchyme does not allow for rigid topological specialization. Moreover, mesenchymal migration is mechanistically different from epithelial movement. Epithelial cells move as a sheet en block, whereas mesenchymal migration is considerably more dynamic. Mesenchymal cells move individually and can leave part of the trailing region behind. Elizabeth Hay (Harvard University, Boston, MA), who first described the EMT (Hay, 2005), illustrated the fundamental differences of such movement in embryogenesis (subtle/controlled) and

tumorigenesis (aggressive/uncontrolled) to define the distinct EMT mechanisms at the EMT conference.

Turning an epithelial cell into a mesenchymal cell requires alterations in morphology, cellular architecture, adhesion, and migration capacity. Commonly used molecular markers for EMT include increased expression of N-cadherin and vimentin, nuclear localization of β-catenin, and increased production of the transcription factors such as Snail1 (Snail), Snail2 (Slug), Twist, EF1/ZEB1, SIP1/ZEB2, and/or E47 that inhibit E-cadherin production. Phenotypic markers for an EMT include an increased capacity for migration and three-dimensional invasion, as well as resistance to anoikis/apoptosis. A summary of common EMT markers is listed in Table I. Importantly, these developmental regulators can induce EMT in a nondevelopmental context and thereby have an important role in cancer and fibrosis.

Signaling pathways in EMT

Much of the meeting highlighted signaling pathways that regulate or mediate the EMT, focusing both on refinement and extension of known pathways, but also on the discovery of new regulators and novel pathways (Fig. 1).

One of the first cell surface receptors identified that was able to stimulate scattering of epithelial cells was the Met receptor tyrosine kinase. Activation of Met by its ligand, hepatocyte growth factor, enhances the migration of multiple cell lines in vitro, and scattering of cultured multicystic dysplastic kidney cells is a classical EMT assay. Morag Park (McGill University, Montreal, Quebec, Canada) reported that transgenic mice expressing wild-type or active variants of Met under the control of the mouse mammary tumor virus promoter develop nodal and ductal hyperplasia and spontaneous mammary tumors, albeit with a long latency period (∼1.5 yr). Park suggested that Met cooperates with the Her2/neu oncogene in activating EMT, and that the Crk family of SH2 and SH3 adaptor proteins are critical in Met-mediated EMT. Crk proteins are highly expressed in human breast tumors, and Park reported that small interfering RNA (siRNA) ablation of Crk inhibits Met-dependent cell migration and EMT.

Although the Met receptor-mediated signaling results in cell scattering, it has not been made clear whether Met signaling also has a more permanent effect on the expression or localization of some of the effectors of EMT, such as E-cadherin and β-catenin. Recent work by Walter Birchmeier (Max Delbruck Center, Berlin, Germany) suggests that Met also regulates intracellular localization of β-catenin. β-Catenin has a dual role in the EMT; it enhances cell–cell adhesion when bound to cadherin complexes in adherens junctions and also functions as a transcriptional coactivator upon entry into the nucleus (van Es et al., 2003). The ability of β-catenin to enhance cadherin-dependent adhesion depends on β-catenin binding to α-catenin and on α-catenin binding to the cadherin (Chu et al., 2004). Phosphorylation of β-catenin residue Y142 prevents α-catenin interaction and enhances the binding of β-catenin to BCL9-2, which is the vertebrate homologue of the *Drosophila melanogaster* legless gene (Brembeck et al., 2004). Interaction of β-catenin with BCL9-2 enhances nuclear accumulation of both proteins, simultaneously decreasing cadherin-mediated adhesion

Table I. **EMT markers**

Proteins that increase in abundance
 N-cadherin
 Vimentin
 Fibronectin
 Snail1 (Snail)
 Snail2 (Slug)
 Twist
 Goosecoid
 FOXC2
 Sox10
 MMP-2
 MMP-3
 MMP-9
 Integrin αvβ6

Proteins that decrease in abundance
 E-cadherin
 Desmoplakin
 Cytokeratin
 Occludin

Proteins whose activity increases
 ILK
 GSK-3β
 Rho

Proteins that accumulate in the nucleus
 β-catenin
 Smad-2/3
 NF-κβ
 Snail1 (Snail)
 Snail2 (Slug)
 Twist

In vitro functional markers
 Increased migration
 Increased invasion
 Increased scattering
 Elongation of cell shape
 Resistance to anoikis

and activating catenin target gene transcription. Ectopic BCL9-2 expression is sufficient to induce EMT in cultured cells, and siRNA-mediated BCL9-2 inactivation drives the reverse mesenchymal–epithelial transition (MET). Birchmeier reported that Y142 can be phosphorylated by the Met tyrosine kinase, indicating the existence of an EMT activation pathway where Met induces β-catenin nuclear translocation by enhancing BCL9-2 interaction. This pathway satisfactorily links these two well known EMT regulators.

Interestingly, Pez/PTPN14, which is a tyrosine phosphatase that is frequently mutated in colorectal tumors (Wang et al., 2004), induces Snail1 expression and can also activate cell migration (Yeesim Khew-Goodall, Hanson Institute, Adelaide, Australia). Pez can dephosphorylate β-catenin on tyrosine residues that regulate its interaction with the adherens junction complex, suggesting that Pez mutations contribute to EMT by preventing cytoplasmic β-catenin–cadherin interaction and enhancing its nuclear translocation. However, Pez overexpression in MDCK and MDA-MB468 cells was shown to be sufficient to
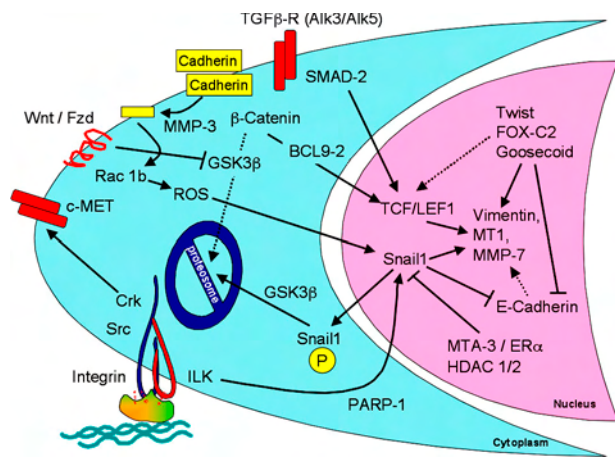
Figure 1. **Signaling events during EMT.** The major signaling events that were reported in the meeting are summarized. Cleavage of E-cadherin (yellow) by MMP-3 resulted in activation of Snail1 through ROS. Snail1 localization to the nucleus is controlled by phosphorylation of a nuclear export motif and a proteosomal degradation motif, which are each phosphorylatable by GSK-3β. An ILK-responsive element in the Snail1 promoter binds PARP-1. Snail1 expression is inhibited by the MTA3–NuRD chromosomal rearrangement complex, acting downstream of the activated estrogen receptor. Repression of E-cadherin by Snail1, Twist, or other repressors leads indirectly to expression of vimentin and other mesenchymal gene products, partly because of β-catenin/Tcf–Lef1 activation. FOX-C2, as well as SIP1, can also directly activate mesenchymal gene expression. Translocation of β-catenin to the nucleus requires BCL9-2, which itself can induce EMT. Abundance of β-catenin is regulated by phosphorylation-dependent proteosomal degradation, unless GSK-3β is silenced through Wnt signaling. TGF-β is known to activate this canonical Wnt pathway, but TGF-β also directly activates the Tcf–Lef1 transcription complex through tyrosine phosphorylation of SMAD-2. The c-Met receptor tyrosine kinase, through the Crk adaptor, also stimulates EMT.

cause EMT, and knockdown in zebrafish causes multiple developmental abnormalities, including aberrant pigmentation and craniofacial deformation. These defects are broadly consistent with dysfunctional neural crest EMT in the absence of Pez.

Cancer-relevant insights into EGF signaling were provided by Erik Thompson (University of Melbourne, Melbourne, Australia), who has identified EGF as a novel EMT inducer in human breast cancer, as measured by EGF's ability to decrease E-cadherin and increase vimentin production in PMC42 cells. Interestingly, EMT may influence the response of certain cancers to EGF receptor (EGFR)–targeted therapeutics. John Haley (OSI Pharmaceuticals, Melville, NY) presented data showing that the sensitivity of nonsmall cell lung cancer cell lines to erlotinib, which is an EGFR-targeted monoclonal antibody, did not correlate with EGFR levels, but rather depended on their EMT status, with those having undergone EMT showing resistance (Thomson et al., 2005).

An interesting and novel aspect of EGFR signaling was presented by Mien-Chie Hung (The University of Texas MD Anderson Cancer Center, Houston, TX), who reported that EGFR, which is a transmembrane receptor tyrosine kinase, complexes with the STAT3 transcription factor in the nucleus and can be immunoprecipitated from the EGF-responsive iNos promoter (Lo et al., 2005a). The role that promoter-complexed EGFR has in EMT is uncertain, but high nuclear EGFR is associated with a poor prognosis in breast carcinoma (Lo et al., 2005b).

The observation that a transmembrane receptor is found in functional promoter complexes in the nucleus was one of the meeting's most surprising observations, and it will be of great interest to characterize the topological and structural mechanisms through which a membrane receptor enters the nucleus and activates transcription (Giri et al., 2005).

TGF-β is a major regulator of EMT and has been implicated in skin cancer development (Zavadil and Bottinger, 2005). Jiri Zavadil (New York University School of Medicine, New York, NY) reported that TGF-β activates EMT through Smad-3–dependent activation of the HEY1 gene, a member of the Hairy/Enhancer-of-split family of transcriptional repressors. Zavadil used extensive gene expression profiling to identify HEY1 targets that are important in EMT induction (Zavadil et al., 2004). He reported on the profiling of EMT in the following three different contexts: HaCaT human keratinocyte EMT in response to TGF-β, mouse model of aristolochic acid nephropathy, and human kidney-proximal tubule cells. Satisfyingly, one of these targets is *Dishevelled 2* (*DVL2*), which is a gene that regulates EMT by repressing the production of Notch, GSK3β, and β-catenin. Another HEY1 target seen in all three systems was the polycomb family histone methyltransferases EZH1/EZH2, suggesting that TGF-β–activated EMT could be controlled through structural histone modification. Other TGF-β targets include integrins β4 and α6. Richard Bates (University of Massachusetts, Worcester, MA) reported that the integrin αvβ6 is up-regulated during colon cancer development and highly expressed in metastatic samples (Bates, 2005).

Christopher Gebeshuber showed that TGF-β induced Smad-2 tyrosine phosphorylation and that TGF-β–induced EMT was blocked upon expression of nonphosphorylatable Smad-2 mutant, the expression of which inhibited metastases formation. Gebeshuber also reported that this mutant had a reduced ability to interact with the Tcf–Lef1 transcription factor. This suggests that tyrosine phosphorylation of Smad-2 may potentiate Tcf–Lef1 interaction and stimulate both EMT and metastatic induction. Ali Nawshad (University of Nebraska, Lincoln, NE) and Elizabeth Hay reported a similar noncanonical role for TGF-β in the EMT of mouse palatal epithelial seam and kidney-proximal tubule cells. They reported that Smad-2/4 repressed E-cadherin transcription through Tcf–Lef1 (Masszi et al., 2004; Nawshad et al., 2005).

One of the functions of TGF-β is to stimulate expression of ECM proteins. Do ECM proteins initiate EMT? Andre Menke (University of Ulm, Ulm, Germany) showed that extracellular collagen that is deposited during a fibrotic disease can be an initiator of EMT. Menke reported that pancreatic cancer cell lines cultured on collagen I have a reduced capacity to cluster E-cadherin at points of cell–cell contact and have a more mesenchyme-like morphology. Menke postulated an EMT pathway where collagen induces both the recruitment of FAK to cadherin adhesion complexes and the phosphorylation of β-catenin. Phosphorylated β-catenin then translocates to the nucleus, activating EMT target genes. Conceptually, this may be similar to work by Mina Bissell describing the capacity of mechanical forces or the shape of the cell to initiate EMT.

Regulating Snail1

The Snail1 transcriptional repressor is a key EMT regulator (Barrallo-Gimeno and Nieto, 2005). There was much interest in signaling pathways converging on Snail1 production, stability, and intracellular localization. Derek Radisky (Mayo Clinic, Jacksonville, FL) reported that matrix metalloproteinase-3 (MMP-3) activates Snail1 production in mammary cells. MMP-3 is expressed in many primary breast tumors, induces mammary carcinogenesis in transgenic mice, and causes an in vitro EMT in mouse mammary cells (Lochter et al., 1997; Sternlicht et al., 1999). Radisky reported that MMP-3 activates EMT by inducing the production of an alternatively spliced variant of Rac1, which is a small GTPase that regulates cell migration through control of actin polymerization (Burridge and Wennerberg, 2004). This splice variant, termed Rac1b, activates the mitochondrial production of reactive oxygen species (ROS), which subsequently activates Snail1 production (Radisky et al., 2005). However, the mechanism by which MMP-3 stimulates alternative splicing, or how the Rac1 variant activates ROS, is unclear. Snail genes can be considered regulators of cell survival, adhesion, and migration, and the triggering of the EMT is just one of the mechanisms they use to promote cell movement (Barrallo-Gimeno and Nieto, 2005). Pierre Savagner (Batiment de Recherche en Cancerologie, Montpellier, France) reported that Snail2-deficient mice show delayed mammary gland tubule growth, and precocious branching morphogenesis similar to that seen in the mammary gland lacking P-cadherin, which is a cadherin that is selectively expressed in myoepithelial cells (Radice et al., 1997). Snail2-deficient mammary gland retained normal smooth muscle actin-staining myoepithelial cells. These cells lack P-cadherin, suggesting that Snail2 controls a progenitor-like phenotype in the mammary gland through P-cadherin.

Several investigators reported new insights into the control of Snail1 expression. Shoukat Dedhar (University of British Columbia, Vancouver, British Columbia, Canada) reported that integrin-linked kinase (ILK) activates Snail1 expression. Using proteomic approaches, Dedhar and coworkers made the surprising finding that ILK-mediated induction of Snail1 transcription maps to a portion of the Snail1 promoter that is bound by poly-ADP-ribose polymerase 1 (PARP-1). PARP-1 regulates transcription by modifying chromatin structure and through interaction with other transcription factors (Kim et al., 2005). ILK activation promotes PARP-1 binding to the Snail1 promoter, whereas siRNA ILK knockdown and drug inhibition of ILK activity prevents PARP-1 from binding to the promoter. siRNA knockdown of PARP-1 in mesenchymally transformed PC-3 cells inhibited Snail1 expression and stimulated E-cadherin expression, suggesting the novel idea that PARP-1 itself is an important factor in EMT control. It is unclear whether direct phosphorylation of PARP-1 by ILK controls its ability to interact with the Snail1 promoter. Inhibiting ILK activity with the small molecular inhibitor QLT0267 inhibited production of urokinase type plasminogen activator and the invasion of MDA-MB231 breast cancer cells (Nancy Dos Santos, University of British Columbia, Vancouver, British Columbia, Canada).

Anna Bagnato (Regina Elena Cancer Institute, Rome, Italy) also reported that endothelin 1 induced EMT in ovarian carcinomas in in vitro and in vivo cells through a phosphoinositide 3 kinase– and ILK-mediated signaling pathway, leading to glycogen synthase kinase-3β (GSK-3β) inhibition, Snail and β-catenin stabilization, and transcriptional programs that control repression of E-cadherin. Inhibition of the endothelin A receptor reversed the EMT, suppressed ILK and Snail1 expression, and restored E-cadherin expression. Snail1 represses E-cadherin expression by binding to three independent E-boxes in the cadherin promoter. Snail1 prevents E-cadherin expression through at least two pathways, one dependent on class I histone deacetylases and the other independent of it (Antonio Garcia de Herreros, Universitat Pompeu Fabra, Barcelona, Spain).

Snail transcription is regulated by the estrogen receptor (ER; Paul Wade, National Institute of Environmental Health Sciences, Research Triangle Park, NC). ER is an EMT inhibitor and is critical in maintaining the epithelial status of normal breast cells. Wade reported that MTA3, which is a component of the Mi-2–NuRD transcriptional repressor complex, is an ER-responsive gene, and its expression correlates well with ER expression in primary breast tissue samples. Wade reported that MTA3 binds to the Snail1 promoter and inhibits Snail1 transcription (Fujita et al., 2003). Because expression of the ER is a marker for good breast cancer prognosis, the observation that ER is an EMT inhibitor provides further evidence in support of a role for EMT in oncogenesis.

Snail1 levels can also be controlled posttranslationally, and Garcia de Herreros and Hung both reported that Snail1 is a phosphoprotein. Garcia de Herreros reported that Snail1 phosphorylation prevents its nuclear accumulation and inhibits its ability to activate EMT (Dominguez et al., 2003). Hung reported that Snail1 is phosphorylated by GSK-3β on two distinct motifs. Phosphorylation of two serines in the first motif directs Snail1 ubiquitination and proteolytic destruction. Phosphorylation of four serines on the second motif directs nuclear export. Mutation of all six GSK-3β phosphorylation sites increased the half-life of the Snail1 protein and ensured that it was constitutively nuclear. Consistent with a role for Snail1 phosphorylation in EMT, expression of Snail1 that could not be phosphorylated caused a loss of E-cadherin production and an EMT-like morphological change in human tumor lines (Zhou et al., 2004). Jim Woodgett (Samuel Lunenfeld Research Institute, Toronto, Ontario, Canada) described an important role for GSK-3β in controlling embryonic stem cell differentiation and the maintenance of pluripotency.

EMT in embryogenesis and adults

During embryogenesis, the neural crest develops from a small portion of the dorsal neural tube (Huang and Saint-Jeannet, 2004; Newgreen and McKeown, 2005). After an EMT, neural crest cells migrate away from the neural tube and differentiate into bone, smooth muscle, peripheral neurons and glia, and melanocytes. Don Newgreen (Murdoch Children's Research Institute, Melbourne, Australia) reported that the Sox transcription factors control this EMT and subsequent migration. Using an electroporation system that delivers Sox genes to cells on one side of the neural tube in living chicken embryos, Newgreen reported that ectopic expression of Sox-8, -9, or -10 was sufficient

to induce EMT and activate migration away from the neural tube while suppressing terminal differentiation. This migratory capacity was conferred to all cells of the neural tube, indicating that Sox expression was overriding inhibitory signals that normally restrict neural tube EMT to cells of the neural crest.

Nelly Auersperg (University of British Columbia, Vancouver, British Columbia, Canada) provided evidence that EMT occurs in the ovaries of adult women. The mature mammalian ovary is enveloped by the ovarian surface epithelium (OSE), and the bulk of ovarian carcinomas arise from these cells. As a result of wound repair after egg extrusion, OSE cells are trapped in the ovarian follicle or stroma of postovulatory ovaries. Dr. Auersperg presented evidence showing that normal human OSE cells have a strong propensity to undergo EMT in vitro and in vivo in response to growth factor stimulation and alteration in their extracellular matrix. Auersperg suggested that normal OSE trapped within the ovary may undergo EMT as a means of maintaining ovarian homeostasis.

Cell adhesion and EMT

A defining feature of EMT is a reduction in E-cadherin levels and a concomitant production of N-cadherin. Cadherins are transmembrane proteins whose homotypic interaction between neighboring cells creates adherens junctions (Gumbiner, 2005). Alteration of cadherin-based adhesion has a key role in modulating development and organogenesis. At the cell membrane, cadherin proteins are found as homodimers tethered to the actin cytoskeleton by a multiprotein complex that includes α-, β-, and p120-catenin.

To characterize the physical forces underlying cadherin-based adhesion, Jean-Paul Thiery (Institut Pasteur, Paris, France) reported on an elegant system designed to measure the force necessary to separate two cells that are adhered solely to each other (Chu et al., 2004, 2005). Thiery reported that the development of intercellular adhesion by N- or E-cadherin is a two-step process. The first step relies on interactions between the cadherins on the surface of adjacent cells. This interaction takes 30 s to develop and requires a force of ∼10 nanoNewtons to break apart. The second step, which takes up to 30 min to maximize, strengthens the initial interaction and requires ∼200 nanoNewtons to separate it. This strengthening depends on Rac- and Cdc42-mediated induction of actin polymerization, presumably to anchor the cell surface cadherins to the cytosol. Thiery also reported that four times more force is required to separate adhesions between E-cadherin molecules compared with N-cadherin ones. In addition, there is no detectable interaction strength between E- and N-cadherin. This supports the current EMT paradigm, where the presence of E-cadherin in epithelial cells allows for greater cell–cell adhesive strength compared with that of the N-cadherin–expressing mesenchyme. Moreover, the minimal adhesive interaction between E- and N-cadherin would be predicted to allow an N-cadherin–expressing cell to migrate through a layer of E-cadherin–expressing cells.

Alpha Yap (University of Queensland, Brisbane, Australia) reported evidence that E-cadherin clustering at cell–cell junction sites requires dynamic microtubules. Yap reported visual evidence that the plus ends of microtubules terminate in E-cadherin puncta and that agents that block dynamic plus ends inhibit the ability of cells to concentrate cadherin at cell–cell contacts. This suggests that the actin and microtubule cytoskeletons both serve to anchor E-cadherin adhesions. This would contrast cadherin adhesions to integrin-containing focal adhesions because microtubule association with focal adhesions triggers their disassembly (Ezratty et al., 2005).

Mina Bissell (Lawrence Berkeley National Laboratory, Berkeley, CA) described data suggesting that cell shape changes brought about by the destruction of the basement membrane cause EMT. She then described a model of branching morphogenesis of the mammary gland and showed data to support a transient EMT at the tip of the branching structures. This was demonstrated by the activation of the vimentin promoter (visualized by a GFP reporter) at the branch tip. Bissell went on to describe studies that provided an understanding of how branching structures are created. She used engineered matrices and biomaterials to show that the architecture of the created vessel in collagen gels can determine where and how branches are created. Although the role of cell geometry in growth (Folkman and Moscona, 1978; Chen et al., 1997), apoptosis (Chen et al., 1997), and metabolic regulation (Bissell et al., 1977) has been known for decades, the molecular pathways that link cell shape to these events, and also to EMT, are only now beginning to be elucidated (Weaver et al., 2002; Paszek et al., 2005; Radisky et al., 2005). The orientation of a cell to its growth substrate may also regulate EMT. Marcia McCoy and Calvin Roskelley (University of British Columbia, Vancouver, British Columbia, Canada) reported that overexpression or mislocalization of the apical marker podocalyxin destabilized cell polarity in vitro, which may explain why podocalyxin overexpression is an independent marker of in vivo breast carcinoma progression (Somasiri et al., 2004).

EMT in cancer

The occurrence of EMT during tumor progression allows benign tumor cells (i.e., ones that are noninvasive and nonmetastatic) to acquire the capacity to infiltrate surrounding tissue and to ultimately metastasize to distant sites. The pathological staging of tumors supports this paradigm. The most compelling evidence for the involvement of EMT in oncogenesis is the ability of multiple EMT regulators to enhance tumor formation and/or metastasis (Thiery, 2002). For example, expression of Snail1 increases the aggressiveness of experimentally induced breast tumors, and high Snail1 expression correlates with an increased risk of tumor relapse and poor survival rates in human breast cancer (Moody et al., 2005). Loss of E-cadherin is a hallmark of metastatic carcinoma (Cavallaro and Christofori, 2004), and proteomic analysis of breast cancer reveals that circulating mammary tumor cells, or those found as micrometastases, show evidence of mesenchymal conversion (Willipinski-Stapelfeldt et al., 2005). The EMT meeting added to the growing list of EMT regulators that control some aspect of oncogenesis, which includes MMP-3, BCL9–2, EGFR, Met, Goosecoid, Kaiso, TGF-β, FOXC2, GSK-3β, Smad-3, Pez, Snail1, Snail2, and ILK (Table I).

However, there remains some controversy in the cancer community, particularly among pathologists, as to whether the

transformation of a normal cell into a cancerous cell or a non-invasive tumor into a metastatic tumor is truly an EMT (Tarin et al., 2005). Skepticism about the role of EMT in cancer stems from the apparent rarity of the EMT–like morphological changes that are observed in primary tumor sections, and also from the observation that metastases appear histologically similar to the primary tumor from which they are derived. Of central importance, therefore, is the direct visualization of EMT during tumor progression. Garcia de Herreros used a new Snail1 antibody that is suitable for mouse and human immunohistochemistry (EC3) to show that Snail1 protein is expressed specifically at the invading front of colorectal tumors. Snail antibodies have been difficult to use in immunohistochemistry, and Karl-Friedrich Becker (Technical University of Munich, Munich, Germany) used another new Snail1 antibody (Sn9H2; Rosivatz et al., 2005) to demonstrate nuclear Snail1 in gastric, mammary, and endometrial tumors. Richard Bates reported that integrin αvβ6 is specifically expressed at the invading edge of colorectal cancer xenografts. Thomas Brabletz (University of Erlangen, Erlangen, Germany) reported that tumor cells at the invading edge of colorectal carcinomas have nuclear β-catenin and loss of E-cadherin. Nuclear localization of β-catenin is frequently used as an EMT marker, and nuclear β-catenin is a marker for a poor prognosis in colorectal cancer. The ability of EMT markers to identify a subset of tumor cells raises the possibility that EMT could be associated with the maintenance of cancer stem cells. Brabletz reported that invading cells with nuclear β-catenin also express the stem cell markers hTert and survivin, possibly implicating EMT in cancer stem cell maintenance (Brabletz et al., 2005). The presence of EMT markers at the tumor–host interface, but not in the bulk tumor, is strong evidence that EMT occurs during tumor development and that it regulates invasiveness and tumor aggressiveness.

The histological similarity of secondary, metastasis-derived tumors to the primary tumor indicates that EMT-mediated metastatic development must be followed by a reverse MET to allow colonization of secondary sites. Brabletz reported that metastases derived from tumors originally expressing nuclear β-catenin were found to reexpress E-cadherin, and their β-catenin became cytoplasmic, which is suggestive of a MET (Brabletz et al., 2001). Similarly, Christine Chaffer (Bernard O'Brien, Institute of Microsurgery, Melbourne, Australia) reported that variants of the metastatic T24/TSU-Pr1 bladder carcinoma line that were selected for enhanced metastatic potential have more epithelial markers (E-cadherin and keratins) than their less metastatic counterparts, but continue to express some mesenchymal markers (vimentin and MMPs). This ability of cells to express attributes of both epithelial and mesenchymal phenotypes was referred to by Savagner as a "metastable phenotype" (Fig. 2). Consistent with this idea, Savanger reported that Rac distribution can be found with both epithelial-like (adherens junctions) and mesenchyme-like (lamellopodia) patterns during the migration of cohesive epithelial cells, and probably during tumor invasion as well. Metastability is consistent with the expression of stem cell markers in colorectal cells undergoing EMT and suggests that such plasticity may be found in progenitor cells in various organs. This plasticity could also be

an explanation for the difficulty in observing EMT in cancer development; acquisition of mesenchymal characteristics may be transitory and undergo a reversal during later tumorigenesis.

Robert Weinberg (Whitehead Institute, Cambridge, MA) reported that three transcription factors regulating developmental EMT—Twist, Goosecoid, and FOXC2—have important roles in metastasis. Each of these gene products enhances metastasis in experimental mouse models and is highly expressed in primary human tumors and metastases. Twist is a basic helix-loop-helix transcription factor that was originally identified as a *D. melanogaster* EMT activator (Castanon and Baylies, 2002). Weinberg reported that Twist expression is sufficient to induce an in vitro EMT in breast cells and that Twist inactivation inhibits metastasis development in vivo (Yang et al., 2004). Goosecoid is a homeobox transcriptional repressor that marks the Spemann organizer in vertebrate gastrulation and is one of the first identified regulators of embryological patterning (De Robertis et al., 2001). Both Twist and Goosecoid regulate FOXC2, which is a transcription factor of the FOX family of forkhead helix-turn-helix DNA-binding proteins that regulates EMT and organ development in multiple tissues (Carlsson and Mahlapuu, 2002). Twist, Goosecoid, and Snail1 all repress E-cadherin and induce FOXC2; they also enhance cell migration in vitro and metastatic potential in vivo. It is not yet known whether these three genes regulate individual or overlapping pathways of EMT and metastases. Importantly, FOXC2 also directly up-regulated mesenchymal gene transcription, rather than causing an EMT through E-cadherin repression.

Frans van Roy and Geert Berx (Ghent University, Ghent, Belgium) reported on the identification of a series of novel target genes of the E-cadherin repressors Snail1 and SIP1/ZEB2 that control the establishment of junctional complexes, intermediate filament networks, and the actin cytoskeleton (De Craene et al., 2005). They also showed some direct effects on mesenchymal factor transcription via these pathways. Christine Gilles (University of Liege, Liege, Belgium) reported that vimentin

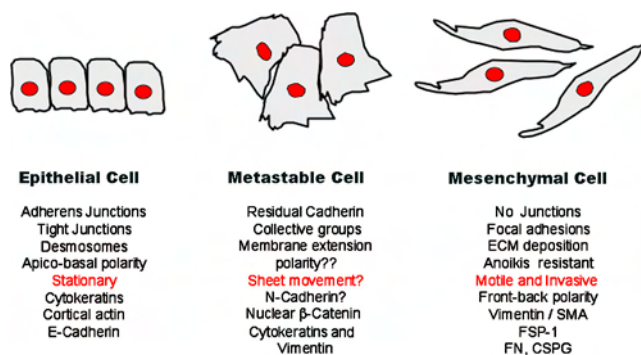| Epithelial Cell	Metastable Cell	Mesenchymal Cell
Adherens Junctions	Residual Cadherin	No Junctions
Tight Junctions	Collective groups	Focal adhesions
Desmosomes	Membrane extension	ECM deposition
Apico-basal polarity	polarity??	Anoikis resistant
Stationary	Sheet movement?	Motile and Invasive
Cytokeratins	N-Cadherin?	Front-back polarity
Cortical actin	Nuclear β-Catenin	Vimentin / SMA
E-Cadherin	Cytokeratins and	FSP-1
	Vimentin	FN, CSPG

Figure 2. **The metastable cell phenotype.** Several studies have identified a hybrid cell showing both epithelial and mesenchymal traits. These cells are summarized here, in conjunction with their epithelial and mesenchymal counterparts. The term metastable was introduced at the meeting by Pierre Savagner, who showed evidence of epithelial and mesenchymal Rac localization within the same cells. Similar scenarios of hybrid cells were shown by Chaffer (metastasis-derived T24 human bladder carcinoma cells) and Thompson (EGF-treated PMC42 human breast cancer cells). Coexpression of mixed lineage traits within the same cell may be consistent with the stem cell–like profiles reported by Brabletz in colon carcinoma cells at the invasive front.

transcription was activated by SIP1/ZEB2, as well as a Tcf–β-catenin complex.

EMT in fibrosis

The accumulation of fibroblasts, excess collagen, and other matrix components at sites of chronic inflammation lead to scar tissue formation and progressive tissue injury. These fibroblasts derive from the bone marrow, but also arise from an EMT of cells at injury sites (Kalluri and Neilson, 2003; Neilson, 2005). EMT is likely involved in the progressive fibrotic diseases of the heart, lung, liver, and kidney.

Eric Neilson (Vanderbilt University, Nashville, TN) presented work using fibroblast-specific protein 1 (FSP1) as a marker for EMT that occurs during fibrosis (Iwano et al., 2002). FSP1-positive cells appear during kidney fibrosis and in IgA nephropathy; increased expression of FSP1 correlates with the prognosis and extent of fibrosis (Nishitani et al., 2005). The ablation of FSP1 cells attenuates fibrosis and collagen deposition, indicating a causal role for these cells in fibrotic disease (Iwano et al., 2001). Kidney FSP1-positive cells derive from two sources; from the bone marrow and from an EMT at sites of renal fibrosis (Iwano et al., 2002). Inactivation of FSP1 with a LacZ "knock in" mouse produced fibroblasts that were less motile in wound healing assays and had impaired angiogenesis in an aortic ring outgrowth model. Neilson also introduced studies on the FSP1 promoter and reported the identification a new zinc finger protein, fibroblast transcription factor 1, which binds in the FSP1 promoter. Fibroblast transcription factor 1 also up-regulates Twist and Snail1 and suppresses β-catenin, E-cadherin, and ZO-1 during EMT, indicating that it may be a key regulator of the EMT transcriptome.

Raghu Kalluri (Harvard University, Boston, MA) introduced the novel concept of endothelial–mesenchymal transition, which is probably an important process in TGF-β1–mediated cardiac fibrosis. Kalluri also reported that an inhibitor of TGF-β signaling, bone-morphogenic protein 7 (BMP7), could inhibit cardiac fibrosis in two mouse models of this disease. BMP7 belongs to the BMP family of TGF-β growth factors, and has a specific role as a morphogen during liver development. Kalluri also discussed the functional interconnection between EMT and angiogenesis, suggesting that angiogenesis inhibition could be therapeutic for fibrosis as well as cancer. Michael Zeisberg (Harvard University, Boston, MA) reported that BMP7 can inhibit fibroblast migration and prevent fibrotic disease in mouse models of liver fibrosis.

Emerging concepts and future directions of EMT

The detection of EMT in vivo during disease progression in adult organisms remains one of the central challenges of EMT physiology. Pioneering work by Iwano et al. (2002) established that fibrosis involves EMT, and this approach has been extended to include the formation of metastatic tumor cells (Xue et al., 2003). Evidence of EMT markers at the leading edge of invading tumors was provided by Bates (integrin αvβ6), Garcia de Herreros (using a new Snail1 antibody), and Brabletz (nuclear β-catenin), and these new findings were some of the highlights of the meeting, strongly suggesting an important role for EMT in driving tumor invasion and metastasis.

Because it is now possible to visualize the movement and morphology of individual tumor cells in real-time in a living animal (Condeelis and Segall, 2003), the examination of EMT in real-time is a possibility for the future. The detailed molecular studies of many investigators at the EMT meetings will hopefully provide additional markers for this task (Table I). These markers may allow further investigation into the role of metastability in cancer. Metastability indicates the existence of cells with features of both epithelial and mesenchymal cells. This concept is consistent with the sequential steps of junctional dissolution that were described by Thiery (Thiery and Huang, 2005) and is gaining momentum through the accumulation of evidence in favor of such hybrid states. The predominantly epithelial, yet somewhat mesenchymal, phenotype of highly aggressive and metastatic bladder cancer cells presented by Chaffer reinforces the potential of many cancer cells for plastic differentiation. In addition, Savagner showed evidence of both epithelial and mesenchymal patterning of Rac in epithelial cells that were induced to migrate. The importance of MET or other partial loss of mesenchymal markers in the successful growth of metastases could add further opportunities for therapies that block metastases. The possibility that softer boundaries exist between epithelial and mesenchymal tumor cells and the possibility of hybrid cells may help explain the current lack of robust clinical evidence for EMT as a metastasis mediator (Tarin et al., 2005).

Most importantly, the meeting witnessed the emergence of EMT as a target for drug development in cancer and fibrosis. For example, BMP7 mimetics antagonize TGF-β–driven EMT in fibrotic kidney and heart and inhibit disease development. In addition, small molecule ILK inhibitors inhibit Snail1 production, induce E-cadherin expression, and inhibit invasion. Also discussed at the meeting was the possibility that angiogenesis, EMT, fibrosis, and cancer have common regulatory pathways and that the angiogenesis inhibition may be useful in both fibrosis and cancer. The involvement of ILK in angiogenesis, EMT, fibrosis, and cancer suggest that ILK inhibition may be one useful therapy. In addition, EMT could be used as a functional screen for novel anticancer agents, a strategy that led to the identification of motuporamine (Calvin Roskelley). Motuporamine was derived from a library of marine invertebrate compounds and inhibits in vitro invasion and migration by activating the Rho GTPase and stimulating actin stress fiber formation. Continued identification of new EMT inhibitors holds the promise of novel cancer and fibrosis treatment options.

We anticipate considerable progress in this field in the year leading up to the 2007 EMT meeting, which is planned to take place in Montpellier, France (http://www.mtci.com.au/temtia.html), building on the current exponential trend of EMT observations in numerous cellular systems of physiological and pathophysiological importance.

References

Barrallo-Gimeno, A., and M.A. Nieto. 2005. The Snail genes as inducers of cell movement and survival: implications in development and cancer. *Development*. 132:3151–3161.

Bates, R.C. 2005. Colorectal cancer progression: integrin alphavbeta6 and the epithelial-mesenchymal transition (EMT). *Cell Cycle*. 4:1350–1352.

Bissell, M.J., D. Farson, and A.S. Tung. 1977. Cell shape and hexose transport in normal and virus-transformed cells in culture. *J. Supramol. Struct.* 6:1–12.

Brabletz, T., A. Jung, S. Reu, M. Porzner, F. Hlubek, L.A. Kunz-Schughart, R. Knuechel, and T. Kirchner. 2001. Variable beta-catenin expression in colorectal cancers indicates tumor progression driven by the tumor environment. *Proc. Natl. Acad. Sci. USA*. 98:10356–10361.

Brabletz, T., A. Jung, S. Spaderna, F. Hlubek, and T. Kirchner. 2005. Opinion: migrating cancer stem cells - an integrated concept of malignant tumour progression. *Nat. Rev. Cancer*. 5:744–749.

Brembeck, F.H., T. Schwarz-Romond, J. Bakkers, S. Wilhelm, M. Hammerschmidt, and W. Birchmeier. 2004. Essential role of BCL9-2 in the switch between beta-catenin's adhesive and transcriptional functions. *Genes Dev.* 18:2225–2230.

Burridge, K., and K. Wennerberg. 2004. Rho and Rac take center stage. *Cell*. 116:167–179.

Carlsson, P., and M. Mahlapuu. 2002. Forkhead transcription factors: key players in development and metabolism. *Dev. Biol.* 250:1–23.

Castanon, I., and M.K. Baylies. 2002. A Twist in fate: evolutionary comparison of Twist structure and function. *Gene*. 287:11–22.

Cavallaro, U., and G. Christofori. 2004. Cell adhesion and signalling by cadherins and Ig-CAMs in cancer. *Nat. Rev. Cancer*. 4:118–132.

Chen, C.S., M. Mrksich, S. Huang, G.M. Whitesides, and D.E. Ingber. 1997. Geometric control of cell life and death. *Science*. 276:1425–1428.

Chu, Y.S., O. Eder, W.A. Thomas, I. Simcha, F. Pincet, A. Ben-Ze'ev, E. Perez, J.P. Thiery, and S. Dufour. 2005. Prototypical type-I E-cadherin and type-II cadherin-7 mediate very distinct adhesiveness through their extracellular domain. *J. Biol. Chem.* 281:365–373.

Chu, Y.S., W.A. Thomas, O. Eder, F. Pincet, E. Perez, J.P. Thiery, and S. Dufour. 2004. Force measurements in E-cadherin–mediated cell doublets reveal rapid adhesion strengthened by actin cytoskeleton remodeling through Rac and Cdc42. *J. Cell Biol.* 167:1183–1194.

Condeelis, J., and J.E. Segall. 2003. Intravital imaging of cell movement in tumours. *Nat. Rev. Cancer*. 3:921–930.

De Craene, B., B. Gilbert, C. Stove, E. Bruyneel, F. van Roy, and G. Berx. 2005. The transcription factor snail induces tumor cell invasion through modulation of the epithelial cell differentiation program. *Cancer Res.* 65:6237–6244.

De Robertis, E.M., O. Wessely, M. Oelgeschlager, B. Brizuela, E. Pera, J. Larrain, J. Abreu, and D. Bachiller. 2001. Molecular mechanisms of cell–cell signaling by the Spemann-Mangold organizer. *Int. J. Dev. Biol.* 45:189–197.

Dominguez, D., B. Montserrat-Sentis, A. Virgos-Soler, S. Guaita, J. Grueso, M. Porta, I. Puig, J. Baulida, C. Franci, and A. Garcia de Herreros. 2003. Phosphorylation regulates the subcellular location and activity of the snail transcriptional repressor. *Mol. Cell. Biol.* 23:5078–5089.

Ezratty, E.J., M.A. Partridge, and G.G. Gundersen. 2005. Microtubule-induced focal adhesion disassembly is mediated by dynamin and focal adhesion kinase. *Nat. Cell Biol.* 7:581–590.

Folkman, J., and A. Moscona. 1978. Role of cell shape in growth control. *Nature*. 273:345–349.

Fujita, N., D.L. Jaye, M. Kajita, C. Geigerman, C.S. Moreno, and P.A. Wade. 2003. MTA3, a Mi-2/NuRD complex subunit, regulates an invasive growth pathway in breast cancer. *Cell*. 113:207–219.

Giri, D.K., M. Ali-Seyed, L.Y. Li, D.F. Lee, P. Ling, G. Bartholomeusz, S.C. Wang, and M.C. Hung. 2005. Endosomal transport of ErbB-2: mechanism for nuclear entry of the cell surface receptor. *Mol. Cell. Biol.* 25:11005–11018.

Gumbiner, B.M. 2005. Regulation of cadherin-mediated adhesion in morphogenesis. *Nat. Rev. Mol. Cell Biol.* 6:622–634.

Hay, E.D. 2005. The mesenchymal cell, its role in the embryo, and the remarkable signaling mechanisms that create it. *Dev. Dyn.* 233:706–720.

Huang, X., and J.P. Saint-Jeannet. 2004. Induction of the neural crest and the opportunities of life on the edge. *Dev. Biol.* 275:1–11.

Iwano, M., A. Fischer, H. Okada, D. Plieth, C. Xue, T.M. Danoff, and E.G. Neilson. 2001. Conditional abatement of tissue fibrosis using nucleoside analogs to selectively corrupt DNA replication in transgenic fibroblasts. *Mol. Ther.* 3:149–159.

Iwano, M., D. Plieth, T.M. Danoff, C. Xue, H. Okada, and E.G. Neilson. 2002. Evidence that fibroblasts derive from epithelium during tissue fibrosis. *J. Clin. Invest.* 110:341–350.

Kalluri, R., and E.G. Neilson. 2003. Epithelial-mesenchymal transition and its implications for fibrosis. *J. Clin. Invest.* 112:1776–1784.

Kim, M.Y., T. Zhang, and W.L. Kraus. 2005. Poly(ADP-ribosyl)ation by PARP-1: 'PAR-laying' NAD+ into a nuclear signal. *Genes Dev.* 19:1951–1967.

Lo, H.W., S.C. Hsu, M. Ali-Seyed, M. Gunduz, W. Xia, Y. Wei, G. Bartholomeusz, J.Y. Shih, and M.C. Hung. 2005a. Nuclear interaction of EGFR and STAT3 in the activation of the iNOS/NO pathway. *Cancer Cell*. 7:575–589.

Lo, H.W., W. Xia, Y. Wei, M. Ali-Seyed, S.F. Huang, and M.C. Hung. 2005b. Novel prognostic value of nuclear epidermal growth factor receptor in breast cancer. *Cancer Res.* 65:338–348.

Lochter, A., A. Srebrow, C.J. Sympson, N. Terracio, Z. Werb, and M.J. Bissell. 1997. Misregulation of stromelysin-1 expression in mouse mammary tumor cells accompanies acquisition of stromelysin-1-dependent invasive properties. *J. Biol. Chem.* 272:5007–5015.

Masszi, A., L. Fan, L. Rosivall, C.A. McCulloch, O.D. Rotstein, I. Mucsi, and A. Kapus. 2004. Integrity of cell–cell contacts is a critical regulator of TGF-beta 1-induced epithelial-to-myofibroblast transition: role for beta-catenin. *Am. J. Pathol.* 165:1955–1967.

Moody, S.E., D. Perez, T.C. Pan, C.J. Sarkisian, C.P. Portocarrero, C.J. Sterner, K.L. Notorfrancesco, R.D. Cardiff, and L.A. Chodosh. 2005. The transcriptional repressor Snail promotes mammary tumor recurrence. *Cancer Cell*. 8:197–209.

Nawshad, A., D. Lagamba, A. Polad, and E.D. Hay. 2005. Transforming growth factor-beta signaling during epithelial-mesenchymal transformation: implications for embryogenesis and tumor metastasis. *Cells Tissues Organs*. 179:11–23.

Neilson, E.G. 2005. Setting a trap for tissue fibrosis. *Nat. Med.* 11:373–374.

Newgreen, D.F., and S.J. McKeown. 2005. Neural crest cells migration. *In* Rise and Fall of Epithelial Phenotype: Concepts of Epithelial-Mesenchymal Transition. P. Savagner, editor. Landes Bioscience, Texas. 29–39.

Nishitani, Y., M. Iwano, Y. Yamaguchi, K. Harada, K. Nakatani, Y. Akai, T. Nishino, H. Shiiki, M. Kanauchi, Y. Saito, and E.G. Neilson. 2005. Fibroblast-specific protein 1 is a specific prognostic marker for renal survival in patients with IgAN. *Kidney Int.* 68:1078–1085.

Paszek, M.J., N. Zahir, K.R. Johnson, J.N. Lakins, G.I. Rozenberg, A. Gefen, C.A. Reinhart-King, S.S. Margulies, M. Dembo, D. Boettiger, et al. 2005. Tensional homeostasis and the malignant phenotype. *Cancer Cell*. 8:241–254.

Radice, G.L., M.C. Ferreira-Cornwell, S.D. Robinson, H. Rayburn, L.A. Chodosh, M. Takeichi, and R.O. Hynes. 1997. Precocious mammary gland development in P-cadherin–deficient mice. *J. Cell Biol.* 139:1025–1032.

Radisky, D.C., D.D. Levy, L.E. Littlepage, H. Liu, C.M. Nelson, J.E. Fata, D. Leake, E.L. Godden, D.G. Albertson, M.A. Nieto, et al. 2005. Rac1b and reactive oxygen species mediate MMP-3-induced EMT and genomic instability. *Nature*. 436:123–127.

Rosivatz, E., K.F. Becker, E. Kremmer, C. Schott, K. Blechschmidt, H. Hofler, and M. Sarbia. 2005. Expression and nuclear localization of Snail, an E-cadherin repressor, in adenocarcinomas of the upper gastrointestinal tract. *Virchows Arch.* 17:1–11.

Shook, D., and R. Keller. 2003. Mechanisms, mechanics and function of epithelial-mesenchymal transitions in early development. *Mech. Dev.* 120:1351–1383.

Somasiri, A., J.S. Nielsen, N. Makretsov, M.L. McCoy, L. Prentice, C.B. Gilks, S.K. Chia, K.A. Gelmon, D.B. Kershaw, D.G. Huntsman, et al. 2004. Overexpression of the anti-adhesin podocalyxin is an independent predictor of breast cancer progression. *Cancer Res.* 64:5068–5073.

Sternlicht, M.D., A. Lochter, C.J. Sympson, B. Huey, J.P. Rougier, J.W. Gray, D. Pinkel, M.J. Bissell, and Z. Werb. 1999. The stromal proteinase MMP3/stromelysin-1 promotes mammary carcinogenesis. *Cell*. 98:137–146.

Tarin, D., E.W. Thompson, and D.F. Newgreen. 2005. The fallacy of epithelial mesenchymal transition in neoplasia. *Cancer Res.* 65:5996–6000.

Thiery, J.P. 2002. Epithelial-mesenchymal transitions in tumour progression. *Nat. Rev. Cancer.* 2:442–454.

Thiery, J.P., and R. Huang. 2005. Linking epithelial-mesenchymal transition to the well-known polarity protein Par6. *Dev. Cell.* 8:456–458.

Thompson, E.W., D.F. Newgreen, and D. Tarin. 2005. Carcinoma invasion and metastasis: a role for epithelial-mesenchymal transition? *Cancer Res.* 65:5991–5995.

Thomson, S., E. Buck, F. Petti, G. Griffin, E. Brown, N. Ramnarine, K.K. Iwata, N. Gibson, and J.D. Haley. 2005. Epithelial to mesenchymal transition is a determinant of sensitivity of non-small-cell lung carcinoma cell lines and xenografts to epidermal growth factor receptor inhibition. *Cancer Res.* 65:9455–9462.

van Es, J.H., N. Barker, and H. Clevers. 2003. You Wnt some, you lose some: oncogenes in the Wnt signaling pathway. *Curr. Opin. Genet. Dev.* 13:28–33.

Wang, Z., D. Shen, D.W. Parsons, A. Bardelli, J. Sager, S. Szabo, J. Ptak, N. Silliman, B.A. Peters, M.S. van der Heijden, et al. 2004. Mutational analysis of the tyrosine phosphatome in colorectal cancers. *Science.* 304:1164–1166.

Weaver, V.M., S. Lelievre, J.N. Lakins, M.A. Chrenek, J.C. Jones, F. Giancotti, Z. Werb, and M.J. Bissell. 2002. beta4 integrin-dependent formation of polarized three-dimensional architecture confers resistance to apoptosis in normal and malignant mammary epithelium. *Cancer Cell.* 2:205–216.

Willipinski-Stapelfeldt, B., S. Riethdorf, V. Assmann, U. Woelfle, T. Rau, G. Sauter, J. Heukeshoven, and K. Pantel. 2005. Changes in cytoskeletal protein composition indicative of an epithelial-mesenchymal transition in human micrometastatic and primary breast carcinoma cells. *Clin. Cancer Res.* 11:8006–8014.

Xue, C., D. Plieth, C. Venkov, C. Xu, and E.G. Neilson. 2003. The gatekeeper effect of epithelial-mesenchymal transition regulates the frequency of breast cancer metastasis. *Cancer Res.* 63:3386–3394.

Yang, J., S.A. Mani, J.L. Donaher, S. Ramaswamy, R.A. Itzykson, C. Come, P. Savagner, I. Gitelman, A. Richardson, and R.A. Weinberg. 2004. Twist, a master regulator of morphogenesis, plays an essential role in tumor metastasis. *Cell.* 117:927–939.

Zavadil, J., and E.P. Bottinger. 2005. TGF-beta and epithelial-to-mesenchymal transitions. *Oncogene.* 24:5764–5774.

Zavadil, J., L. Cermak, N. Soto-Nieves, and E.P. Bottinger. 2004. Integration of TGF-beta/Smad and Jagged1/Notch signalling in epithelial-to-mesenchymal transition. *EMBO J.* 23:1155–1165.

Zhou, B.P., J. Deng, W. Xia, J. Xu, Y.M. Li, M. Gunduz, and M.C. Hung. 2004. Dual regulation of Snail by GSK-3beta-mediated phosphorylation in control of epithelial-mesenchymal transition. *Nat. Cell Biol.* 6:931–940.

Expression of protein elongation factor eEF1A2 predicts favorable outcome in breast cancer

Geeta Kulkarni · Dmitry A. Turbin · Anahita Amiri · Sujeeve Jeganathan · Miguel A. Andrade-Navarro · Thomas D. Wu · David G. Huntsman · Jonathan M. Lee

Abstract Breast cancer is the most common malignancy among North American women. The identification of factors that predict outcome is key to individualized disease management and to our understanding of breast oncogenesis. We have analyzed mRNA expression of protein elongation factor eEF1A2 in two independent breast tumor populations of size $n = 345$ and $n = 88$, respectively. We find that eEF1A2 mRNA is expressed at a low level in normal breast epithelium but is detectably expressed in approximately 50–60% of primary human breast tumors. We have derived an eEF1A2-specific antibody and measured eEF1A2 protein expression in a sample of 438 primary breast tumors annotated with 20-year survival data. We find that high levels of eEF1A2 protein are detected in 60% of primary breast tumors independent of HER-2 protein expression, tumor size, lymph node status, and estrogen receptor (ER) expression. Importantly, we find that high eEF1A2 is a significant predictor of outcome. Women whose tumor has high eEF1A2 protein expression have an increased probability of 20-year survival compared to those women whose tumor does not express substantial eEF1A2. In addition, eEF1A2 protein expression predicts increased survival probability in those breast cancer patients whose tumor is HER-2 negative or who have lymph node involvement.

Geeta Kulkarni and Dmitry A. Turbin contribute equally to the work

G. Kulkarni · A. Amiri · S. Jeganathan · J. M. Lee (✉)
Department of Biochemistry, Microbiology and Immunology, University of Ottawa, 451 Smyth Road, K1H 8M5 Ottawa, ON, Canada
e-mail: jlee@uottawa.ca

D. A. Turbin · D. G. Huntsman
Genetic Pathology Evaluation Centre of the Department of Pathology and Prostate Research Centre at the Vancouver General Hospital, British Columbia Cancer Agency and University of British Columbia, Vancouver, BC, Canada

M. A. Andrade-Navarro
Department of Cellular and Molecular Medicine, University of Ottawa and the Ottawa Health Research Institute, Ottawa, ON, Canada

T. D. Wu
Department of Bioinformatics, Genentech, South San Francisco, CA, USA

Introduction

Despite early screening programs and new treatment options, an estimated 45,000 North American women will die of breast cancer in 2005 because their tumor recurred after surgery and chemotherapy. The best current predictors of tumor recurrence are lymph node involvement and tumor size [1]. Lack of estrogen receptor (ER) and high expression of the HER-2 receptor tyrosine kinase in the primary tumor are also reliable markers of increased recurrence risk [1]. However, using conventional histo-pathological methods, we can accurately predict recurrence likelihood for only about 1/3 of breast cancer patients [2]. Large-scale analysis of gene expression patterns in breast tumors suggest that relapse is under the aggregate control of dozens of genes [3–5]. Aggregate gene expression patterns, termed gene signatures, can

be used to retrospectively predict chemotherapy response and survival probability [3–5]. The use of gene signatures to predict outcome is useful [6], but it does not lead to the identification of individual genes that regulate tumor recurrence or mechanistic understanding of relapse or to identifying novel therapy targets [7, 8].

We have previously reported that *EEF1A2*, the gene encoding protein elongation factor eEF1A2, is amplified and overexpressed in ~30% of ovarian tumors [9]. eEF1A2 is one of two members of the eEF1A family of proteins (eEF1A1 and eEF1A2) that bind amino-acylated tRNA and facilitate their recruitment to the ribosome during translation elongation [10]. eEF1A proteins have other functions not related to translation such as inducing actin and tubulin cytoskeleton rearrangements [11, 12]. The eEF1A1 and eEF1A2 isoforms share greater than 90% sequence identity but have different expression patterns: eEF1A1 is ubiquitously expressed while eEF1A2 is detectably expressed only in normal heart, brain and muscle [13]. Inactivation of the mouse eEF1A2 homolog, *Eef1a2*, leads to immunodeficiency and neural and muscular defects and death by 30 days of age [14, 15]. eEF1A2 has transforming properties: ectopic expression of wild-type eEF1A2 in mammalian cells enabled growth in an anchorage-independent manner and enhanced tumorigenicity in nude mice [9]. While eEF1A2 is likely to be important in ovarian cancer, it is not known whether eEF1A2 contributes to breast cancer or could be used as a prognostic marker.

In this report we find that eEF1A2 mRNA and protein are highly expressed in 50–60% of primary human breast tumors and metastases but not in normal breast epithelium. Importantly, we find that high eEF1A2 protein expression in the primary tumor is associated with a significantly increased 20-year survival. Our data suggests that there is a relationship between the oncogenic program induced by eEF1A2 and reduced aggressiveness of breast tumors.

Materials and methods

Cell lines, adenovirus and siRNA

Cell lines were obtained from the American Tissue Culture Collection (ATCC). For adenoviral infection, eEF1A2 was cloned into pShuttle-IRES (*EcoRV/XhoI*). The *EEF1A2*-directed siRNA is 5′-UCGAA-CUUCUCAAUGGUCCTT-3′. siPORT Lipid (Ambion) was used for siRNA transfection according to the manufacturer's instructions.
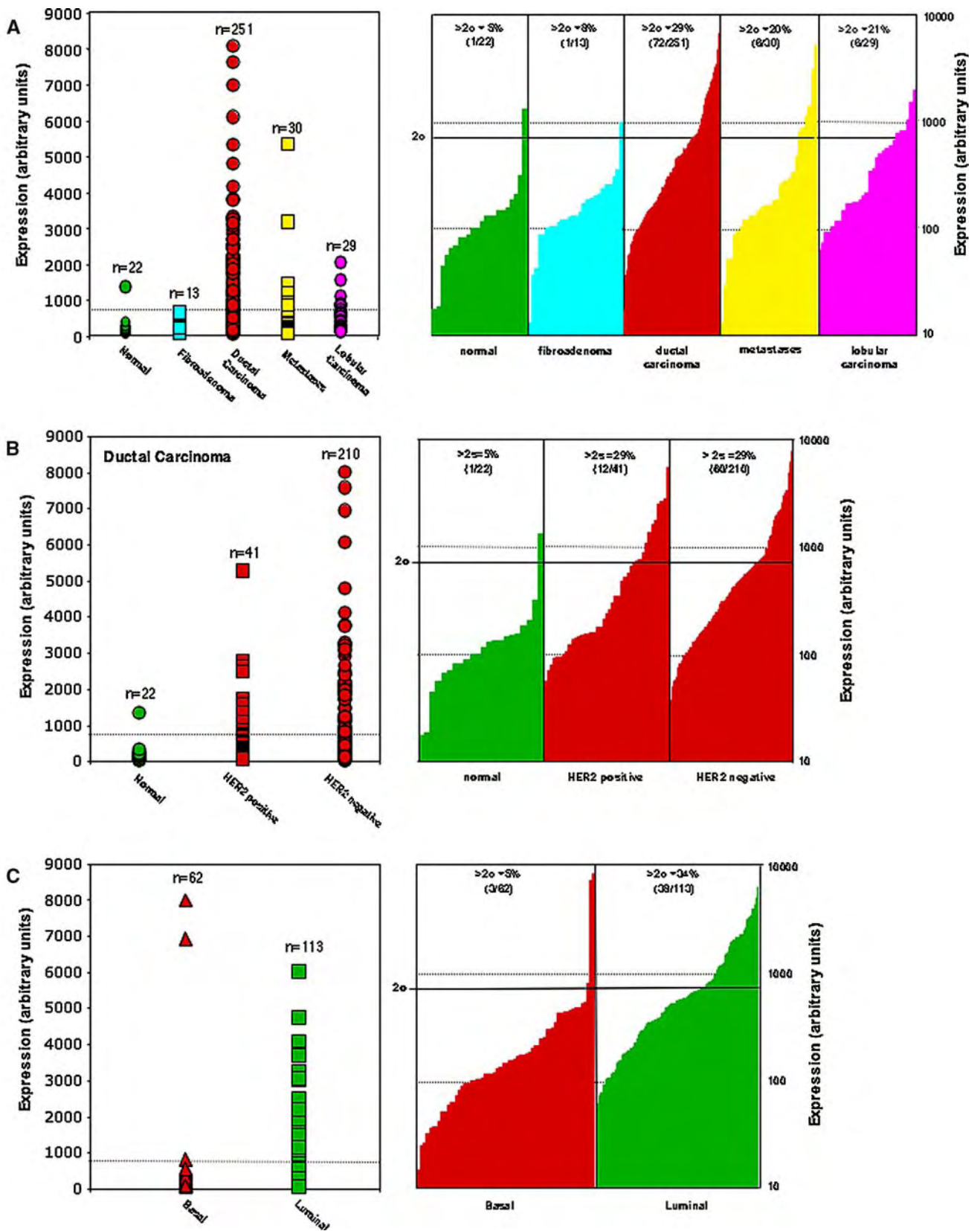
Gene expression analysis

eEF1A2 gene expression data in Fig. 1 was extracted from the GeneExpress database from GeneLogic (Gaithersburg, MD) for probe set 204540_at on the HG-U133A GeneChip from Affymetrix (Santa Clara, CA). Microarray data values were generated by the MAS5 signal algorithm. Data were extracted for samples available as of February 2003. HER-2 gene expression was assessed using the expression of probe set 216836_s_at and a threshold of 8,000 in the signal value. eEF1A2 gene expression data in Fig. 2 were obtained from Huang et al. [3].

Derivation of an eEF1A2 antibody, Western blotting and immunoprecipitation

The KVERKEGNASGVSLLEALDT immunogen was injected into rabbits and sera collected after boost (Cedarlane Laboratories). eEF1A2 peptide was coupled to an Affi-Gel 10 resin (Bio-Rad) according to the manufacturer's instructions and purified as described [16]. Cells were lysed in RIPA buffer (50 mM Tris–Cl; pH 7.4, 1% Triton X-100, 1% sodium deoxycholate, 0.1% SDS, 1 mM EDTA; pH 7.0, 150 mM NaCl, 1% aprotonin, 1 mg/ml leupeptin, 50 mM NAF, 1 mM Na_3VO_4, 10 μg/ml pepstatin, 1 mM PMSF in DMSO). Protein quantification was performed by Bradford protein assay (Bio-Rad), electrophoresed and transferred onto PVDF membranes (Perkin–Elmer). Membranes were blocked in 5% skim milk, 5% BSA, TBST for 2 h RT and eEF1A2 antibody (1:3,000) added overnight. Membranes were washed 3×TBST and HRP goat anti-rabbit added (Upstate) at 1:3,000 added for one hour at room temperature and washed 3×TBST. The membranes were developed using ECL-plus (Western Lightning, Perkin Elmer). α-actin antibody (Sigma) at a 1:12,000 dilution and then HRP conjugated anti-mouse antibody (Upstate) at a 1:5,000 dilution. Immunoprecipitation for the Flag protein was performed by using the anti-Flag M2 affinity gel (Sigma). Two hundred and fifty micrograms of cell lysates were used.

Expression and purification of recombinant eEF1A proteins

eEF1A2 and eEF1A1 cDNA were cloned into *EcoRI/NotI* of pGEX-4T2 (Pharmacia). GST-eEF1A2 and GST-eEF1A1 were transformed into *E coli* BL21 DE3 and grown in LBA to A_{600} ~0.7. 0.5 mM IPTG added for 2 h at 25°C. Bacteria were lysed in 25 mM HEPES; pH 7.9, 100 mM KCl, 2 mM EDTA, 20% glycerol,

2 mM DTT, and protease inhibitor cocktail (Roche). Glutathione Sepharose 4B beads (Amersham Bioscience) were equilibrated in lysis buffer and mixed with sonicated suspensions.

Case selection and tissue microarray (TMA) construction

The study included 438 patients with primary invasive breast carcinoma that underwent surgery between 1974 and 1995 at Vancouver General Hospital. Institutional review board approval was obtained to perform this study (Vancouver General Hospital, Vancouver, BC, Canada). Clinical follow-up was available for all the patients, with median follow-up time 15.4 years. The median age of the patients at diagnosis was 61.5 years, minimum 28.2, and maximum 93.5. The only criterion for including the patients into the study was presence of invasive breast carcinoma. No randomization was performed. Our cohort was heterogeneous in terms of treatment protocols. Thirty-four women underwent biopsy, 2 wide excision, 95 partial or segmental mastectomy, 202 modified radical mastectomy, 40 total mastectomy. Information on chemotherapy or radiotherapy protocols was not available. Formalin-fixed, paraffin embedded primary invasive breast cancer tissue blocks were used to construct tissue microarrays as described previously [31, 32].

Immunocytochemistry and immunohistochemistry

BT549 and MCF7 cells were fixed using 10% neutral-buffered formalin and paraffin embedded. Sections were deparaffinized by automated machine and microwaved for antigen retrieval. The sections were further treated with 3% H_2O_2 in TBS (pH 7.6) for 10 min. Sections were rinsed in TBS for 5 min and blocked in 4% BSA, 10% Sucrose, 1% (v/v) normal swine serum

in TBS) for 1 h at room temperature. eEF1A2 antibody diluted 1:10–1:50 in TBS, 10% sucrose,1% BSA, 0.01% sodium azide in TBS was added overnight at 4°C. Sections were then rinsed 3× TBS, incubated with secondary diluted 1:200 in 3% BSA for 1 hour RT (Amersham Biosciences; #NA934) and washed 3×TBS. Diaminobenzidine (DAB, DAKO Corporation, CA, USA) and 30% H_2O_2 (1:4) were added for 10 min and rinsed under tap water for 5 min.

Immunostaining of TMA sections was performed on a Ventana Discovery Instrument (Ventana Medical Systems, Tucson, Arizona) using DAB Map Kit (HRP labeled Biotin-Streptavidin System). The staining included the following steps: deparaffinization, heat induced antigen retrieval with EDTA pH 8.0 (24 min), hydrogen peroxide quenching 3% H_2O_2 (8 min), eEF1A2 antibody at 1:100 dilution (32 min), biotinylated universal secondary antibody (32 min), streptavidin–biotin peroxidase complex (16 min), DAB (8 min), counterstain with hematoxylin (4 min).

Assessment of eEF1A2 protein expression

Bacus Laboratories Inc. Slide Scanner (BLISS) (Bacus Laboratories, Inc, Lombard, IL) was used to digitize the images of tissue cores, as described previously [33, 34]. WebSlide Browser v.3.98 (Bacus Laboratories, Inc, Lombard, IL) was used for viewing preview images of the arrays and assessment of individual core images. H&E slides cut from the same array were scanned together with immunohistochemical ones, and used as a reference to determine the correspondence of the protein expression to specific structures of breast carcinoma. The images were placed into a web site-based relational database along with identification information and scores for each core. The database is publicly accessible through http://www.gpecimage.ubc.ca/tma/web/viewer.php for reviewing and rescoring of the images.

Scoring of eEF1A2 immunostaining was performed semiquantitatively, using digital images and 22-inch monitor with hardware color calibration capabilities. Protein expression pattern in tumor tissue was diffuse in most cases. Staining was scored as negative (0) if no staining was present in the cytoplasm of the tumor cells, and weak (1+), moderate (2+) and strong (3+), depending on the intensity of staining in the cytoplasm. Scores were entered into a standardized Excel worksheet (Microsoft Excel, Microsoft, Redmond, WA) with a sector map matching each TMA section. Scores for the duplicate cores were consolidated to a single value per case using an Excel macro developed by DT. The higher value was accepted for the case if there

were discrepant scores for the duplicate cores. Cases were marked as missing in the statistical analysis if there were no interpretable data, i.e. if there was no tumor tissue in the cores or the cores were cut through. Original scoring tables were deconvoluted together with core identification file using Deconvoluter 1.10 [35], and the resulting table files imported into SPSS 11.0 for Windows (SPSS Inc., Chicago, IL).

Statistical analysis of TMA

Statistical analysis was performed in SPSS 13.0 for Windows. Univariate analysis of survival was carried out by using Kaplan–Meier survival curves and log-rank statistics to test for significant differences between curves. Multivariate analysis was performed using a proportional hazards model. We used two-tailed Spearman's correlation to assess the relationship between the expression of eEF1A2 and other markers. All tests were two-sided and used a 5% alpha level to determine significance.

Results

eEF1A2 mRNA expression is elevated in human breast tumor tissue independent of HER2

To determine whether eEF1A2 was involved in breast cancer, we analyzed eEF1A2 mRNA expression in human breast tissue derived from normal and tumor samples ($n = 345$). We hypothesized that a role for eEF1A2 in breast oncogenesis could be inferred from high tumor-specific gene expression, an approach used to identify other candidate oncogenes [6]. eEF1A2 expression was measured using hybridization to an Affymetrix HG-U133A DNA microarray (Fig. 1A). eEF1A2 expression was very low in normal breast epithelium ($n = 22$) and in fibroadenomas ($n = 13$). However, approximately 30% of ductal carcinomas (73/251), lobular carcinomas (10/30) and breast tumor metastases (10/29) had eEF1A2 expression greater than 2σ above the normal tissue expression mean (a signal value of 697). This high eEF1A2 expression implicates eEF1A2 as a breast cancer oncogene.

Approximately 10–30% of breast tumors have high expression of the HER-2 receptor tyrosine kinase due to amplification of the *HER-2* gene [17, 18]. We next examined whether eEF1A2 expression correlated with HER-2 expression in the ductal carcinomas (Fig. 1B). HER-2 positive ($n = 41$) and HER-2 negative ($n = 210$) ductal carcinomas had a similar fraction of tumors with eEF1A2 expression above normal and the distribution of eEF1A2 expression between populations was not significantly different by Kolmogorov–Smirnov ($p < 0.39$) analysis. This suggests that any role of eEF1A2 in breast oncogenesis is HER-2 independent.

Using gene expression profiling, breast tumors can broadly divided into two groups: basal-like and luminal-like [19]. To determine whether eEF1A2 was differently expressed in these tumor subtypes, we next
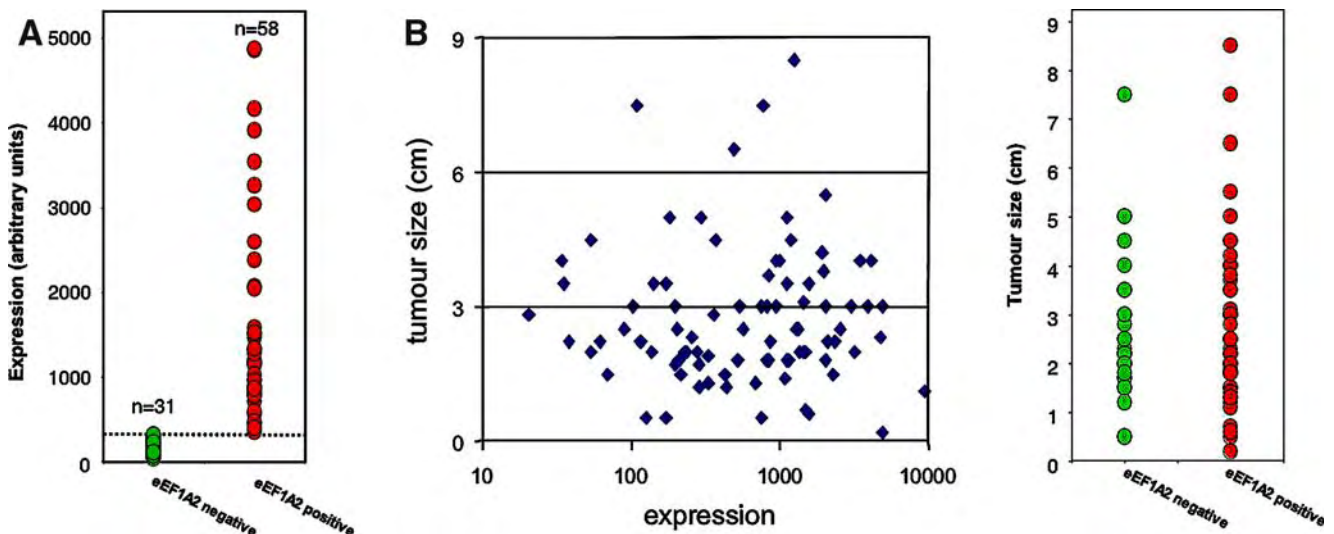

Fig. 2 eEF1A2 expression does not correlate with tumor size. (A) Value of eEF1A2 expression in eEF1A2 positive (red circle) and negative (green circle) breast tumors. The horizontal line indicates the 2σ value above the mean of the distribution of eEF1A2 expression value in the eEF1A2 negative group. (B) Tumor size plotted as a function of eEF1A2 expression (left panel). Tumor size in the eEF1A2 positive (red circle) and negative (green circle) groups (right panel)

measured eEF1A2 expression in basal and luminal types. Tumors were segregated based on the reported 50-gene classifier [20]. As shown in Fig. 1C, eEF1A2 is expressed almost exclusively in the luminal tumors. Of the 62 basal tumors, only three (5%) had a mean eEF1A2 expression above the 2σ normal while 38/113 (34%) of the luminal tumors were above this mark. Mean eEF1A2 expression in the basal tumors was 430 ± 1319 compared to 911 ± 1085 in the luminal ones; expression in the two populations is significantly different by Student's t-test ($p < 0.01$). eEF1A2 is not part of the gene expression profile used to classify the luminal and basal types, but the luminal expression pattern of eEF1A2 suggests its involvement in the luminal tumor phenotype.

To extend this analysis, we analyzed eEF1A2 expression in a publicly available breast tumor expression dataset [3]. This dataset contained expression profiles from 89 primary breast tumors. Using the Affymetrix software (MAS5.0) respective call for eEF1A2 presence or absence/marginal, these tumors can be divided into eEF1A2 negative and positive groups. Of these 89 samples, 58 (65%) are in the in eEF1A2 positive group and 31 (35%) in the negative group. Mean expression in the eEF1A2 negative population was 145 ± 86 (arbitrary units) while that of the positive population was 1609 ± 1224 (Fig. 2A). All tumors in the positive population had an expression value greater than 2σ above the expression mean of the negative population; eEF1A2 expression in the two populations was different by Student's t-test ($p < 0.0001$). Tumor size did not differ substantially between the groups (Fig. 2B; negative: 2.8 ± 1.5 cm, positive: 2.9 ± 1.6 cm). Furthermore, there was no significant correlation between eEF1A2 mRNA expression and ER, progesterone receptor (PR) or lymph node status (not shown).

Derivation of an eEF1A2 antibody

We next derived an antibody against eEF1A2 to determine the relationship between eEF1A2 protein and breast cancer. We used a synthetic peptide corresponding to human eEF1A2 residues 215–233 as an immunogen. eEF1A2 is one of two highly related proteins: eEF1A1 and eEF1A2. Residues 215–233 were used as an immunogen because of the differences between it and the corresponding eEF1A1 sequence (KVTRKDGNASGTTLLEALDC, differences underlined). To test the antiserum generated, we first identified eEF1A2 mRNA expression in a panel of human breast cancer cell lines (Fig. 3a). eEF1A2 expression is detected in MCF7 cells but not BT549. Skeletal muscle

mRNA is used as a positive control. As shown in Fig 3b, our eEF1A2 antibody did not detect protein in BT549 cells but did detect a band of approximately 50 kDa in BT549 cells infected with an eEF1A2 adenovirus. The predicted molecular weight of eEF1A2 is 54 kDa. Similarly, the eEF1A2 antibody recognized a band of ~50 kDa in MCF7 cells and the intensity of this band is reduced in the presence of an eEF1A2 siRNA. The antibody also recognizes GST-eEF1A2 and not GST alone or GST-eEF1A1 (Fig. 3c). Furthermore, Fig. 3d shows that the antiserum detects Flag-tagged eEF1A2 immunoprecipitated from BT549 cells infected with an eEF1A2 adenovirus. Finally, the antiserum stains fixed and paraffin-embedded MCF7 cells and not BT549 cells (Fig. 3e). The staining pattern in MCF7 cells is diffusely cytoplasmic, consistent with the previously reported staining pattern of epitope-tagged eEF1A2 [9]. The magnitude of eEF1A2 staining in MCF7 cells is substantially reduced by treating MCF7 cells with eEF1A2 siRNA. Taken together, this indicates that our eEF1A2 antiserum is specifically recognizing eEF1A2.

eEF1A2 protein expression in breast carcinoma

We next used our antiserum to determine whether eEF1A2 protein expression could be used as a breast cancer prognostic marker. We used a tissue microarray (TMA) of 438 samples. There were 380 interpretable cases out of 438 used for building the array. Fifty eight cases were excluded from the statistical analysis due to either absence of tumor tissue in both cores representing a case, drop-off of the cores from the slides, or cut-through of the cores. The patterns of staining were classified in four levels by visual examination: negative, weak, moderate and strong. Weak staining was seen in 76 cases (20.0%), moderate in 177 (46.6%), and strong in 79 (20.8%) cases; 48 tumors (12.6%) showed no expression of the protein. Representative photomicrographs of different levels of eEF1A2 immunostaining are shown as Fig. 4, together with corresponding H&E staining. All tissue core images can be viewed at https://www.gpecimage.ubc.ca/tma/web/viewer.php.

Analysis of eEF1A2 protein expression on TMA

To determine prognostic significance of eEF1A2 in invasive breast carcinoma, we performed univariate Kaplan–Meier analysis of the survival data associated to the 438 cases. Moderate or strong immunostaining in the breast carcinoma TMA was associated with significantly better survival compared to negative or weak

Fig. 3 Derivation of an eEF1A2 antibody. (**a**) eEF1A2 mRNA expression, measured by northern blot in breast cancer cell lines. RNA staining of the membrane in the lower panel served as a loading control. (**b**) *Left panel*. The eEF1A2 antiserum detects an ~50 kDa band, indicated by an arrow, in Western blots of BT549 cells infected with an eEF1A2 adenovirus but not in the GFP infected control. Both viruses were used at an MOI of 200. *Right panel* A ~50 kDa band is detected in MCF7 cells and the intensity of this band is reduced after transfection of an eEF1A2 siRNA. The control MCF7 has been transfected with a scrambled siRNA. (**c**) The eEF1A2 antiserum detects GST-eEF1A2 (upper arrow) and not GST or GST-eEf1A1 proteins. An MCF7 lysate is used as a positive control fro wild-type eEF1A2 (lower arrow) (**d**) The eEF1A2 antiserum detects eEF1A2 immunoprecipated from BT549 cells infected with an eEf1A2 adenovirus. A whole cell lysate from the infected cells is also shown. (**e**) The eEf1A2 antiserum stains of MCF 7 cells and the intensity of staining is reduced using an eEF1A2 siRNA. The antiserum does not stain BT549 cells
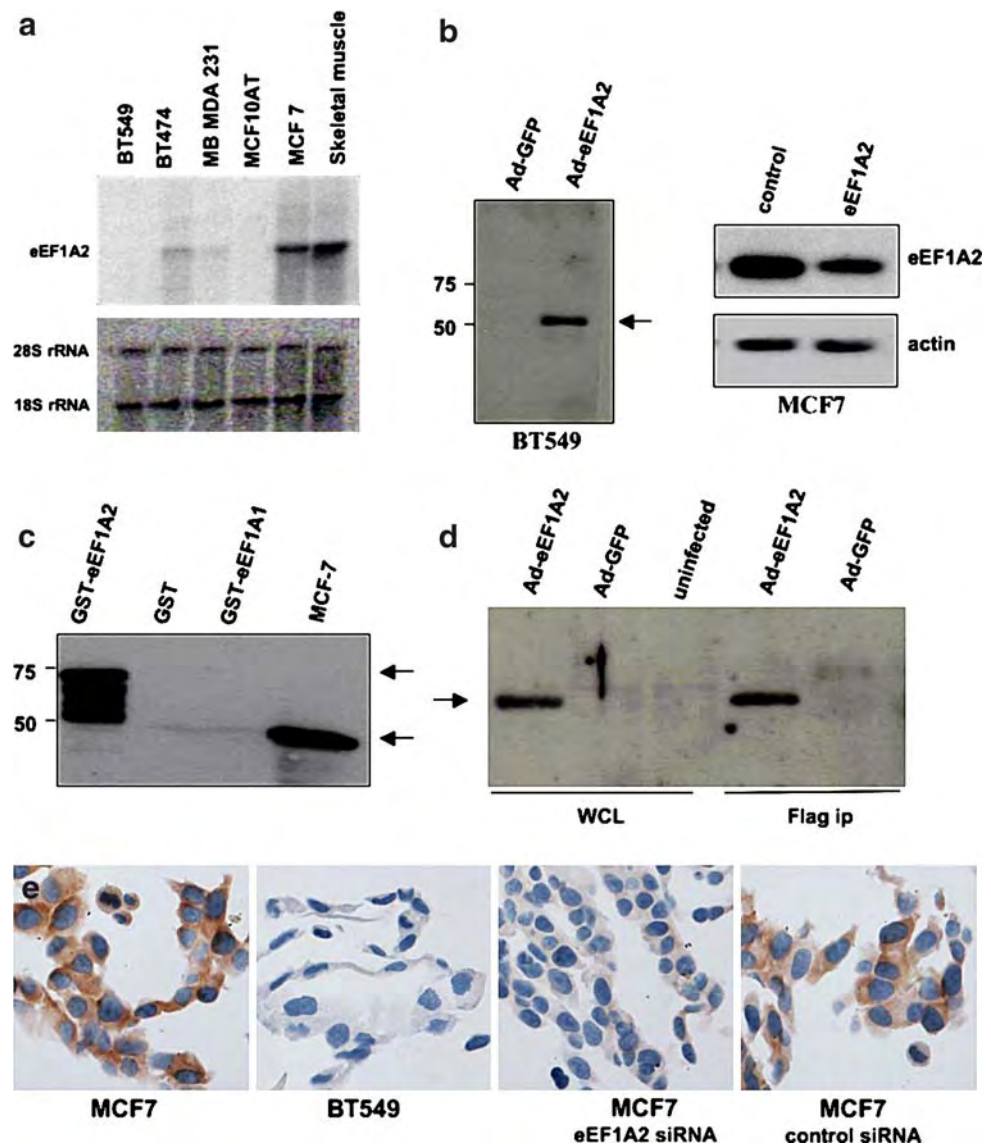
staining ($p = 0.005$, Fig. 5a) in the full cohort of patients. Twenty-year cumulative survival in the moderate or strong staining group was ~75% compared to ~55% in the low to negative group.

To further extend this analysis, we determined the prognostic significance of eEF1A2 protein expression in patients depending on the lymph node status, ER and HER2/neu positivity. Moderate to high expression of the protein remained a good prognostic marker in the subset of the patients with regional lymph node metastases ($p = 0.02$, Fig. 5b), and in the patients with tumors negative for HER2/neu ($p = 0.02$, Fig. 5b). eEF1A2 protein immunostaining was not a significant prognostic marker in node-negative ($p = 0.2$) or in HER2/neu-positive ($p = 0.1$) patients, as well as in the separate subsets of ER-negative or positive cases ($p = 0.1$ and $p = 0.08$, respectively).

eEF1A2 protein expression showed weak but significant negative correlation with p53 and Ki67 ($p = 0.04$ and $p = 0.008$, respectively; Table 1). No significant correlation was observed between eEF1A2 immunostaining and Nottingham grade, nodal status, estrogen and progesterone receptor, and HER2/neu status (Table 1). Negative correlation of eEF1A2 with the well-known proliferation markers supports the idea of favorable prognostic significance of this biomarker.

Multivariate analysis in a Cox model with eEF1A2, tumor grade, tumor size and nodal status in the equation shows that eEF1A2 loses statistical significance for survival in this model ($p = 0.073$, HR = 0.65). eEF1A2 expression was not significant also in the Cox regression model with grade, tumor size, nodal status, and ER and Her2/neu expression added ($p = 0.52$, HR = 0.82), and in the model with ER, Her2/neu,

Fig. 4 eEF1A2 staining in the breast tumor microarray. Examples of eEF1A2 immunostaining in breast carcinoma TMA. H&E staining (left column) of a representative negative, weak, moderate and strong eEF1A2 immuno-staining tumor (centre column). Rightmost column is a higher magnification view of the boxed square in the centre column
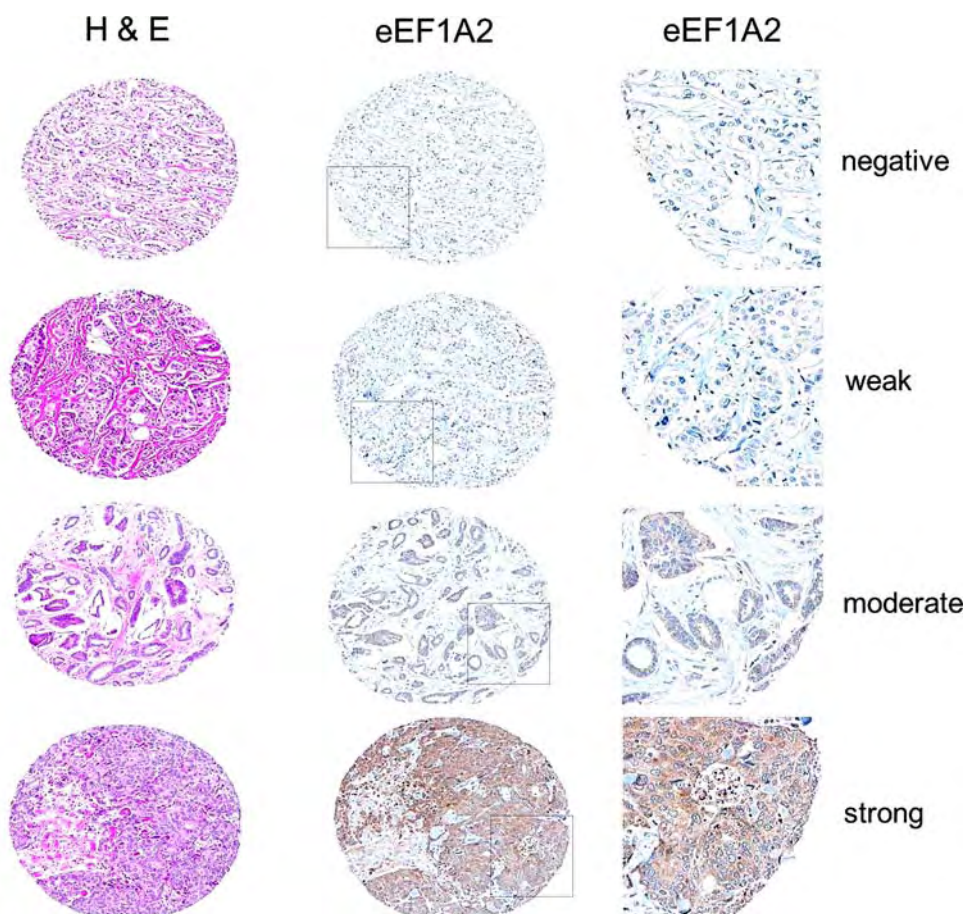
Ki67, and p53 ($p = 0.535$, HR = 0.84). These data suggest that eEF1A2 while eEF1A2 is a prognostic marker in breast cancer, it is less powerful than other well-known clinical and immunohistochemical factors.

Discussion

In this report, we have determined that high protein and mRNA expression of protein elongation factor eEF1A2 occurs in ~60% of primary human breast tumors. In humans, eEF1A2 is expressed only in normal tissue of the brain, heart and skeletal muscle [13]. Consistent with this observation, we find that eEF1A2 mRNA is poorly detected in normal breast epithelium. We have previously reported that eEF1A2 has transforming properties and can enhance focus formation in rodent fibroblasts, allow growth in soft agar and enhance the tumorigenicity of mouse and human cells in nude mice [9]. The specific up-regulation of eEF1A2 in breast tumors and its transforming potential indicate that it is causally involvement in breast tumorigenesis.

We have further determined that eEF1A2 expression is a useful breast cancer prognostic marker. We find that eEF1A2 protein expression is associated with significantly increased probability of 20-year survival. Patients whose breast tumor has moderate or strong eEF1A2 staining had a 20-year cumulative survival of ~75% compared to ~55% in the eEF1A2 low to negative group. At the current time, the best markers for prognosis are ER status, lymph node involvement, tumor size, expression of the Her2/neu receptor tyrosine kinase [2, 21]. However, these four markers only accurately predict outcome for ~30% of breast cancer patients. For example, approximately one third of women who are lymph node positive remain disease-free for 10 years and one third of women who are lymph node negative will have a disease recurrence [2, 21]. The accurate prediction of breast cancer outcome therefore requires the identification and validation of additional markers. Our data indicates that eEF1A2 is one such a marker. Furthermore, moderate to high eEF1A2 expression predicted good prognosis for patients whose tumors had no lymph node involvement or were negative for Her2/neu. Thus, eEF1A2 will have further use in predicting outcome in these specific breast cancer populations.
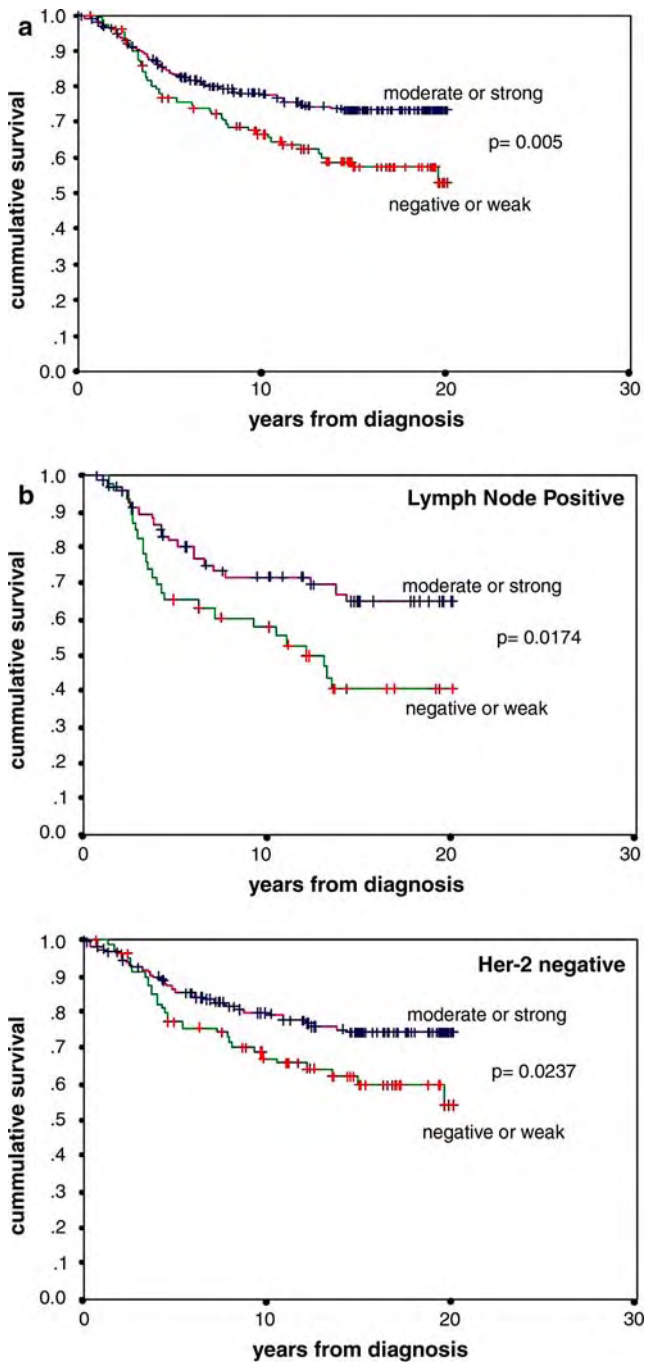
Fig. 5 eEF1A2 expression is associated with increased 20-year survival probability. (**a**) Disease-specific survival comparison for the patients with negative or weak expression of eEF1A2 compared to those with moderate to strong expression. Cumulative survival probability is plotted as a function of years following diagnosis. The difference is significant at $p = 0.005$. (**b**) Disease-specific survival comparison for the patients with negative or weak expression of eEF1A2 compared to those with moderate to strong expression in lymph node positive (upper panel) or Her-2 (lower panel) tumors. In node-positive and her-2 negative patients, eEF1A2 expression is a significant prognostic indicator ($p = 0.02$ for both)

Based on gene expression patterns, breast tumors can be classified into two broad groups: luminal-like and basal-like [19]. Luminal and basal tumors are so named because of their respective keratin expression pattern mirrors that of the basal and luminal cells of the normal mammary epithelium [22]. The luminal/basal division of tumors roughly corresponds to ER status, with luminal tumors generally being ER+ while the basal ones are usually ER– [19, 20, 23]. Patients with basal tumors have a generally poorer prognosis than those with luminal ones, and basal tumors are much more likely to be p53+ compared to their luminal counterparts [19, 20, 23]. eEF1A2 is not one of the genes used to discriminate luminal tumors from basal ones, but we observe high eEF1A2 mRNA expression almost exclusively in luminal tumors. The lack of strong correlation between eEF1A2 and ER expression suggests that eEF1A2 may mark a specific subset of ER– luminal tumors. There are three luminal subtypes (A, B, C) based on gene expression patterns and it is plausible that eEF1A2 may mark one of these [23]. The luminal-expression pattern of eEF1A2 further strengthens our observation that eEF1A2 is a marker for good prognosis.

Gene expression studies indicate that breast cancer outcome is under the control of dozens of genes, groups of which are commonly upregulated or downregulated in the tumor [3–5]. While these gene groups, termed gene signatures [6], have been used in retrospective studies to predict long-term survival, difficulties in using gene expression profiling in routine clinical practice make it simpler to identify new prognostic markers using immunostaining. Of particular importance will be to identify markers have an expression pattern that is independent of other markers. We find that eEF1A2 protein expression in breast tumors does not correlate with Her2/neu, tumor grade, size, nodal status, or ER or progesterone receptor status. We find a very weak, albeit statistically significant, inverse correlation between eEF1A2 expression and p53 and Ki67. The lack of striking correlation between eEF1A2 and other breast cancer prognostic markers indicates that eEF1A2 is an independent prognostic marker as well as a novel one [19, 20, 23].

Since we have previously described eEF1A2 as a strongly transforming gene [9], it is surprising that its high expression is associated with good prognosis. This suggests that high expression of eEF1A2 can enhance transformation and tumorigenesis in breast cells, but some facet of the oncogenic program activated by eEF1A2 or that eEF1A2 is part of, is less malignant than that of other oncogenes such as Her-2/neu. For example, eEF1A2 may not activate an effective metastatic program or induce effective angiogenesis.

Table 1 Correlation of eEF1A2 protein expression with Nottingham grade, nodal status, and other biomarkers

	Correlation coefficient (Spearman's ρ)	p Value (two-tailed)	Number of valid cases
Grade	0.062	0.268	323
Nodal status	–0.093	0.089	333
Estrogen receptor	0.031	0.610	274
Progesterone receptor	0.005	0.935	306
HER2/neu	–0.046	0.432	290
P53	–0.129	0.035	267
Ki67	–0.159	0.008	280

Understanding the mechanism by which eEF1A2 activates tumorigenesis will be necessary to understand why its expression is associated with good prognosis. The small but negative correlation that we have observed between eEF1A2 and Ki67 suggest that eEF1A2 is unlikely to be associated with increased mitotic index, suggesting that eEF1A2 drives oncogenesis through a pathway not obligately tied to enhanced proliferation [24]. However, the mechanism(s) by which eEF1A2 induces tumor formation remains an open one. eEF1A2 is a protein elongation factor and recruits amino-acylated tRNA to the ribosome during the elongation phase of translation [10]. eEF1A2 could therefore enhance tumorigenesis by upregulating the translation of proteins having a direct role in cell growth control or tumorigenesis [25]. The eIF4E protein initiation factor seems to function in this manner and ectopic eIF4E can increase the abundance of several proteins that upregulate cell growth and angiogenesis, among them c-Myc, cyclin D1, VEGF and FGF-2 [26]. Our observation that Her2/neu and ER expression is independent of eEF1A2 expression suggests that eEF1A2-activated oncogenesis is unlikely to involve Her2/neu or ER. It is possible that eEF1A2 may enhance oncogenesis independent of its function in translation. The eEF1As protein binds to actin and can regulate actin and tubulin polymerization [11]. eEF1A proteins have also been reported to activate phosphotidyl-inositol-4-kinase [27] and to be important in ubiquitination [28]. eEF1A2 may regulate tumorigenesis through these processes.

EEF1A2, the gene encoding eEF1A2, maps to 20q13.3 [29]. Genes in 20q13 are frequently amplified in breast cancer [30] and high-level amplification of 20q13 is associated with poor outcome [31]. In addition to *EEF1A2*, the 20q13 amplicon includes several genes that may have a causal relationship with cancer, including the ZNF217 transcription factor, the Aurora-A kinase, and the CYP24 [32]. Our observation that high eEF1A2 expression is associated with good prognosis suggests a complex interplay of oncogenic pathways regulated by 20q13 genes.

In summary, we have identified eEF1A2 as a novel breast cancer oncogene by virtue of its overexpression.

eEF1A2 is likely to be a useful prognostic marker for good outcome. Our current study has been retrospective in nature and the further utility of eEF1A2 in breast cancer prognosis will require prospective analysis of eEF1A2 in breast cancer.

References

1. Cianfrocca M, Goldstein LJ (2004) Prognostic and predictive factors in early-stage breast cancer. Oncologist 9(6):606–616
2. Weigelt B, Peterse JL, van't Veer LJ (2005) Breast cancer metastasis: markers and models. Nat Rev Cancer 5(8):591–602
3. Huang E, Cheng SH, Dressman H, Pittman J, Tsou MH, Horng CF, Bild A, Iversen ES, Liao M, Chen CM et al (2003) Gene expression predictors of breast cancer outcomes. Lancet 361(9369):1590–1596
4. West M, Blanchette C, Dressman H, Huang E, Ishida S, Spang R, Zuzan H, Olson JA Jr, Marks JR, Nevins JR (2001) Predicting the clinical status of human breast cancer by using gene expression profiles. Proc Natl Acad Sci USA 98(20):11462–11467
5. van't Veer LJ, Dai H, van de Vijver MJ, He YD, Hart AA, Mao M, Peterse HL, van der Kooy K, Marton MJ, Witteveen AT et al (2002) Gene expression profiling predicts clinical outcome of breast cancer. Nature 415(6871):530–536
6. Wu TD (2001) Analysing gene expression data from DNA microarrays to identify candidate genes. J Pathol 195(1):53–65
7. Debouck C, Goodfellow PN (1999) DNA microarrays in drug discovery and development. Nat Genet 21(Suppl 1):48–50
8. Marton MJ, DeRisi JL, Bennett HA, Iyer VR, Meyer MR, Roberts CJ, Stoughton R, Burchard J, Slade D, Dai H et al (1998) Drug target validation and identification of secondary drug target effects using DNA microarrays. Nat Med 4(11):1293–1301

9. Anand N, Murthy S, Amann G, Wernick M, Porter LA, Cukier IH, Collins C, Gray JW, Diebold J, Demetrick DJ et al (2002) Protein elongation factor EEF1A2 is a putative oncogene in ovarian cancer. Nat Genet 31(3):301–305

10. Hershey JW (1991) Translational control in mammalian cells. Annu Rev Biochem 60:717–755

11. Condeelis J (1995) Elongation factor 1 alpha, translation and the cytoskeleton. Trends Biochem Sci 20(5):169–170

12. Shiina N, Gotoh Y, Kubomura N, Iwamatsu A, Nishida E (1994) Microtubule severing by elongation factor 1 alpha. Science 266(5183):282–285

13. Knudsen SM, Frydenberg J, Clark BF, Leffers H (1993) Tissue-dependent variation in the expression of elongation factor-1 alpha isoforms: isolation and characterisation of a cDNA encoding a novel variant of human elongation-factor 1 alpha. Eur J Biochem 215(3):549–554

14. Shultz LD, Sweet HO, Davisson MT, Coman DR (1982) 'Wasted', a new mutant of the mouse with abnormalities characteristic to ataxia telangiectasia. Nature 297(5865):402–404

15. Chambers DM, Peters J, Abbott CM (1998) The lethal mutation of the mouse wasted (wst) is a deletion that abolishes expression of a tissue-specific isoform of translation elongation factor 1 alpha, encoded by the Eef1a2 gene. Proc Natl Acad Sci USA 5(8):4463–4468

16. www.bio.com

17. Wiseman SM, Makretsov N, Nielsen TO, Gilks B, Yorida E, Cheang M, Turbin D, Gelmon K, Huntsman DG (2005) Coexpression of the type 1 growth factor receptor family members HER-1, HER-2, and HER-3 has a synergistic negative prognostic effect on breast carcinoma survival. Cancer 103(9):1770–1777

18. Slamon DJ, Clark GM, Wong SG, Levin WJ, Ullrich A, McGuire WL (1987) Human breast cancer: correlation of relapse and survival with amplification of the HER-2/neu oncogene. Science 235(4785):177–182

19. Perou CM, Sorlie T, Eisen MB, van de Rijn M, Jeffrey SS, Rees CA, Pollack JR, Ross DT, Johnsen H, Akslen LA et al (2000) Molecular portraits of human breast tumours. Nature 406(6797):747–752

20. Sorlie T, Perou CM, Tibshirani R, Aas T, Geisler S, Johnsen H, Hastie T, Eisen MB, van de Rijn M, Jeffrey SS et al (2001) Gene expression patterns of breast carcinomas distinguish tumor subclasses with clinical implications. Proc Natl Acad Sci USA 98(19):10869–10874

21. Gradishar WJ (2005) The future of breast cancer: the role of prognostic factors. Breast Cancer Res Treat 89(Suppl 1):S17–26

22. Birnbaum D, Bertucci F, Ginestier C, Tagett R, Jacquemier J, Charafe-Jauffret E (2004) Basal and luminal breast cancers: basic or luminous? (review). Int J Oncol 25(2):249–258

23. Sorlie T, Tibshirani R, Parker J, Hastie T, Marron JS, Nobel A, Deng S, Johnsen H, Pesich R, Geisler S et al (2003) Repeated observation of breast tumor subtypes in independent gene expression data sets. Proc Natl Acad Sci USA 100(14):8418–8423

24. van Diest PJ, van der Wall E, Baak JP (2004) Prognostic value of proliferation in invasive breast cancer: a review. J Clin Pathol 57(7):675–681

25. Thornton S, Anand N, Purcell D, Lee J (2003) Not just for housekeeping protein initiation and elongation factors in cell growth and tumorigenesis. J Mol Med 81(9):536–548

26. De Benedetti A, Harris AL (1999) eIF4E expression in tumors: its possible role in progression of malignancies. Int J Biochem Cell Biol 31(1):59–72

27. Yang W, Burkhart W, Cavallius J, Merrick WC, Boss WF (1993) Purification and characterization of a phosphatidylinositol 4-kinase activator in carrot cells. J Biol Chem 268(1):392–398

28. Gonen H, Smith CE, Siegel NR, Kahana C, Merrick WC, Chakraburtty K, Schwartz AL, Ciechanover A (1994) Protein synthesis elongation factor EF-1 alpha is essential for ubiquitin-dependent degradation of certain N alpha-acetylated proteins and may be substituted for by the bacterial elongation factor EF-Tu. Proc Natl Acad Sci USA 91(16):7648–7652

29. Lund A, Knudsen SM, Vissing H, Clark B, Tommerup N (1996) Assignment of human elongation factor 1alpha genes: EEF1A maps to chromosome 6q14 and EEF1A2 to 20q13.3. Genomics 36(2):359–361

30. Stebbins CE, Russo AA, Schneider C, Rosen N, Hartl FU, Pavletich NP (1997) Crystal structure of an Hsp90-geldanamycin complex targeting of a protein chaperone by an antitumor agent. Cell 89(2):239–250

31. Tanner MM, Tirkkonen M, Kallioniemi A, Holli K, Collins C, Kowbel D, Gray JW, Kallioniemi OP, Isola J (1995) Amplification of chromosomal region 20q13 in invasive breast cancer: prognostic implications. Clin Cancer Res 1(12):1455–1461

32. Lee JM (2003) The role of protein elongation factor eEF1A2 in ovarian cancer Reprod Biol Endocrinol 1:69

33. Ng TL, Gown AM, Barry TS, Cheang MC, Chan AK, Turbin DA, Hsu FD, West RB, Nielsen TO (2005) Nuclear beta-catenin in mesenchymal tumors. Mod Pathol 18:68–74

34. Turbin DA, Cheang MC, Bajdik CD, Gelmon KA, Yorida E, De Luca A, Nielsen TO, Huntsman DG, Gilks CB (2006) MDM2 protein expression is a negative prognostic marker in breast carcinoma. Mod Pathol 19:69–74

35. Liu CL, Prapong W, Natkunam Y, Alizadeh A, Montgomery K, Gilks CB, van de Rijn M (2002) Software tools for high-throughput analysis and archiving of immunohistochemistry staining data obtained with tissue microarrays. Am J Path 161(5):1557–1565

eEF1A2 activates Akt and stimulates Akt-dependent actin remodeling, invasion and migration.

Running title: eEF1A2 activates Akt and actin remodeling

Anahita Amiri, Farahnaz Noei, Sujeeve Jeganathan, Geeta Kulkarni, Dixie E. Pinke, & Jonathan M. Lee[*]

Department of Biochemistry, Microbiology and Immunology, University of Ottawa, 451 Smyth Road, Ottawa, Ontario, Canada. K1H 8M5.

[*]Address Correspondence to:
Dr. Jonathan Lee
Biochemistry, Microbiology, & Immunology
University of Ottawa
451 Smyth Road
Ottawa, Ontario
Canada K1H 8M5
jlee@uottawa.ca
Telephone: 613-562-5800 ext 8640
Facsimile: 613-562-5451

Abstract

eEF1A2 is a protein translation factor that is a likely human oncogene by virtue of its capacity to transform mammalian cells and its high expression in tumours of the ovary, breast and lung. Here, we show that expression of eEF1A2 is sufficient to stimulate the formation of filopodia in BT549 human breast cancer cells and non-transformed Rat2 cells. Filopodia formation in eEF1A2-expressing cells is dependent on the activity of phosphatidylinositol-3 kinase (PI3K), and the ROCK and Akt kinases. Furthermore, eEF1A2 expression is sufficient to activate Akt in a PI3K-dependent fashion and inactivation of eEF1A2 by siRNA reduces Akt activity. Using breast cancer cell line BT 549, we show that eEF1A2 expression stimulates cell migration and invasion in a largely PI3K and Akt dependent manner. These results suggest that eEF1A2 regulates oncogenesis through Akt and PI3K-dependent cytoskeletal remodeling.

Introduction

eEF1A2 (eukaryotic protein elongation factor 1 alpha 2) is one of two isoforms of protein elongation factor eEF1A (eEF1A1 and eEF1A2). eEF1A proteins are GTP-binding proteins that interact with amino-acylated tRNA and recruit them to the ribosome during the elongation phase of protein translation. The two human isoforms share > 90% identity and have essentially the same function during protein translation (Knudsen et al., 1993). eEF1A1 is expressed ubiquitously whereas mammalian eEF1A2 expression is limited to the heart, brain, and skeletal muscle (Kahns et al., 1998; Knudsen et al., 1993; Lee et al., 1993).

eEF1A2 is likely to be an important human oncogene (Lee, 2003). *EEF1A2*, the gene encoding eEF1A2, is amplified and its mRNA overexpressed in ~30% of primary human ovarian cancers (Anand et al., 2002). Expression of wild-type eEF1A2 transforms rodent fibroblasts and increases their tumorigenicity in nude mice (Anand et al., 2002). Amplification of *EEF1A2* and increased eEF1A2 mRNA and protein overexpression has also been reported in lung and breast tumours (Kulkarni et al., 2006; Tomlinson et al., 2005; Wang et al., 2004). In lung cancer, high expression of eEF1A2 correlates with increased Ki-67 expression and is associated with poor prognosis (Wang et al., 2004). Furthermore, eEF1A2 may also have a role in metastatic development and it is overexpressed in metastatic rat mammary adenocarcinoma cell lines relative to non-metastatic controls (Edmonds et al., 1996; Pencil et al., 1993). While these observations implicate eEF1A2 in oncogenesis, little is known about the molecular mechanisms by which eEF1A2 could enhance tumour development.

eEF1A proteins have cellular functions in addition to their canonical role in translation elongation. eEF1A from several species and genera binds to actin filaments and microtubules both *in vivo* and *in vitro* (Condeelis, 1995). Binding of *Dictyostelium* eEF1A to F-actin enhances actin bundling (Yang et al., 1990), suggestive of a role for eEF1A in actin cytoskeleton remodeling. Two C-terminal domains in the *Dictyostelium* eEF1A protein directly bind actin (Condeelis, 1995). These domains are distinct from sequences that bind GTP, tRNA or are responsible for GTP hydrolysis. *Saccharomyces cereviseae* has two eEF1A genes (*TEF1* and *TEF2*), both of which more closely resemble human eEF1A1 than eEF1A2 gene. *TEF1* proteins

that are deficient in actin bundling are competent in translation elongation, indicating that actin interaction and peptide elongation are independent functions of the protein (Gross & Kinzy, 2005). While ectopic *TEF1* or *TEF2* expression in *S. cereviseae* leads to a general disorganization of the actin cytoskeleton (Munshi et al., 2001), the effect that mammalian eEF1A2 expression has on the eukaryotic actin cytoskeleton has yet to be fully investigated.

eEF1A proteins have also been implicated in phosphatidylinositol (PI) signaling. PIs are negatively charged, low-abundant, membrane-bound phospholipids that serve as regulators of multiple signaling pathways (Carpenter & Cantley, 1990; Fruman et al., 1998; Meijer & Munnik, 2003; Overduin et al., 2001). An eEF1A-related protein, PIK-A49, has been purified from carrot cells based on an ability to increase the *in vitro* lipid kinase activity of phosphatidylinositol-4 Kinase (PI4K) (Yang et al., 1993). PI4 kinases catalyze the phosphorylation of the D4 carbon of the inositol ring (PI) (Heilmeyer et al., 2003). Phosphatidylinositol-4 phosphate (PI4P) is an obligate precursor of phosphatidylinositol-(4,5) biphosphate (PIP_2) and phosphatidylinositol-(3,4,5) triphosphate (PIP_3). PIP_3 is a lipid second messenger that activates diverse signaling pathways important in oncogenesis, among them activation of the Akt serine/threonine kinase (Vivanco & Sawyers, 2002). Akt directly and indirectly controls the activity of many oncogenic pathways, including proliferation, growth, apoptosis and actin filament remodeling (Qian et al., 2004; Vivanco & Sawyers, 2002). Recently eEF1A1 has been determined by mass spectroscopy to be a possible binding partner for Akt2 and ectopic eEF1A2 expression has been shown to increase Akt abundance (Lau et al., 2006). However functional aspects of eEF1A/Akt interaction remain unexplored.

In this report, we find that eEF1A2 is a novel activator of Akt. Akt activation by eEF1A2 is dependent on phosphatidylinositol-3 kinase (PI3K). Furthermore, eEF1A2 induces filopodia production in rodent and human cell lines and enhances cell invasion and migration in an Akt- and PI3K-dependent manner. This indicates an important role for eEF1A2 in controlling phosphatidylinositol signaling, actin remodeling and cell motility.

Results

eEF1A2 expression induces rearrangement of the actin cytoskeleton. To examine a role for eEF1A2 in actin remodeling, we ectopically expressed eEF1A2 in cell lines that normally do not express eEF1A2. As shown in Figure 1a, eEF1A2 protein is expressed in the MCF7 human breast adenocarcinoma line but is not detectable in the BT549 human breast ductal carcinoma cancer cell line nor the rat Rat2 non-transformed fibroblast line. eEF1A2 protein is also detectable in the rat ovarian epithelial ROSE 199 cell line (right panel fig 1a)(Adams & Auersperg, 1985). The eEF1A2 antibody used for this analysis recognizes an eEF1A2 epitope (KVERKEGNASGVSLLEALDT) that is identical between the rat and human eEF1A2 isoforms (Kulkarni et al., 2006). High expression level of eEF1A2 protein was detected in selected cell lines (Figure 1c). Cells infected with empty pLXSN or transfected with an empty pCDNA3.1 vector were used as controls.

To examine a role for eEF1A2 in controlling the actin cytoskeleton, we stained eEF1A2-expressing cells and controls with phalloidin. Control BT549 cells showed prominent actin stress fibers, a thin but recognizable lamellipodia, but very few filopodia-like structures (figure 2a). Filopodia are pencil-like bundles of parallel actin fibers that emerge from the cell lamellipod. Filopodia exist in many cell types and have a role in activating and sustaining cell migration (Carragher & Frame, 2004; Chodniewicz & Klemke, 2004). eEF1A2-expressing BT549 cells showed a dramatic increase in the number and length of filopodia-like structures emerging from the lamellipod (Figure 2a). These filopodia are > 10 μM in length. Filopodia in control BT549 cells, when present, were < 1μM. In many eEF1A2-expressing cells, the filopodia are not only greater in number but also exhibit branching as they project outward. Branched filopodia were not observed in any control BT549 cells. Filopodia structures in the eEF1A2 expressing cells are somewhat polarized, meaning that they are often longer and more branched at one side of the cell (Figure 2a). Increased filopodia number and length was observed in all eEF1A2-expressing BT549 clones, independent of whether they were made by retroviral infection or plasmid transfection. This indicates that observed eEF1A2-dependent actin remodeling is unlikely to be due to chance clonal variation. To further confirm that the increase in filopodia formation was dependent on eEF1A2, we inhibited eEF1A2 by adding eEF1A2

siRNA to eEF1A2-expressing BT549 cells. Using this siRNA, we are generally able to reduce the eEF1A2 level by ~90% relative to control siRNA (Figure 2b). Addition of eEF1A2 siRNA resulted in a reduction in filopodia formation relative to control siRNA (Figure 2c) .

To determine whether eEF1A2 could induce filopodia formation in other cell types, we next expressed eEF1A2 in non-transformed rodent Rat2 cells. Rat2 does not express detectable eEF1A2 protein (Figure 1a). Like BT549 cells, eEF1A2 expression activated the appearance of filopodia structures in Rat2 cells (Figure 2d). Filopodia were not observed in control Rat2 cells. No discernable alteration in lamellipodia or stress fibers was observed upon eEF1A2 expression. The ability of eEF1A2 to induce filopodia formation in both transformed (BT549) and non-transformed (Rat2) cell lines, indicates that eEF1A2's effect on actin remodeling is unlikely to be cell-line specific.

To further characterize eEF1A2-induced filopodia, we observed their formation by video time-lapse microscopy. As shown in Figure 3a, filopodia were visible by light microscopy only in eEF1A2 expressing cells. These filopodia protruded outward from the eEF1A2-expressing cell in the general direction of cell movement, indicating that they do not derive from cytoplasmic retraction (Figure 3a). To further study the filopodia structures, we stained eEF1A2-expressing BT549 cells with a VASP antibody and phalloidin (Figure 3b). VASP is a member of the Ena (*Drosophila* enabled)/ VASP (vasodilator-stimulated phosphoprotein) proteins, which are localized to focal adhesions, along stress fibers and at the tips of lamellipodia and many filopodia (Reinhard et al., 1992; Svitkina et al., 2003). VASP is a key player in the formation of filopodia. In eEF1A2 expressing cells, VASP was mostly detectable at the base of the filopodia and between and within the actin fibers.

eEF1A2-dependent actin reorganization requires phosphatidylinositol-3 kinase, Akt and ROCK activity. Phosphatidylinositol-3 kinase (PI3K) is involved in many cellular processes, including growth, survival and actin filament remodeling (Vivanco & Sawyers, 2002). To test the hypothesis that eEF1A2 may regulate filopodia through PI3K-dependent signaling, we added LY294002, a specific inhibitor of PI3K to eEF1A2-expressing cells and observed filopodia

formation. As shown in Figure 4a and 4b, addition of LY294002 reduced the size and number of filopodia structures in both Rat2 and BT549 cells. This reduction was dose-dependent: filopodia shorten to <5 uM in 10 μM LY294002 and branching is reduced in both Rat2 and BT549 cells. 20 μM LY294002 reduced filopodia number to wild type levels in both cells. LY294002 had no visible effect on lamellipodia or stress fibers. These observations indicate that PI3K activity is required for actin filament rearrangement induced by eEF1A2.

Because filopodia formation is dependent on PI3K, we next determined eEF1A2 could directly bind PI3K or was an activator of PI3K activity. To this end, we transiently expressed eEF1A2 in BT549 cells using an eEF1A2-adenovirus. As shown in Figure 4c, ectopically expressed eEF1A2 did non-co-immunoprecipitate with endogenous PI3K. Furthermore, eEF1A2 expression did not alter overall abundance of PI3K (Fig 4c) nor the activation status of PI3K (Figure 4d). PI3K activity was measured by phosphorylation of tyrosine 506 (Y506) the p85 subunit of PI3K, a marker for P13K activity (Chen et al., 2004).

A key target of PI3K is Akt. Akt is involved in many biological processes, among them proliferation, apoptosis and growth (Vivanco & Sawyers, 2002). It has also been shown that PI3K remodels actin filaments through the activation of Akt (Qian et al., 2004). To test whether Akt is also involved in filopodia formation by eEF1A2, we used API-2, a specific inhibitor of Akt (Yang et al., 2004) to eEF1A2-expressing cells. As shown in Figure 4e, addition of API-2 greatly reduced the formation of filopodia in eEF1A2-expressing BT549 cells, indicating that Akt is required for eEF1A2-dependent filopodia formation .

Recently, it has been shown that PI3K regulates filopodia dynamics through Akt and ROCK (Tornieri et al., 2006). ROCK kinase is a downstream effector of the RhoA GTPase (Riento & Ridley, 2003). To investigate whether Rho signaling has any role in the formation of filopodia by eEF1A2, we used ROCK inhibitor Y27632. As shown in Figure 4f, addition of Y27632 decreased the number and length of filopodia to the wild-type level in eEF1A2-expressing BT549 cells, suggesting the importance of ROCK kinase in the formation of filopodia by eEF1A2.

Expression of eEF1A2 is sufficient to activate Akt in a PI3K-dependent manner. Because filopodia production by eEF1A2 was, at least in part, dependent on Akt activity, we determined whether eEF1A2 might be involved in Akt activation. Akt is activated by its membrane translocation and phosphorylation at Thr 308 and Ser 473. Thus, phosphorylations of Thr 308 and Ser 473 serve as surrogate markers of Akt activation. To determine whether the expression of eEF1A2 has any effect on Akt activation, we transiently expressed eEF1A2 in BT549 cells using an eEF1A2-adenovirus and then used Western blotting to determine the phosphorylation status of Thr 308 and Ser 473. As shown in Figure 5a, infection of eEF1A2 increased phosphorylation of both Thr 308 and Ser 473 relative to GFP-infected cells. Moreover, BT549 cells that stably express eEF1A2 also showed increased levels of phosphorylation at both Thr (308) and Ser (473) sites relative to control cells (Figure 5b). We next used siRNA to inactivate eEF1A2 in MCF7 breast cancer cells. Endogenous eEF1A2 is readily detectable in wild-type MCF7 cells (Figure 1a). In these cells, EF1A2 siRNA reduced Akt phosphorylation somewhat (1.8 when normalized to actin). Inhibition of Akt activity was not complete, suggesting that while eEF1A2 has a physiological role in controlling Akt activity, there are likely to be eEF1A2-independent pathways of Akt activation. To determine whether Akt activation by eEF1A2 was dependent on PI3K activity, we treated eEF1A2-overexpressing BT549 cells with LY294002. As shown in Figure 5d, LY294002 inhibited the activation of Akt in a dose-dependent manner. However, addition of Rapamycin, an inhibitor of mTOR/Raptor complex, had no affect on Akt activation by eEF1A2 (Figure 5e). Taken together our results indicate that eEF1A2 is a functional regulator of Akt activity.

Expression of eEF1A2 increases cell migration. Filopodia structures are critical for cell migration and invasion (Chodniewicz & Klemke, 2004) and activation of Akt has previously been reported to increase cell migration and invasion (Arboleda et al., 2003). Enhanced formation of filopodia and Akt activation in eEF1A2-overexpressing cells suggests that eEF1A2 might be involved in both migration and invasion. To assess whether overexpression of eEF1A2 is sufficient to increase cell migration, we measured the migration of BT549 cells using transwell migration assays. As shown in Figure 6a, eEF1A2 expression significantly enhanced cell migration relative to control cells (Student's t-test, $p<0.05$). To determine whether PI3K activity is required for this increase in cell migration, we measured migration in the presence of

LY294002. As shown in Figure 6b, PI3K inhibition significantly reduced the extent of migration in eEF1A2 expressing cells (Student's t-test, $p<0.05$). However, the magnitude of this migration in the presence of 20 µM LY294002 was still higher than the control and increasing LY294002 dosage had no further inhibitory effect on migration but did cause cytotoxicity (data not shown). To investigate whether Akt has any effect on the cell migration by eEF1A2, we added Akt inhibitor, API-2, to the BT549 cells overexpressing eEF1A2. As in the case of LY294002 and wortmannin, addition of API-2 significantly reduced cell migration (student's t-test, $p<0.05$) but it did not completely abolish it to the same level as control cells (Figure 6c). Similarly, addition of wortmannin, another PI3K inhibitor, at the concentration of 10 nM significantly (Student's t-test, $p<0.05$) decreased the magnitude of cell migration in eEF1A2-expressing cells (Figure 6c).   These results suggest that activation of PI3K and Akt is important in eEF1A2-induced cell migration.

Expression of eEF1A2 is sufficient to increase cell invasion. To investigate a role for eEF1A2 in invasion we coated transwells with Matrigel to simulate the basal lamina. As shown in Figure 7, significantly (Student's t-test, $p<0.05$) more eEF1A2-expressing cells invaded through the matrix than control cells, suggesting that eEF1A2 is an enhancer of cell invasion. Furthermore, this enhanced invasion in eEF1A2-expressing cells was significantly (Student's t-test, $p<0.05$) inhibited by LY294002 and API-2, indicating a dependence of eEF1A2-induced invasion on PI3K and Akt activities (Figure 7a and 7b). However, like the case with eEF1A2-induced migration by LY294002/wortmannin or API-2 never completely reduced invasion to wild-type levels, suggesting the existence of PI3K-independent pathways through which eEF1A2 stimulates invasion and migration. Addition of mTOR/Raptor inhibitor, rapamycin, had no effect on either cell migration or invasion by eEF1A2, indicating that mTOR/Raptor pathway is not involved in these processes (Figures 6c and 7b).

Expression of eFF1A2 has no effect on spreading and adhesion. Cell adhesion and spreading are cellular processes that occur during cell migration. To determine whether eEF1A2 had any effect on cell spreading, we used video microscopy to observe the behavior of BT549 cells on fibronectin-coated plates. eEF1A2-expressing cells and controls were trypsinized, plated and observed for lamellipodia formation. As shown in Figure 8a, by 10 minutes, control cells begin

to form a visible lamellipod (arrow) and by 28 minutes have developed large lamellipodia. eEF1A2-expressing cells formed a lamellipod with similar kinetics, indicating that eEF1A2 expression is not affecting cell spreading, as measured by lamellipod formation. This result is consistent with our observation (Figure 2) that eEF1A2 does not affect lamellipodia appearance. To determine whether eEF1A2 affected cell adhesion, we trypsinized BT549 cells and added them to fibronectin-coated coverslips. At various times after cell addition, coverslips were washed and fixed to remove the unstably attached or detached cells and to observe cells that had strongly adhered to their growth substrate. The number of adhering cells therefore serves as an indirect measure of cell adhesion. As shown in Figure 8b, control and eEF1A2 expressing cells had similar adhesive parameters. Thus, eEF1A2 detectably affects neither cell spreading nor the kinetics of the adhesion process.

Discussion

eEF1A2, protein elongation factor eEF1A2, is likely to be an important oncogene (Thornton et al., 2003). eEF1A2 is highly expressed in 30-60% of tumors of the ovary, breast, and lung (Kulkarni et al., 2006; Lee, 2003; Li et al., 2005; Tomlinson et al., 2005). Wild-type eEF1A2 has transforming properties: it enhances focus formation, allows growth in soft agar, and increases the tumorigenicity of mouse and human cells in nude mice (Anand et al., 2002). However, the mechanism by which eEF1A2 induces oncogenesis is unclear. Here, we show that eEF1A2 activates the Akt serine/threonine kinase and stimulates actin remodeling that is dependent on PI3K, Akt and ROCK. eEF1A2 expression also makes cells more motile and invasive *in vitro*. We propose that eEF1A2 promotes tumour development through PI3K-dependent activation of Akt and an Akt-dependent increase in filopodia formation and motility.

eEF1A2 is one of two isoforms of eEF1A, eEF1A1 and eEF1A2. eEF1A proteins are relatively well conserved during evolution, and eEF1A homologues have been identified in yeast and *C. elegans*, among others. Beyond its role in translation, eEF1A has additional cellular functions. Interaction of eEF1A with the actin cytoskeleton was first demonstrated in *Dictyostelium* (Yang et al., 1990) and eEF1A proteins of several animal genera have been reported to bind F-actin and bundle them *in vitro* (Edmonds et al., 1996; Munshi et al., 2001; Yang et al., 1990). There are two *S. cerevisiae* eEF1A homologues (*TEF1*, *TEF2*); both are more related to eEF1A1 than eEF1A2. In the Tef1 protein, actin bundling and translation elongation are separable enzymatic activities because Tef1 point mutations that inhibit actin binding and bundling have no substantial effect on translation (Gross & Kinzy, 2005). The two functions are also physically separate on the eEF1A protein: two domains in the C terminus of eEF1A bind actin while the GTP binding, hydrolysis and tRNA interacting domains are found in the eEF1A N-terminus (Condeelis, 1995; Hershey, 1991). Ectopic expression of Tef1 or Tef2 proteins in *S. cereviseae* reduces the accumulation of F-actin structures at the bud (Munshi et al., 2001) but the effect of eEF1A on the actin cytoskeleton of mammalian cells has not been previously reported. We find that eEF1A2 expression increases the formation of filopodia structures in rodent and human cells. Filopodia are bundles of parallel actin that protrude outward from the cell membrane. Protrusive actin structures have an important role in driving cell migration and

invasion, particularly in metastatic tumour cells (Yamaguchi et al., 2005). Consistent with an involvement of filopodia in cell movement, we found that eEF1A2 causes cells to be more migratory and invasive *in vitro*.

The increased invasiveness of eEF1A2-expressing cells suggests that eEF1A2 might have a role in tumor metastasis. In fact, eEF1A has previously been reported to be overexpressed in metastatic rat mammary adenocarcinoma cell lines compared to non-metastatic ones (Edmonds et al., 1996; Pencil et al., 1993). Because metastatic development is the ultimate cause of death in cancer, the ability of eEF1A2 to increase migration predicts that eEF1A2 expression would be associated with poor prognosis. Consistent with this idea, lung cancer patients whose tumour have high levels of eEF1A2 have a reduced probability of survival compared to their non-eEF1A2 expressing counterparts (Li et al., 2005). In addition, high eEF1A2 expression is associated with severe tumor grades and metastasis in several cancer cell lines (Edmonds et al., 1996; Li et al., 2005; Pencil et al., 1993). We have recently determined the prognostic significance of eEF1A2 in breast cancer (Kulkarni et al., 2006). To our astonishment, we find that high eEF1A2 protein expression correlates with an increased probability of 20-year survival (Kulkarni et al., 2006). eEF1A2 expression is independent of other breast cancer prognostic factors. It is a surprise to us that expression of an Akt activator and an enhancer of cell migration correlates with enhanced survival probability. For example, expression of Snail, an inducer of cell migration, correlates with poor survival in breast cancer (Moody et al., 2005). Because of its transforming capacity and its high tumour-specific expression, eEF1A2 is likely to be promoting tumour growth in breast cells. However, we speculate that while eEF1A2 may activate several oncogenic processes (i.e. Akt activation and enhancing migration), it may be a less potent breast cancer oncogene than others. Alternatively, eEF1A2 may alter some malignant process that inhibits patient mortality. For example, a capacity for eEF1A2 to promote cell proliferation may make the tumour more susceptible to chemotherapy or eEF1A2 expression may drive tumour cells into a more differentiated and therefore less malignant state. Possibly, the enhancement of motility by eEF1A2 may preclude the successful colonization of metastatic sites because migratory cells that leave the primary tumour may be too motile to stably colonize secondary sites. The observation that eEF1A2 expression is a marker of good prognosis in breast (Kulkarni

et al., 2006) and a marker of poor prognosis in lung (Li et al., 2005). may reflect the different microenvironments and physiology of these two malignancies.

The PI3K and Akt pathway regulates many cellular processes, including cell adhesion, proliferation, survival, and cytoskeletal rearrangement (Vivanco & Sawyers, 2002). Our observation that eEF1A2 activates Akt suggests a plausible explanation for the capacity of eEF1A2 to transform cells *in vitro* and suggests that eEF1A2 promotes tumour development through Akt. Furthermore, we find that the capacity of eEF1A2 to stimulate cell migration is Akt dependent. Over-expression of Akt2 has been shown to increase invasion and metastasis in human breast and ovarian cancer cells in a PI3K-dependent manner (Arboleda et al., 2003). The mechanism by which eEF1A2 could activate Akt is unknown, although we speculate that phosphatidyl-inositol signaling is involved (see below). Akt2 has recently been identified as an interacting partner of eEF1A1 (Lau et al., 2006). It is therefore possible that binding of eEF1A1 or eEF1A2 to Akt may directly activate the kinase, although the biological significance of eEF1A1/Akt interaction has yet to be determined. It is also unknown whether eEF1A2 directly binds any Akt isoform. Chang and Wang, 2006 found that overexpression eEF1A2 in mouse NIH 3T3 fibroblast cells resulted in increase of the Akt level in these cells. However, we did not see any increase in steady state of Akt levels in BT 549 breast cancer cells or Rat2 cell. While a role for eEF1A2 in controlling Akt abundance is possible, eEF1A2 does not alter steady-state Akt levels in our hands.

We have found that induction of filopodia by eEF1A2 is dependent on PI3K, Akt, and ROCK signaling. The ability of eEF1A2 to activate migration and invasion in breast cancer cells *in vitro* is largely, but not completely, PI3K-dependent. Therefore, eEF1A2 is likely to be involved in both PI3K-dependent and independent pathways that control filopodia formation and cell migration and invasion. Overexpression of PI3K has been shown to cause an increase of both lamellipodia and filopodia formation in chicken embryo fibroblast cells as well as a decrease of actin stress fibers (Qian et al., 2004). Akt has been postulated to modulate actin remodeling through two substrates: Girdin (Enomoto et al., 2005) and Pak1 (Zhou et al., 2003). Girdin is an actin bundling protein (Enomoto et al., 2005) and Pak1 is a member of the PAK (p21-activated kinase) family serine/threonine kinases that phosphorylate several proteins that

directly or indirectly stimulate actin remodeling(Kumar et al., 2006). In the future it will be interesting to determine whether either Girdin or Pak1 is involved in eEF1A2-dependent filopodia formation.

Our study shows that eEF1A2 overexpression only affects filopodia but not lamellipodia or stress fiber formation in a PI3K/Akt-dependent manner. The ability of eEF1A2 to activate filopodia only indicates that eEF1A2 does not regulate all types of actin structures in mammalian cells . While eEF1A proteins from yeast and *Dictyostelium* have been reported to have actin bundling activity, it is not clear whether eEF1A2 regulates filopodia by directly bundling actin. It has been suggested however, that eEF1A cross-links actin filaments in a way that exclude other proteins to cross-link F-actin (Owen et al., 1992), suggesting a direct interaction between eEF1A2 and actin filaments. Because eEF1A2 induction of filopodia is dependent on PI3K, eEF1A2 may regulate actin rearrangement not through direct actin bundling but through phosphoinositide-dependent signaling. The dependence of eEF1A2 induction of filopodia on ROCK as well as PI3K is consistent with this idea. Because ROCK is a Rho effector and Rho activity is dependent on PI3K, we hypothesize that eEF1A2 activates actin rearrangement by stimulating PI(3,4,5)P generation and activating ROCK through Rho A. Because we find the eEF1A2-dependent activation of Akt is dependent on PI3K activity, we also propose that Akt activation by eEF1A2 is via PIP_3 generation.

A role for eEF1A proteins in phospho-inositol signaling has previously been suggested by the identification of the carrot eEF1A homologue PIK-A49 as direct activator of phosphatidylinositol-4 kinase (PI4K) (Yang et al., 1993). Because PIK-A49 has not been cloned as a full-length cDNA, it is unclear whether PIK-A49 is a bona fide eEF1A gene, but protein sequences of PIK1A9 have a high homology to eEF1A proteins from multiple species. Because PI4K activity has the potential to regulate the downstream abundance of important lipid second messengers PI(4,5)P and PI (3,4,5)P, eEF1A2 may also activate filopodia formation through activation of PI (3,4,5)P abundance by increasing PI4K activity. A recent report by Pendaries and colleagues indicate that PI5P created by the *Shigella* parasite can activate Akt in a PI3K-dependent fashion, suggesting that phospholipids abundance may activate PI3K-dependent signaling (Pendaries et al., 2006). It is possible that eEF1A2 may enhance PI (3,4,5)P generation

by activating PI4K. Recent identification of Akt2 as a potential interacting partner of eEF1A1 and Fascin (an actin bundling protein) and mRif (mouse Rho in Filopodia) as eEF1A2 binding proteins (Chang & Wang, 2006; Lau et al., 2006) suggest that eEF1A2 controls filopodia formation by bringing a complex of actin and PI4K/Akt/Rho signaling proteins together.

The two human eEF1A isoforms (eEF1A2 and eEF1A2) are very similar proteins (92% amino acid identity). The two isoforms appear to have the same activity in protein elongation (Kahns et al., 1998). However, it has yet to be determined whether both isoforms have equivalent oncogenic capacity or have the same ability to alter cell motility. We have been unable to directly test the *in vitro* effect of high eEF1A1 expression because we have been unsuccessful at generating cell lines ectopically expressing high levels of eEF1A1 (D. Purcell & J.M. Lee, unpublished observations). We speculate that high levels of eEF1A1 may be toxic to a cell or that some cellular feedback mechanism exists to prevent steady-state eEF1A1 levels from increasing beyond some threshold level. If eEF1A1, like eEF1A2, were oncogenic, we would expect that, like eEF1A2 (Lee, 2003), the gene for eEF1A1 would be commonly amplified during oncogenesis and that some tumours would have high eEF1A1 mRNA expression. The eEF1A1gene, *EEF1A1*, maps to 6q14.1. This region is not frequently amplified in any malignancy and is deleted in squamous cell carcinoma, osteosarcoma and prostate cancer (Fitzsimmons et al., 2003; Nathrath et al., 2002; Verhagen et al., 2002). This suggests that 6q14.1 contains a tumour suppressor. Similarly, we have not detected high expression of eEF1A1 in ovarian or breast tumours (Anand et al., 2002 and unpublished data). While the issue of eEF1A1's oncogenicity will require further investigation, based on the lack of tumour-specific *EEF1A1* amplification or gene overexpression, we speculate that eEF1A1 is unlikely to be an oncogene, an idea consistent with the high level of eEF1A1 expression in normal tissue.

The ability of eEF1A2 to enhance migration and Akt activation suggests that eEF1A2 can be a target for anti-cancer therapy. The drug Aplidin, a derivative of didemnin B, an eEF1A binding drug that inhibits GTP hydrolysis and translation elongation (Crews et al., 1994), is currently undergoing clinical trials as an anti-cancer agent (Jimeno et al., 2004). Because eEF1A2 is associated with poor prognosis in lung cancer (Li et al., 2005), these patients would be predicted to benefit from eEF1A2 inactivation.

In summary, we report several novel functions of the eEF1A2 oncogene: eEF1A2 expression activates Akt and stimulates cell migration, invasion and filopodia formation in an Akt and PI3K-dependent pathway. These observations are consistent with the idea that eEF1A2 may promote tumour development through phosphatidyl-inositol signaling and actin remodeling.

Material and methods

Cell lines. Rat2, Phoenix and BT549 cell lines were purchased from the American Tissue Culture Collection (ATCC) and were grown in ATCC recommended media in 5% CO_2 at 37°C in 1005 humidity. ROSE 199 cells were a gift of Dr. Nelly Auersperg (UBC).

Plasmid constructs, siRNA and cell line preparation. To generate an eEF1A2 retrovirus, full-length eEF1A2 with the C-terminal V5 tag was subcloned into pLXSN (Clontech) in *EcoRI* and *XhoI* sites. Retrovirus was generated in Phoenix Ampho cells. 50% confluent BT549 were infected with 1 ml of viral supernatant in the presence of 4 µg polybrene (Sigma) and selected using G418 for 2 weeks. For eEF1A2 adenovirus generation, eEF1A2 was subcloned into pShuttle-IRES-hrGFP-1 in *EcoRV* and *XhoI* sites and the virus was manufactured by the central facility of the University of Ottawa. eEF1A2 and GFP control adenovirus were used at a MOI of 200. To produce eEF1A2-pCDNA 3.1, full-length eEF1A2 with the C-terminal V5 tag was subcloned into pcDNA 3.1/GS (Invitrogen) in *EcoRI* and *XhoI* sites. Lipofectamine 2000 (Invitrogen) was used for transfection as manufacturer recommended. Zeocin was used to select stable cell lines. The sequence of eEF1A2- siRNA is 5'UCGAACUUCUCAAUGGUCCTT-3'. Transient transfection of siRNA was carried out using 4 μl of Lipofectamine 2000 and 5μl of siRNA (100 nM).

Western blotting and immunoprecipitation. Cells were lysed using RIPA buffer (50 mM Tris-Cl; pH7.4, 1% Triton X-100, 1% Sodium deoxycholate, 0.1% SDS, 1mM EDTA; pH7.0, 150 mM NaCl) supplemented with 1% aprotonin, 1 mg/ml leupeptin, 50 mM NaF, 1 mM Na_3VO_4, 10 µg/ml pepstatin in ethanol, 1mM PMSF in DMSO. Protein concentrations determined by Bradford protein assay (Pierce). Approximately 30 µg of protein extracts were separated by SDS-PAGE and transferred to PVDF membrane. Anti-V5-HRP (Invitrogen), anti-FLAG (Sigma), beta actin (Sigma), Akt, phospho-Akt (Cell Signaling Technology), goat anti-mouse IgG, HRP-conjugate (Upstate Cell Signaling Solutions) and anti-rabbit IgG, HRP-linked antibody (Cell Signaling Technology) were used according to manufacturer recommendations. Anti-eEF1A2 was manufactured as described (Kulkarni et al., 2006) and was used at 1:2000 dilution. Protein bands were visualized by chemiluminescence reagent ECL (Amersham). For PI3K/eEF1A2 interaction, BT549 cells were grown to 50% confluence and transduced with

either GFP or eEF1A2 adenovirus (MOI of 200) or left untransduced. After a 24 hour infection period, cells were lysed in RIPA buffer. 100μg of total protein from each case were pre-cleared with protein A agarose (Upstate Cell Signaling Solutions) or protein G sepharose (Amersham Biosciences) for one hour at 4ºC. 2-4 μg of anti-PI3K p85 (Upstate Cell Signaling Solutions) or anti-V5 (Sigma) antibody were added to lysates and incubated overnight at 4ºC. The antibodies used for the western are: PI3Kp85 (1:2000 in TBST), Y-pPI3Kp85 (Santa Cruz Biotechnology Inc.; 1:1000 in TBST), Flag M2 (Sigma; 1:2000 in TBST), and V5 (1:2000 in TBST), anti-rabbit IgG-HRP conjugate (Cell Signaling Technology, 1:5000 in TBST), and anti-mouse IgG (Upstate Cell Signaling Solutions, 1:5000 in TBST).

Immunofluorescence and video microscopy. Cells were grown on coverslips coated with 50 µg/ml poly-D-lysin (Sigma) prior to fixation or video microscopy. For immunofluorescence staining, cells were fixed with 3.7% formaldehyde for 1 h and permeabilized by 0.1% triton X-100 for 5 min. Following blocking with 2% goat serum and 1% BSA, cells were labeled with Alexa Fluor 546 phalloidin (Molecular Probes) at 1:40 dilution for 1 hr. VASP monoclonal antibody (Transduction Laboratories) was used at 1:50 dilution followed by secondary antibody Alexa Fluor 488- goat antibody at 1:450 dilution. After washing 3 times with PBS, cells were mounted on slides using fluorescent mounting medium (Dako Cytomation). Slides were analyzed by Leica DM IRE2 using 635 nm filter. Images were acquired by Retiga 12 bit camera (Leica) and deconvoluted using Volocity 3.1 software (Improvision). Images for time lapse microscopy were captured using the Axiovert 200 ZEISS microscope and ZEISS camera, and analyzed by Axioversion Rel.4.5 software .

Cell migration and invasion assays. Cells were serum-starved overnight. The top chambers of 6.5-mm Corning Costar transwells (Corning, NY) were loaded with 0.2 ml of cells (5 X 10^5 cells/ml) in serum-free media. 0.6 ml of complete media was added to the bottom wells and cells were incubated at 37ºC overnight. Cells on the top layer were removed and the images of the cells at the bottom of the membrane were captured using Canon camera and a Zeiss Axio Vert microscope. The mean values were obtained from three individual experiments using Excel

Microsoft software and subjected to t-tests. For cell invasion assay, cells were serum-starved overnight. 24-well cell culture inserts (8 μm pore size, BD Biosciences) were loaded with 0.5 ml of cells ((5 X 10^5 cells/ml) in serum-free media. 0.5 ml of complete media was added to the bottom wells and cells were incubated at 37ºC for about 2 days. Cells were fixed, stained, and analyzed as above.

Adhesion and Spreading assays. Adhesion and Spreading assays were performed as described in Podrigues et al., 2005. Images were acquired by Retiga 12 bit camera (Leica). Images for time lapse microscopy for adhesion assay were captured using the Leica DM IRE2 microscope.

Figure legends

Figure 1. eEF1A2 expression in cell lines. (a) Western blot of eEF1A2 expression. Human BT549 and rat Rat2 cells do not naturally express eEF1A2 whereas human MCF7 breast cancer and rat ROSE 199 cells do express eEF1A2 protein. Expression was measured using an eEF1A2-specific antibody. (b) Stable expression of eEF1A2 protein in BT549 and Rat2 cell lines. 1A2-1, 1A2-2, 1A2-3, 1A2-A, and 1A2-B refer to clonal cell lines. 1A2-polyclonal and Rat2-1A2 are cell lines derived from pooling several (>10) drug resistant colonies after selection. The expression of eEF1A2 was analyzed by immunoblotting using anti-eEF1A2 or anti-V5 antibodies. Actin was used as a loading control. eEF1A2-expressing BT549 cells were generated using a plasmid vector or a retrovirus.

Figure 2. eEF1A2 expression induces actin cytoskeletal rearrangement. (a) Fluorescence deconvolution micrographs of eEF1A2-expressing and control BT549 cells with actin visualized by phalloidin (Alexa Fluor 546). Right panels are magnified versions of the boxed area of the left panel. The scale bars in each of the left and right panels are 30 μM and 12 μM in length respectively. (b) Western blot of eEF1A2-expressing BT549 cells with eEF1A2 siRNA or negative siRNA control. (c) Fluorescence micrographs of eEF1A2-expressing cells treated with either eEF1A2 or control siRNA for 24 h and stained with phalloidin to examine actin filaments. (d) Fluorescence micrographs of eEF1A2-expressing and control Rat2 cells stained with phalloidin. Right panels are magnified versions of the boxed area of the left panel. The scale bars in each of the left and right panels are 30 μM and 12 μM in length respectively.

Figure 3. Structures seen in eEF1A2-expressing cells have the criteria of filopodia. *Upper panels* Phase contrast micrographs of control and eEF1A2-expressing BT549 cells. Filopodia are indicated by an arrow. *Lower panels* Time-lapse phase contrast microscopy of filopodia in an eEF1A2-expressing BT549 cell. Elapsed time is indicated in each panel. Images were captured every 5 seconds for 4 hours. A full video of this sequence is found in the supplementary figures (S1) (c) Fluorescence micrographs of eEF1A2-expressing BT549 cell stained for actin (phalloidin) and VASP.

Figure 4. PI3K is required for eEF1A2-induced filopodia formation. (a and b) BT549 and Rat2 cells expressing eEF1A2 were cultured in the presence of the indicated concentrations of LY294002, a PI3K specific inhibitor, overnight. Right panels are magnified versions of the boxed area of the left panel. The scale bar in the left and right pictures is 30 μM and 12 μM in length respectively. (c) eEF1A2 does not physically interact with PI3K. BT549 cells were infected with an adenovirus for GFP or eEF1A2 or mock infected. Antibodies for either eEF1A2 or PI3K were used for immunoprecipitation (IP) from whole cell lysates. An anti-V5 antibody is used as an immunoprecipitation control. Co-immunoprecipitating proteins were detected by Western blotting (WB) using antibodies specific for eEF1A2 and PI3K. The whole cell lysate lane (WCL) lane contains 100 μg of total cellular protein and each immunoprecipitation was performed using 100 μg of protein lysate. (d) eEF1A2 does not activate PI3K. BT549 cells were infected with an Adenovirus for GFP or eEF1A2 and the levels of the indicated proteins assayed by Western blot. PI3K activation is measured by phosphorylation of tyrosine 508 (e and f) cells were treated with 1 μM API-2, an Akt inhibitor (e) or 10 μM Y27632, a ROCK kinase inhibitor overnight and stained with phalloidin. Vehicles applied to control cells.

Figure 5. eEF1A2 activates Akt in a PI3K-dependent manner. Total protein extracts from eEF1A2-expressing cells were analyzed by western blot using Akt, phospho-Akt (Ser 473), or phospho-Akt (Thr 308) antibodies. The protein extracts from cells expressing GFP or the empty vector were used as controls and actin used as a loading control. (a) Akt-phosphorylation 24 hours after infection with an eEF1A2- of GFP-adenovirus. (b) Akt-phosphorylation in stable eEF1A2-expressing BT549 cells (c) Akt phosphorylation in wild-type MCF7 cells that have been treated with an eEF1A2 siRNA. Numbers reflect pAkt band intensity normalized to the actin loading control and is representative of three independent experiments. (d) Akt-phosphorylation, 24 hours after infection with an eEF1A2 adenovirus and a two-hour treatment with indicated concentrations of LY294002. (e) Akt-phosphorylation of eEF1A2-expressing BT549 cells which were treated with Rapamycin for 2 h.

Figure 6. eEF1A2 expression increases cell migration (a) The indicated clones of eEF1A2-expressing BT549 cells were serum-starved overnight and placed in a transwell migration

chamber. The photographs show a representative field from each of the cell lines that have migrated into the chamber. In the lower panel, migration is expressed as a percentage of vector only controls and is the mean and standard deviation of triplicate independent experiments. Enhanced migration is statistically significant ($p<0.05$, Students's t-test) and marked by an asterix. (b) eEF1A2-induced migration is inhibitable by PI3K inhibition. Indicated eEF1A2-expressing BT549 cells were serum-starved overnight, and incubated with LY294002 for 2 h at the indicated concentrations before being placed in the transwell chamber. The micrographs show a representative field of cells that have migrated into the chamber. In the lower panel, migration is expressed as a percentage of vector only controls and is the mean and standard deviation of triplicate independent experiments each with triplicate counts. (c) eEF1A2-expressing BT549 cells were treated with 1 μM API-2 (overnight), 10 ng/ml Rapamycin (2 h) or 10 nM wortmannin (30 min) and subjected to cell migration as above. As control cells were treated with vehicles only. Migration is expressed as a percentage of vector only controls and is the mean and standard deviation of triplicate independent experiments each with triplicate counts. Migration inhibition is statistically significant ($p<0.05$, Students's t-test) and marked by an asterix

Figure 7. eEF1A2 expression increases cell invasion. eEF1A2-overexpressing BT549 were serum-starved overnight. After pre-incubation with LY294002 or DMSO (vehicle) for 2 h, cells were subjected to the invasion assay using Matrigel-coated transwells for approximately 48 hours. The photographs show a representative field from each of the cell lines that have invaded through the Matrigel. In the lower panel, invasion is expressed as a percentage of vector only controls and is the mean and standard deviation of triplicate independent experiments with triplicate counts. Enhanced migration of 1A2 relative to the vector only control is statistically significant ($p<0.05$, Students's t-test) and marked by a single asterix. Similarly, the ability of LY294002 to attenuate migration inhibition is statistically significant ($p<0.05$, Students's t-test) and marked by a double asterix (b) eEF1A2-expressing BT549 cells were treated with 1 μM API-2 (overnight), 10 ng/ml Rapamycin (2 h) or 10 nM wortmannin (30 min) and subjected to cell migration as above. As control cells were treated with vehicles only. Migration is expressed as a percentage of vector only controls and is the mean and standard deviation of triplicate

independent experiments each with triplicate counts. Migration inhibition is statistically significant ($p<0.05$, Students's t-test) and marked by a single asterix

Figure 8. eEF1A2 expression has no effect on cell spreading and adhesion. (a) eEF1A2 expressing cells were trypsinized, and placed on a growth substrate containing fibronectin and observed as a function of time using time-lapse video microscopy on a heated stage. White arrows mark the first appearance of lamellipodia in the plated cells. (b) Cells were trypsinized and plated onto fibronectin-coated coverslips. At indicated time points, cells were washed with PBS , fixed using 3.7% formaldehyde and adherent cells were counted.

Acknowledgements

References

Adams, A.T. & Auersperg, N. (1985). *Exp Cell Biol*, **53,** 181-8.

Anand, N., Murthy, S., Amann, G., Wernick, M., Porter, L.A., Cukier, I.H., Collins, C., Gray, J.W., Diebold, J., Demetrick, D.J. & Lee, J.M. (2002). *Nat Genet*, **31,** 301-5.

Arboleda, M.J., Lyons, J.F., Kabbinavar, F.F., Bray, M.R., Snow, B.E., Ayala, R., Danino, M., Karlan, B.Y. & Slamon, D.J. (2003). *Cancer Res*, **63,** 196-206.

Carpenter, C.L. & Cantley, L.C. (1990). *Biochemistry*, **29,** 11147-56.

Carragher, N.O. & Frame, M.C. (2004). *Trends Cell Biol*, **14,** 241-9.

Chang, R. & Wang, E. (2006). *J Cell Biochem*. epub ahead of print.

Chen, J., Deangelo, D.J., Kutok, J.L., Williams, I.R., Lee, B.H., Wadleigh, M., Duclos, N., Cohen, S., Adelsperger, J., Okabe, R., Coburn, A., Galinsky, I., Huntly, B., Cohen, P.S., Meyer, T., Fabbro, D., Roesel, J., Banerji, L., Griffin, J.D., Xiao, S., Fletcher, J.A., Stone, R.M. & Gilliland, D.G. (2004). *Proc Natl Acad Sci U S A*, **101,** 14479-84.

Chodniewicz, D. & Klemke, R.L. (2004). *Exp Cell Res*, **301,** 31-7.

Condeelis, J. (1995). *Trends Biochem Sci*, **20,** 169-70.

Crews, C.M., Collins, J.L., Lane, W.S., Snapper, M.L. & Schreiber, S.L. (1994). *J Biol Chem*, **269,** 15411-4.

Edmonds, B.T., Wyckoff, J., Yeung, Y.G., Wang, Y., Stanley, E.R., Jones, J., Segall, J. & Condeelis, J. (1996). *J Cell Sci*, **109 (Pt 11),** 2705-14.

Enomoto, A., Murakami, H., Asai, N., Morone, N., Watanabe, T., Kawai, K., Murakumo, Y., Usukura, J., Kaibuchi, K. & Takahashi, M. (2005). *Dev Cell*, **9,** 389-402.

Fitzsimmons, S.A., Ireland, H., Barr, N.I., Cuthbert, A.P., Going, J.J., Newbold, R.F. & Parkinson, E.K. (2003). *Oncogene*, **22,** 1737-46.

Fruman, D.A., Meyers, R.E. & Cantley, L.C. (1998). *Annu Rev Biochem*, **67,** 481-507.

Gross, S.R. & Kinzy, T.G. (2005). *Nat Struct Mol Biol*, **12,** 772-8.

Heilmeyer, L.M., Jr., Vereb, G., Jr., Vereb, G., Kakuk, A. & Szivak, I. (2003). *IUBMB Life*, **55,** 59-65.

Hershey, J.W. (1991). *Annu Rev Biochem*, **60,** 717-55.

Jimeno, J., Lopez-Martin, J.A., Ruiz-Casado, A., Izquierdo, M.A., Scheuer, P.J. & Rinehart, K. (2004). *Anticancer Drugs*, **15,** 321-9.

Kahns, S., Lund, A., Kristensen, P., Knudsen, C.R., Clark, B.F., Cavallius, J. & Merrick, W.C. (1998). *Nucleic Acids Res*, **26,** 1884-90.

Knudsen, S.M., Frydenberg, J., Clark, B.F. & Leffers, H. (1993). *Eur J Biochem*, **215,** 549-54.

Kulkarni, G., Turbin, D.A., Amiri, A., Jeganathan, S., Andrade-Navarro, M.A., Wu, T.D., Huntsman, D.G. & Lee, J.M. (2006). *Breast Cancer Res Treat*.

Kumar, R., Gururaj, A.E. & Barnes, C.J. (2006). *Nat Rev Cancer*, **6,** 459-71.

Lau, J., Castelli, L.A., Lin, E.C. & Macaulay, S.L. (2006). *Mol Cell Biochem*, **286,** 17-22.

Lee, J.M. (2003). *Reprod Biol Endocrinol*, **1,** 69.

Lee, S., Wolfraim, L.A. & Wang, E. (1993). *J Biol Chem*, **268,** 24453-9.

Li, R., Wang, H., Bekele, B.N., Yin, Z., Caraway, N.P., Katz, R.L., Stass, S.A. & Jiang, F. (2005). *Oncogene*.

Meijer, H.J. & Munnik, T. (2003). *Annu Rev Plant Biol*, **54,** 265-306.

Moody, S.E., Perez, D., Pan, T.C., Sarkisian, C.J., Portocarrero, C.P., Sterner, C.J., Notorfrancesco, K.L., Cardiff, R.D. & Chodosh, L.A. (2005). *Cancer Cell*, **8,** 197-209.

Munshi, R., Kandl, K.A., Carr-Schmid, A., Whitacre, J.L., Adams, A.E. & Kinzy, T.G. (2001). *Genetics*, **157,** 1425-36.

Nathrath, M.H., Kuosaite, V., Rosemann, M., Kremer, M., Poremba, C., Wakana, S., Yanagi, M., Nathrath, W.B., Hofler, H., Imai, K. & Atkinson, M.J. (2002). *Oncogene*, **21,** 5975-80.

Overduin, M., Cheever, M.L. & Kutateladze, T.G. (2001). *Mol Interv*, **1,** 150-9.

Owen, C.H., DeRosier, D.J. & Condeelis, J. (1992). *J Struct Biol*, **109,** 248-54.

Pencil, S.D., Toh, Y. & Nicolson, G.L. (1993). *Breast Cancer Res Treat*, **25,** 165-74.

Pendaries, C., Tronchere, H., Arbibe, L., Mounier, J., Gozani, O., Cantley, L., Fry, M.J., Gaits-Iacovoni, F., Sansonetti, P.J. & Payrastre, B. (2006). *Embo J*, **25,** 1024-34.

Qian, Y., Corum, L., Meng, Q., Blenis, J., Zheng, J.Z., Shi, X., Flynn, D.C. & Jiang, B.H. (2004). *Am J Physiol Cell Physiol*, **286,** C153-63.

Reinhard, M., Halbrugge, M., Scheer, U., Wiegand, C., Jockusch, B.M. & Walter, U. (1992). *Embo J*, **11,** 2063-70.

Riento, K. & Ridley, A.J. (2003). *Nat Rev Mol Cell Biol*, **4,** 446-56.

Svitkina, T.M., Bulanova, E.A., Chaga, O.Y., Vignjevic, D.M., Kojima, S., Vasiliev, J.M. & Borisy, G.G. (2003). *J Cell Biol*, **160,** 409-21.

Thornton, S., Anand, N., Purcell, D. & Lee, J. (2003). *J Mol Med*, **81,** 536-48.

Tomlinson, V.A., Newbery, H.J., Wray, N.R., Jackson, J., Larionov, A., Miller, W.R., Dixon, J.M. & Abbott, C.M. (2005). *BMC Cancer*, **5,** 113.

Tornieri, K., Welshhans, K., Geddis, M.S. & Rehder, V. (2006). *Cell Motil Cytoskeleton*, **63,** 173-92.

Verhagen, P.C., Hermans, K.G., Brok, M.O., van Weerden, W.M., Tilanus, M.G., de Weger, R.A., Boon, T.A. & Trapman, J. (2002). *Int J Cancer*, **102,** 142-7.

Vivanco, I. & Sawyers, C.L. (2002). *Nat Rev Cancer*, **2,** 489-501.

Wang, Z., Shen, D., Parsons, D.W., Bardelli, A., Sager, J., Szabo, S., Ptak, J., Silliman, N., Peters, B.A., van der Heijden, M.S., Parmigiani, G., Yan, H., Wang, T.L., Riggins, G., Powell, S.M., Willson, J.K., Markowitz, S., Kinzler, K.W., Vogelstein, B. & Velculescu, V.E. (2004). *Science*, **304,** 1164-6.

Yamaguchi, H., Wyckoff, J. & Condeelis, J. (2005). *Curr Opin Cell Biol*, **17,** 559-64.

Yang, F., Demma, M., Warren, V., Dharmawardhane, S. & Condeelis, J. (1990). *Nature*, **347,** 494-6.

Yang, L., Dan, H.C., Sun, M., Liu, Q., Sun, X.M., Feldman, R.I., Hamilton, A.D., Polokoff, M., Nicosia, S.V., Herlyn, M., Sebti, S.M. & Cheng, J.Q. (2004). *Cancer Res*, **64,** 4394-9.

Yang, W., Burkhart, W., Cavallius, J., Merrick, W.C. & Boss, W.F. (1993). *J Biol Chem*, **268,** 392-8.

Zhou, G.L., Zhuo, Y., King, C.C., Fryer, B.H., Bokoch, G.M. & Field, J. (2003). *Mol Cell Biol*, **23,** 8058-69.

1A
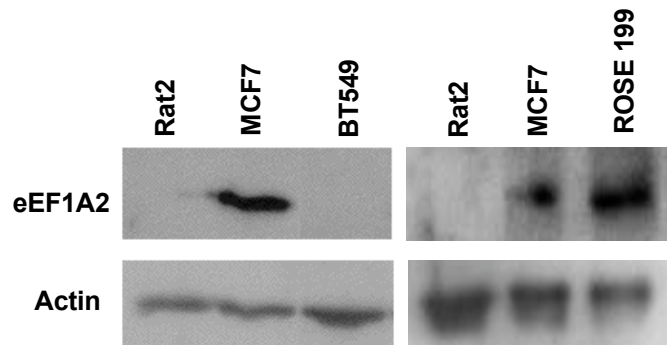
B
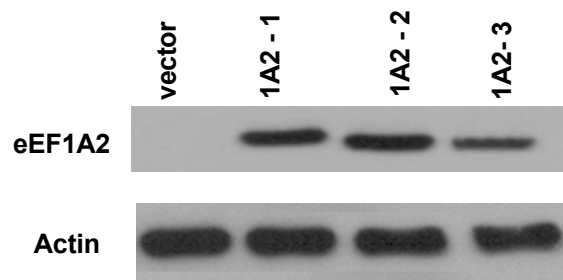
BT549-plasmid
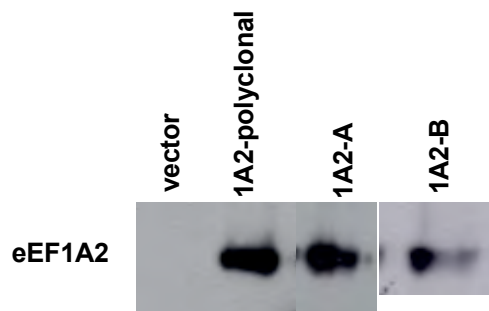
BT549-retrovirus
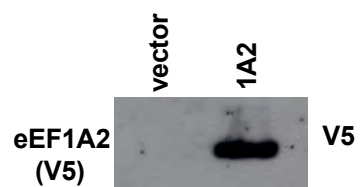
Rat2-plasmid

2A

B

2C

D

Rat2

3A

BT549 1A2   BT549 control

Time = 0'   20'   50'   80'

110'   140'   170'   200'

B   actin   VASP   merge

4A **BT549**

1A2-A

1A2-B

10 μM LY294002 **20 μM LY294002**

B **Rat2**

1A2

10 μM LY294002 **20 μM LY294002**

C

IP

| | WCL | eEF1A2 | PI3K | V5 | WB |

PI3K

eEF1A2

GFP - + -   - + -   - + -   - + -
eEF1A2 - - +   - - +   - - +   - - +

D

GFP   eEF1A2

Y-p85

p85

Actin
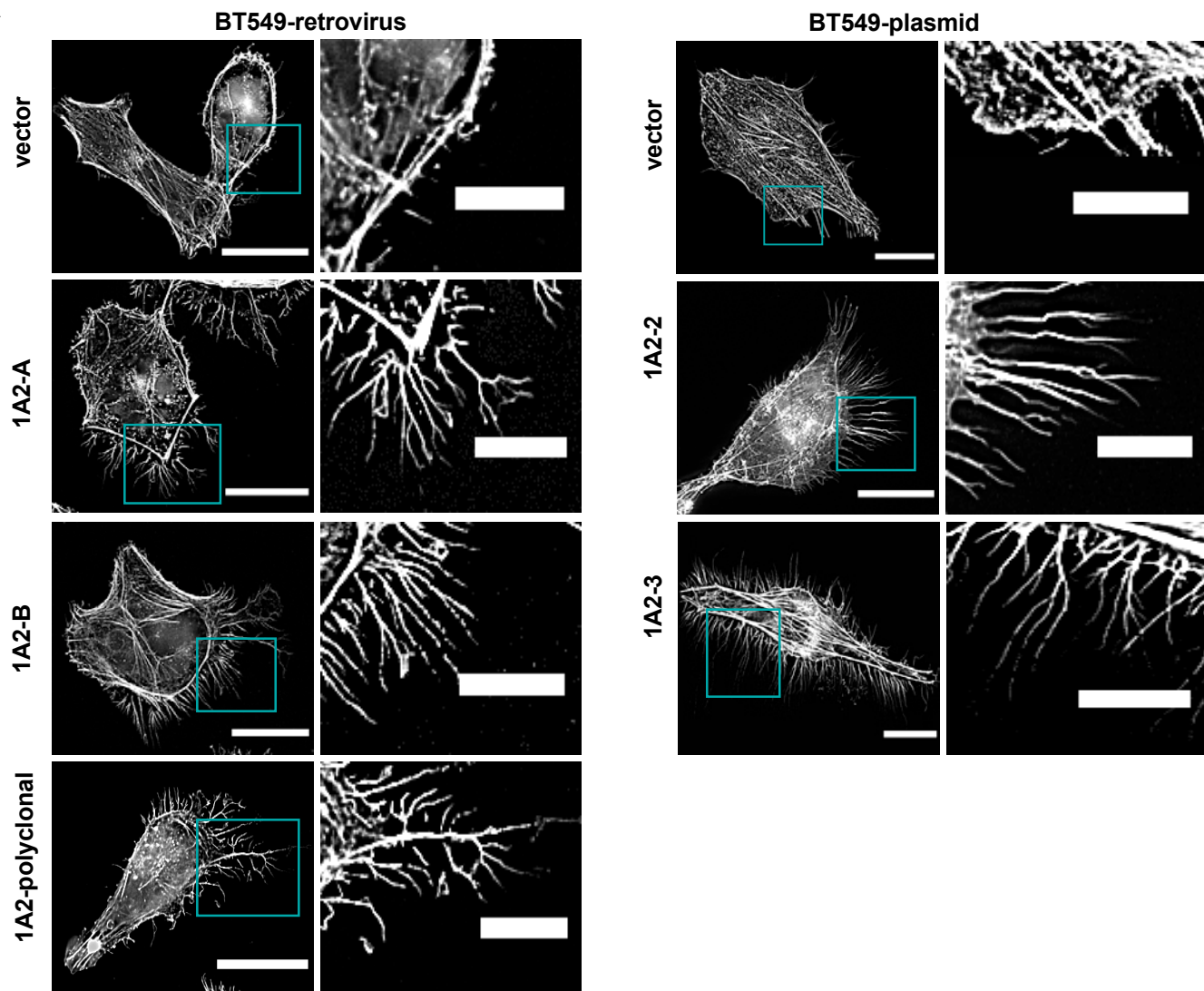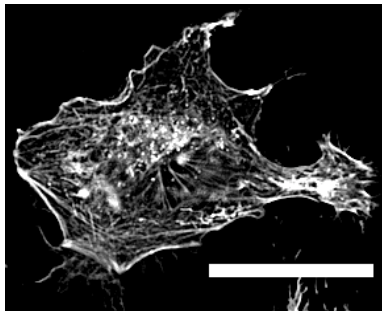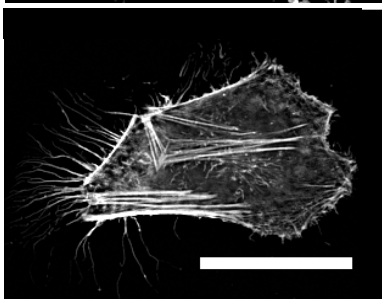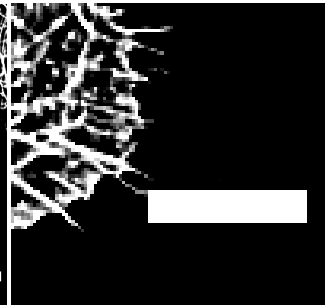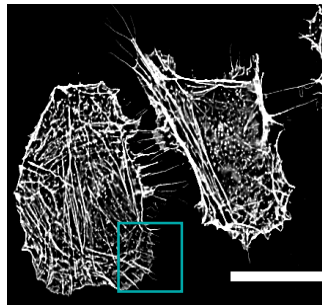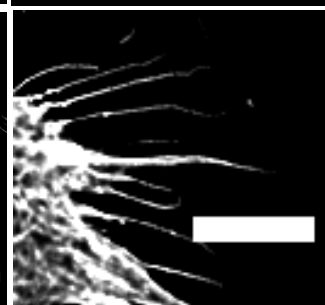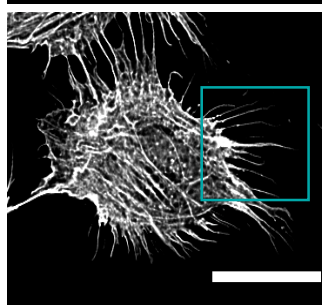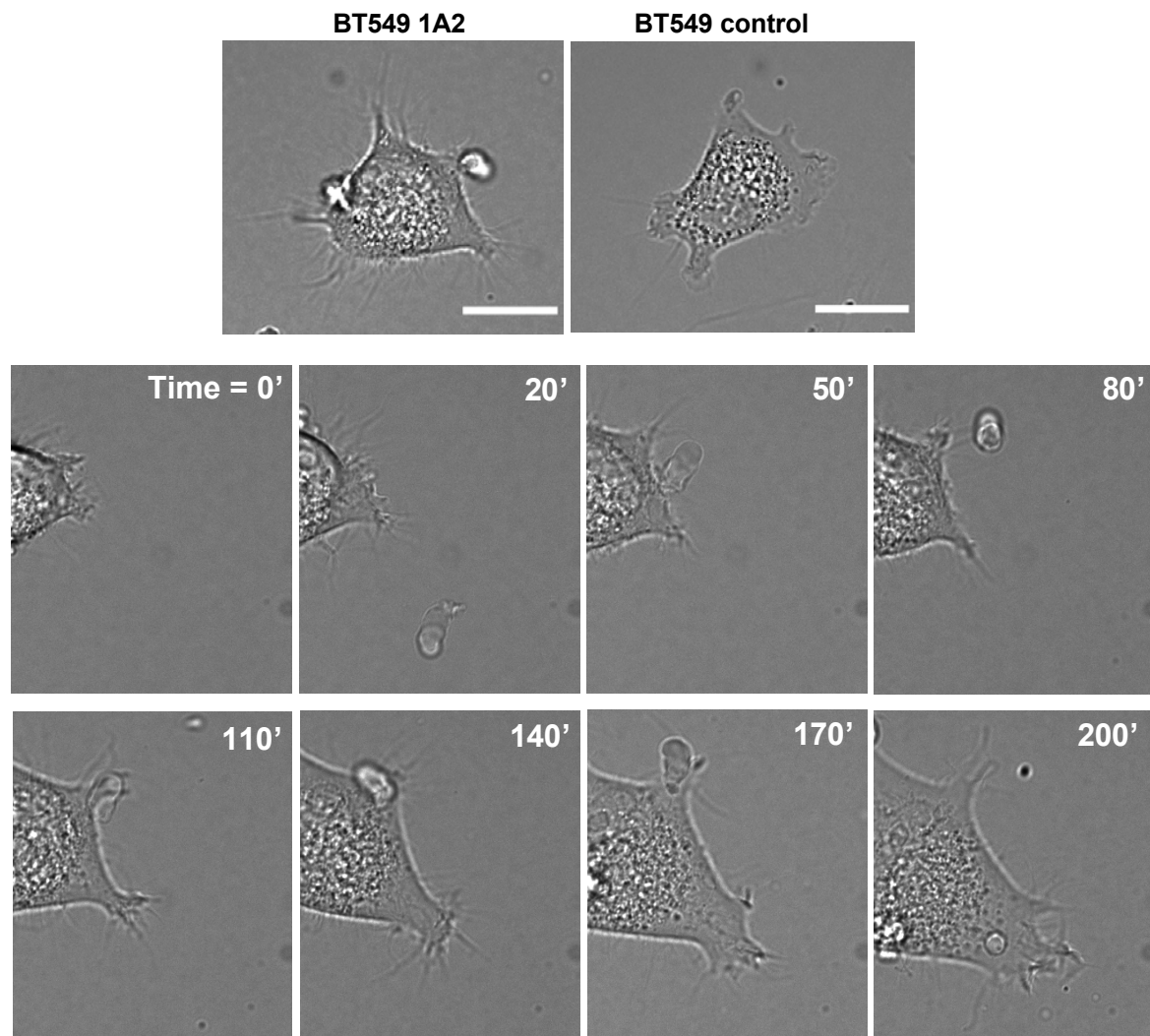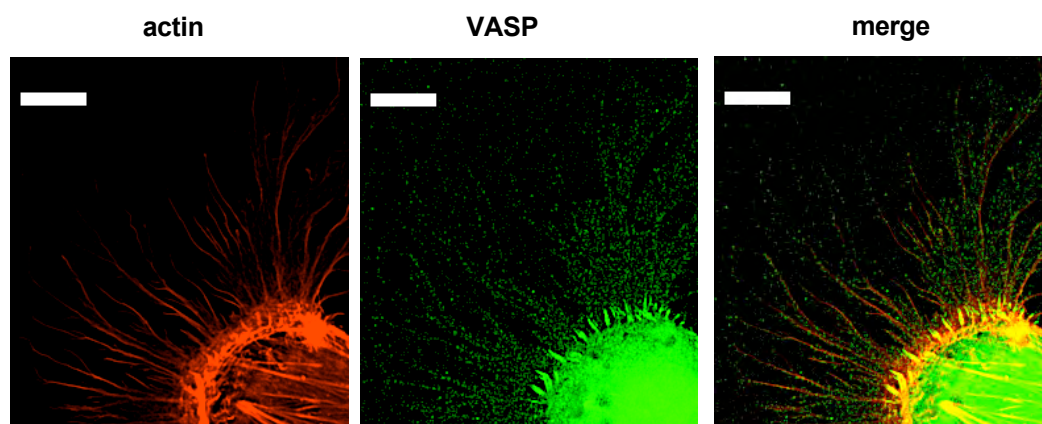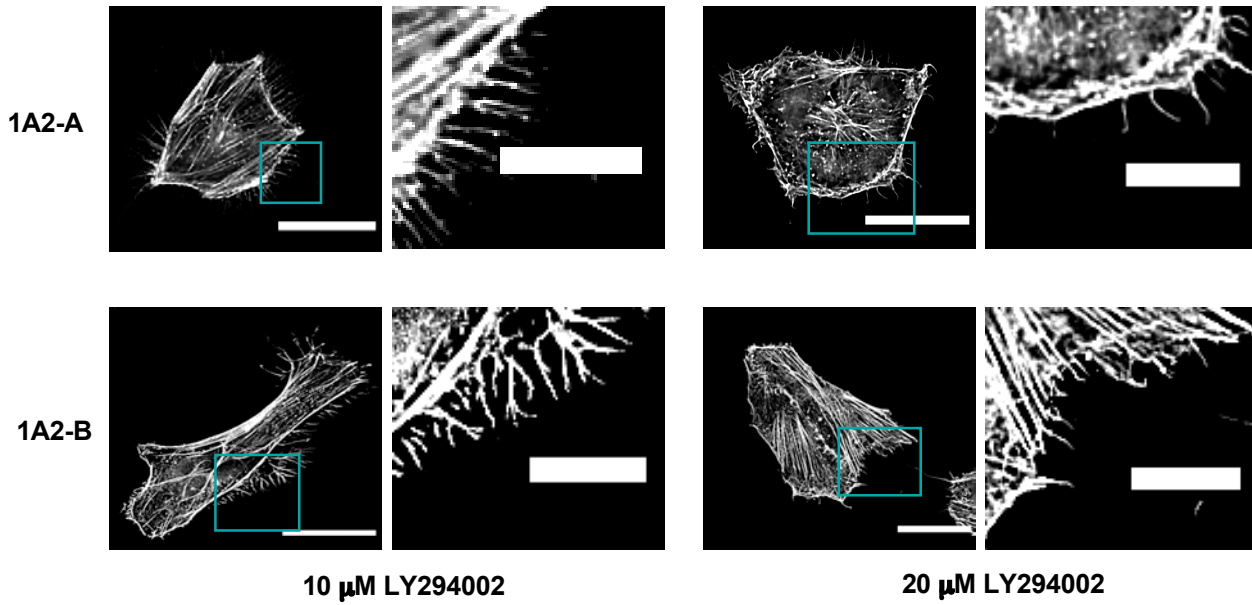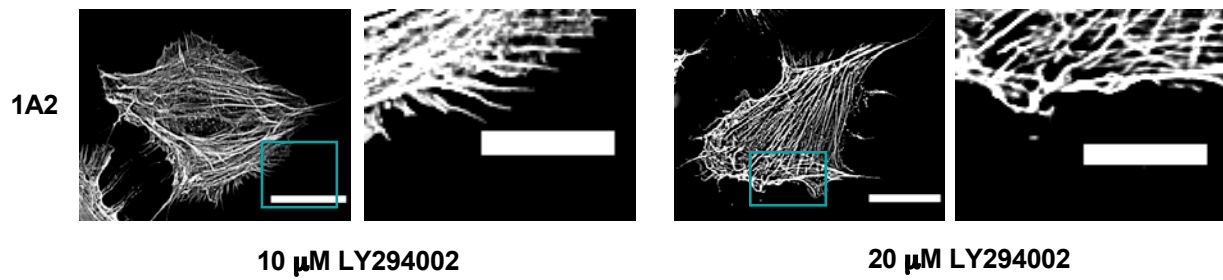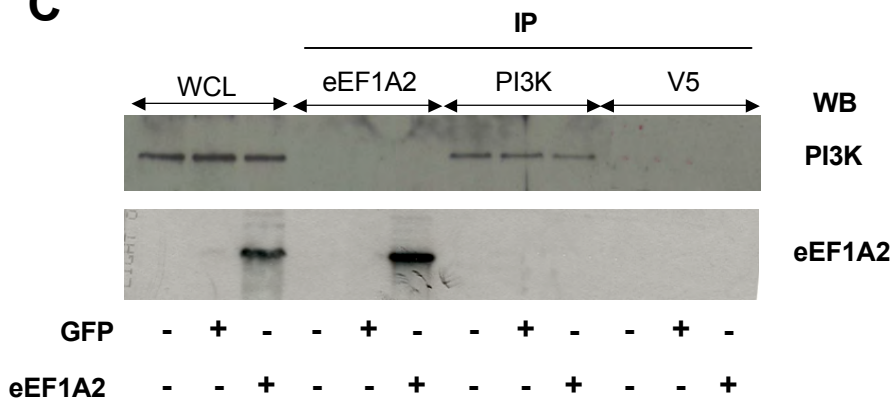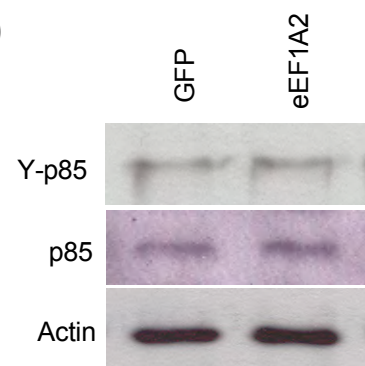
E

API
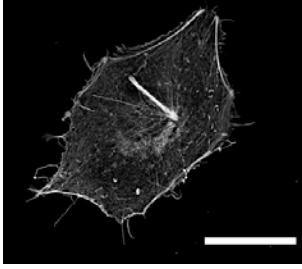
control

F

Y27632

control
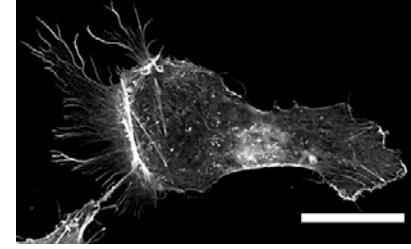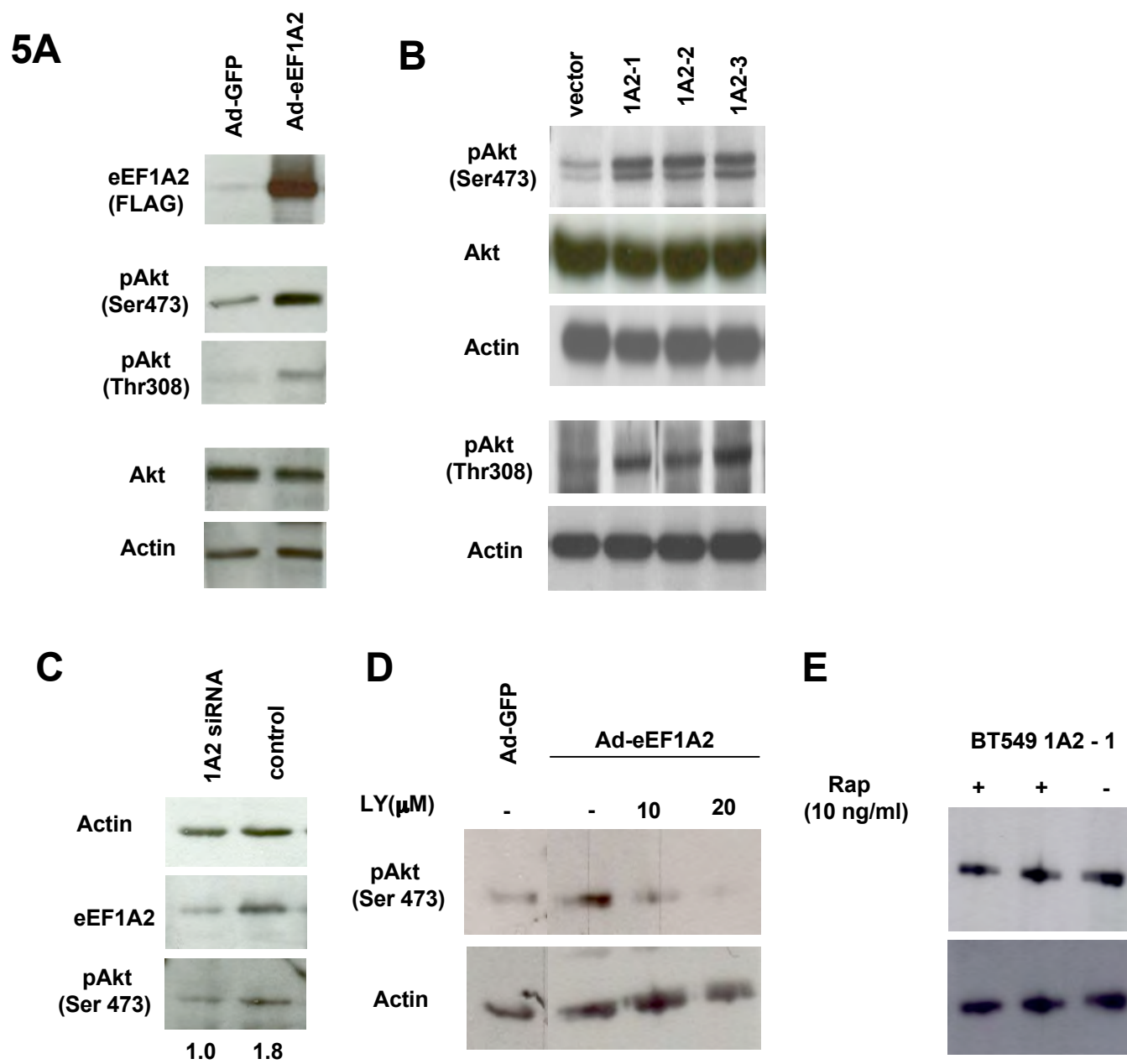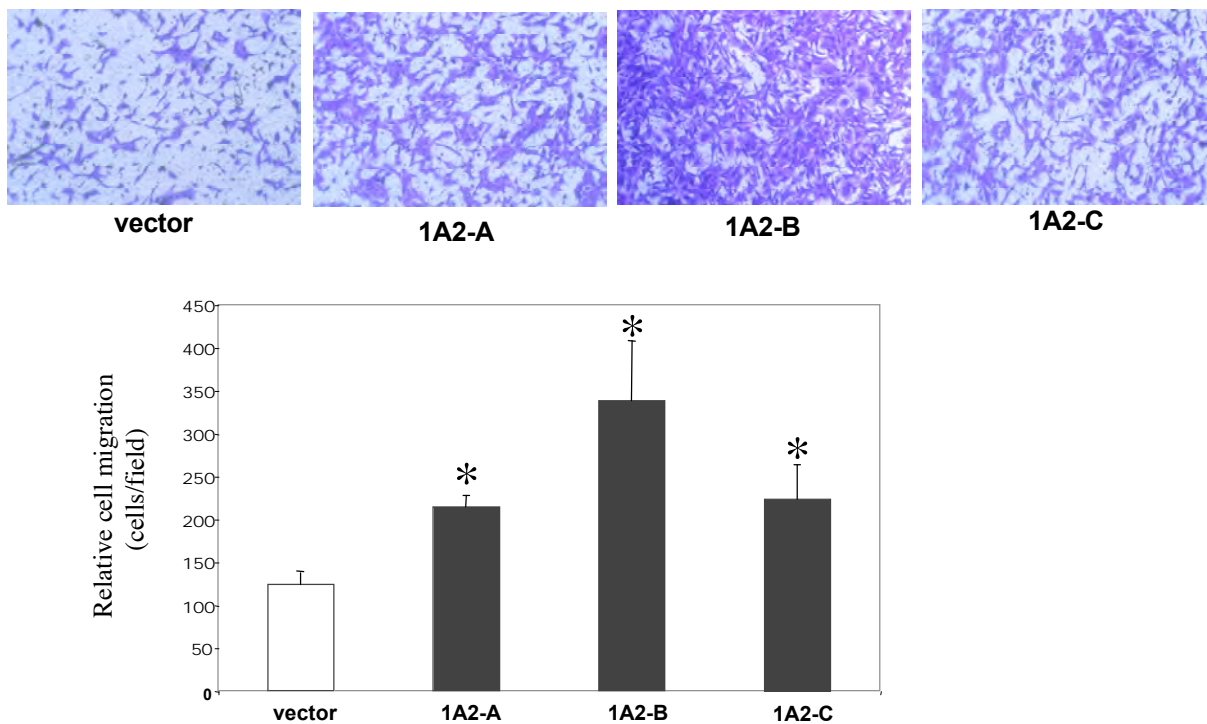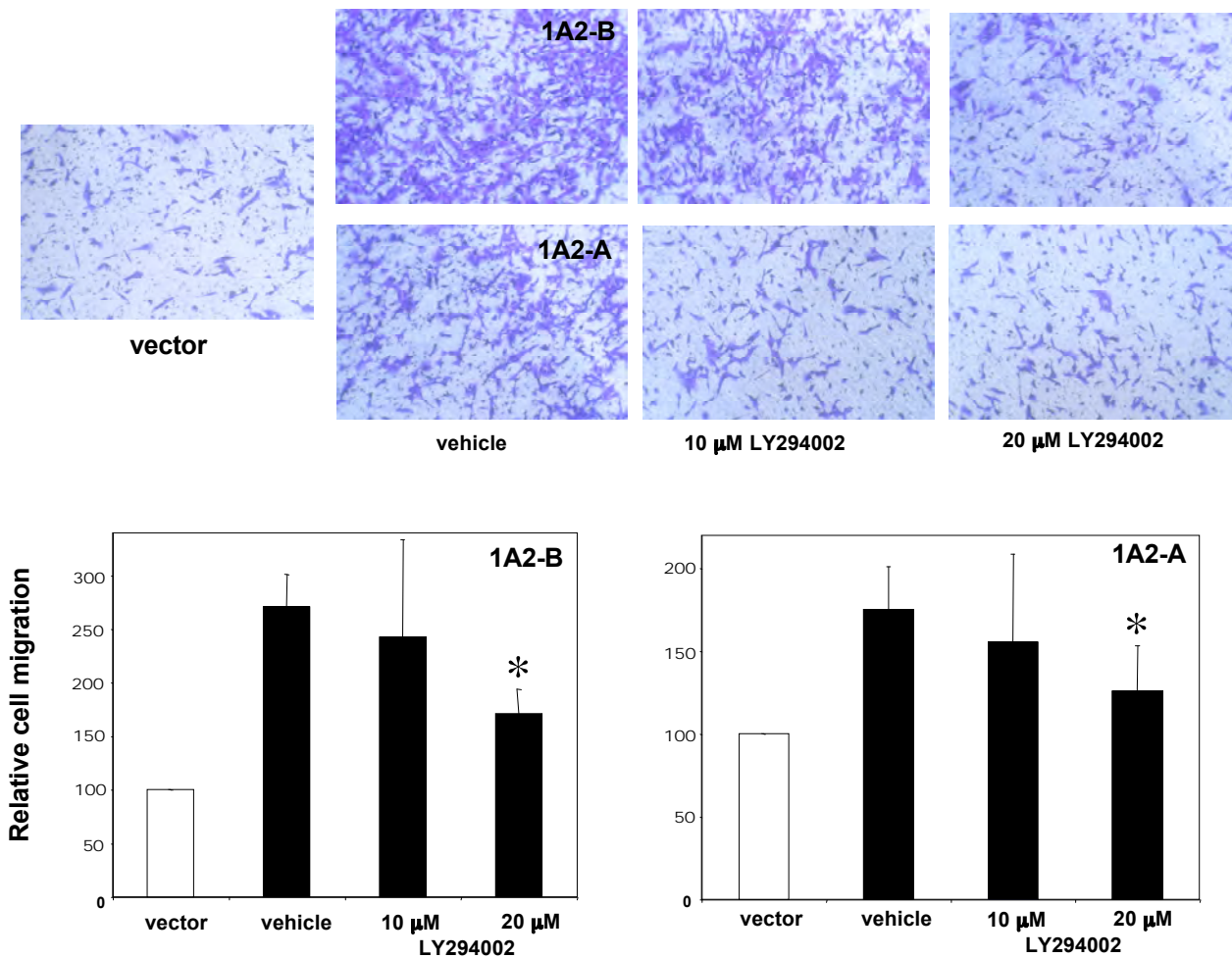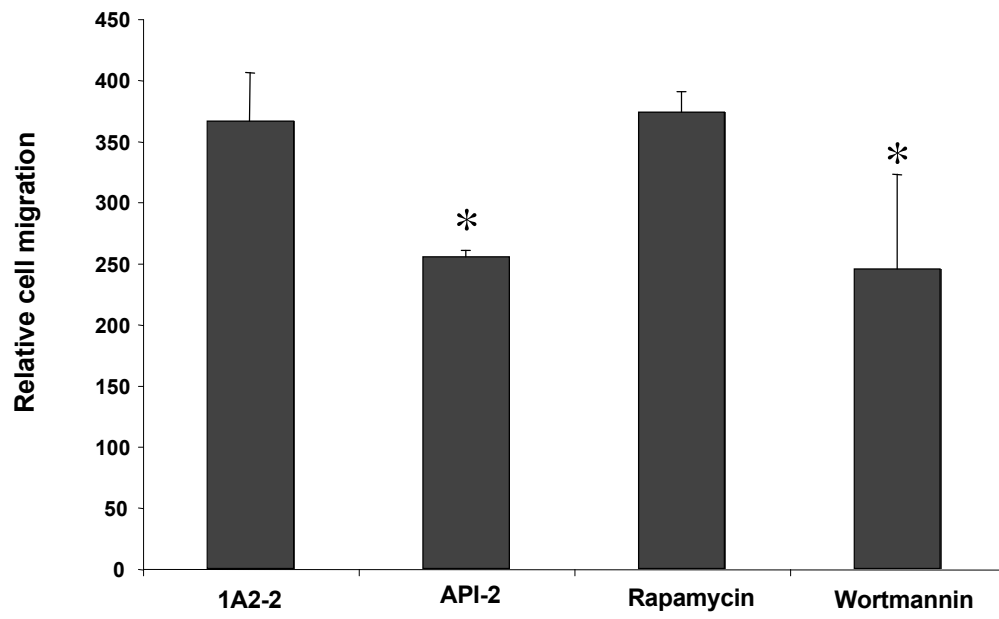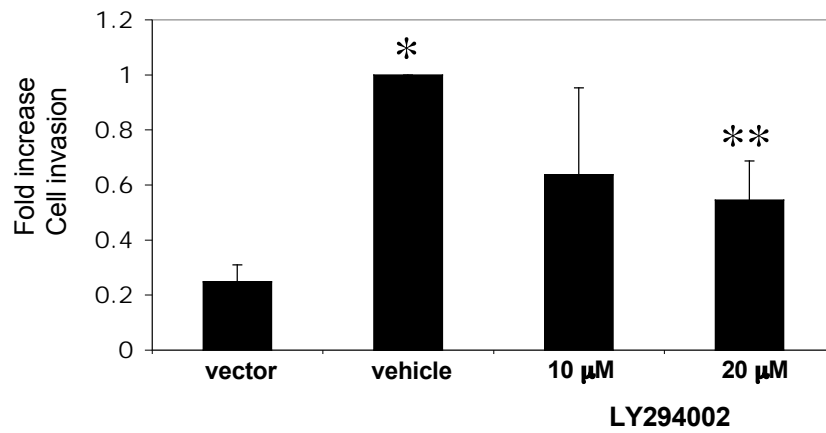
5A

B

C

D

E

6A

vector   1A2-A   1A2-B   1A2-C

B

1A2-B

vector

1A2-A

vehicle   10 μM LY294002   20 μM LY294002

C

7A

1A2-A

vector

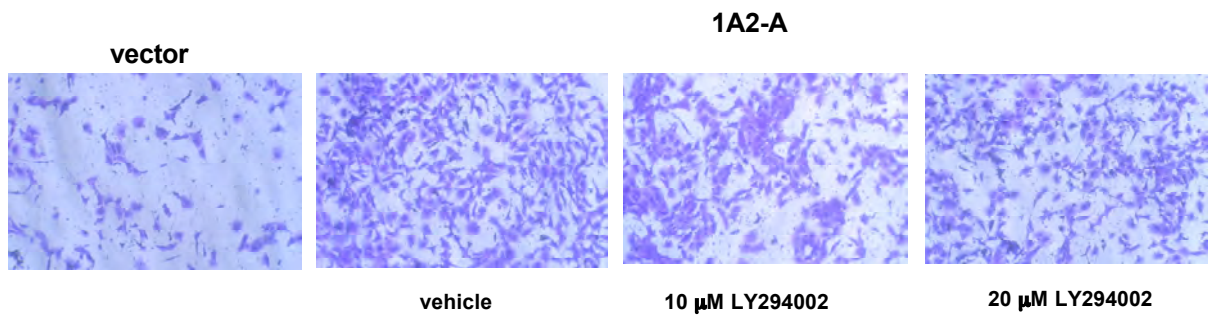vehicle   10 μM LY294002   20 μM LY294002
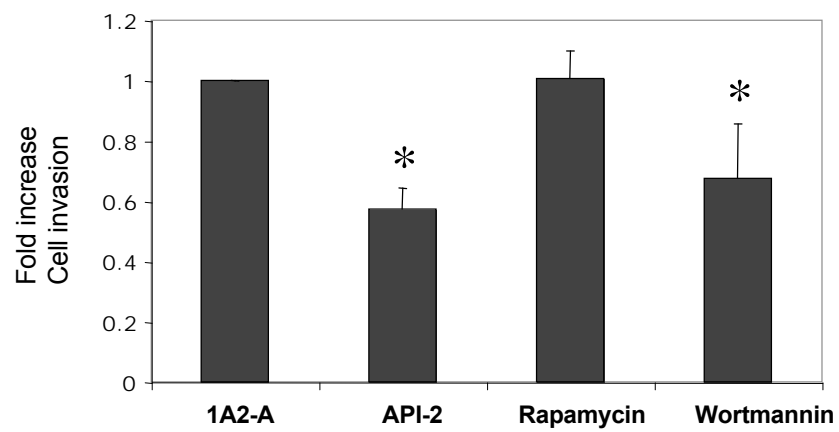

B

8A

Time (minutes)

B

Time (minutes)
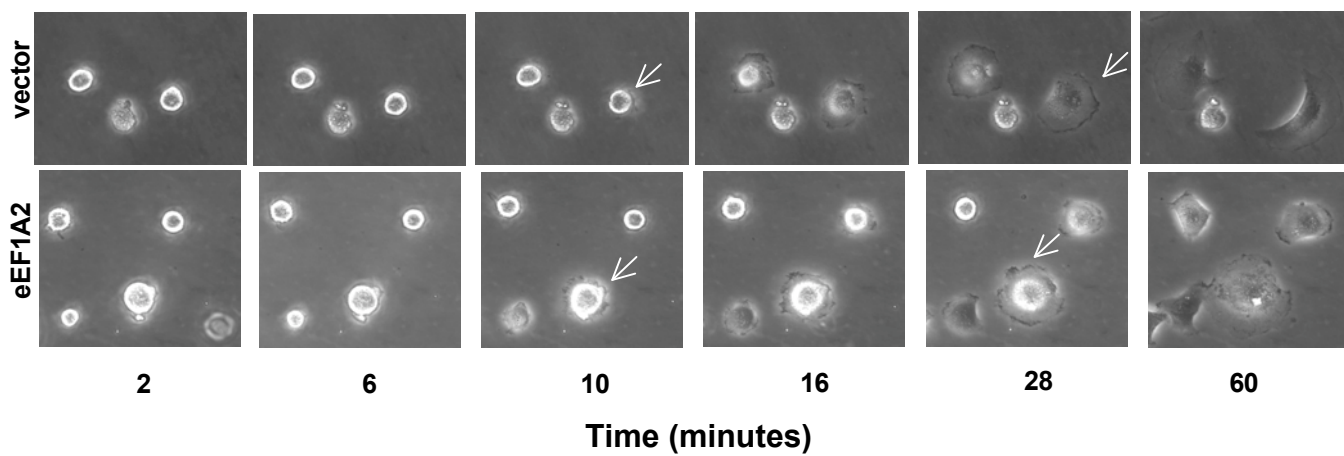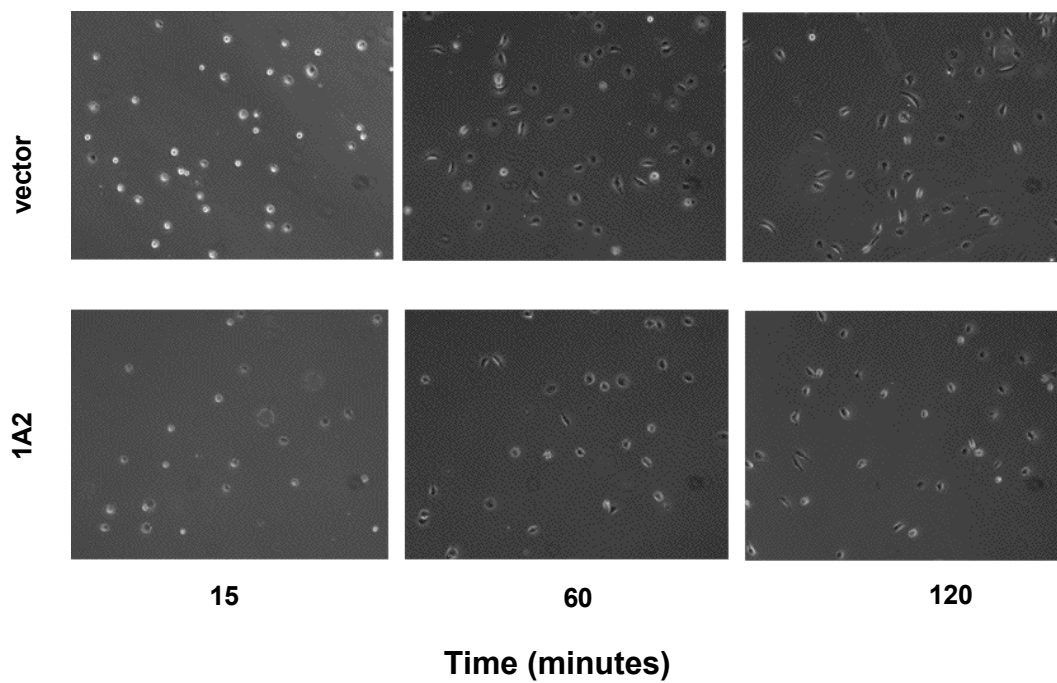
Binding of Elongation Factor eEF1A2 to Phosphatidylinositol-4 Kinase β Stimulates Lipid Kinase Activity and Phosphatidylinositol-4 Phosphate Generation.*

Sujeeve Jeganathan[1] and Jonathan M. Lee[1,2]

Running Title: eEF1A2 activates PI4KIIIβ

[1]Department of Biochemistry, Microbiology, & Immunology, University of Ottawa, 451 Smyth Road, Ottawa, Ontario, Canada K1H 8M5.
[2]To whom correspondence should be addressed: Department of Biochemistry, Microbiology, & Immunology, University of Ottawa, 451 Smyth Road, Ottawa, Ontario, Canada K1H 8M5. Tel: 613-562-5800 x8640. Fax: 613-562-5452. Email: jlee@uottawa.ca

Eukaryotic Protein Translation Elongation Factor 1 alpha 2 (eEF1A2) is an oncogene that transforms mammalian cell lines and increases their tumorigenicity in nude mice. Increased expression of eEF1A2 occurs during the development of breast, ovarian and lung cancer. Here, we report that eEF1A2 directly binds to and activates phosphatidylinositol-4 kinase IIIβ (PI4KIIIβ), an enzyme that converts phosphatidylinositol to phosphatidyl-inositol-4 phosphate (PI4P). Purified recombinant eEF1A2 increases PI4KIIIβ lipid kinase activity *in vitro* and expression of eEF1A2 in rat and human cells is sufficient to increase overall cellular phosphatidylinositol-4 kinase (PI4K) activity and intracellular PI4P abundance. siRNA-mediated reduction in eEF1A2 expression concomitantly reduces PI4K activity. This identifies a physical and functional relationship between eEF1A2 and PI4KIIIβ.

eEF1A2 is one of two members of the eEF1A family of proteins (eEF1A1 and eEF1A2). During protein translation elongation, eEF1A proteins bind amino-acylated tRNA and facilitate their recruitment to the ribosome (1). Aside from their canonical role in protein translation, eEF1A proteins have other functions, including binding actin and inducing rearrangements of the actin and tubulin cytoskeleton (2,3). The inactivation of the mouse eEF1A2 homolog, *Eef1a2*, leads to immunodeficiency and death by 30 days of age (4,5).

Mammalian eEF1A2 mRNA can be detected only in normal mammalian heart, brain and skeletal muscle tissues (6-8). However, high levels of eEF1A2 protein and mRNA are observed in a 30-60% fraction of ovarian, breast and lung tumors (9-12). We have previously reported that eEF1A2 has transforming properties: ectopic expression of wild type human eEF1A2 in mammalian cells enables anchorage-independent growth and enhances tumorigenicity in nude mice (9). Thus, eEF1A2 has an important role in promoting tumor development. However, the mechanism by which eEF1A2 promotes oncogenicity remains unclear.

It has previously been reported that an eEF1A-like protein purified from carrots,

PIK-A49, binds and activates carrot phosphatidylinositol-4 kinase (PI4K) (13,14). This suggests an important relationship between translation elongation and phosphatidylinositol (PI) generation. PIs are negatively charged, membrane-bound phospholipids that serve as regulators of multiple signaling pathways (15-18). PIs are composed of an inositol ring covalently bound to a lipid phosphatidic acid backbone by a phosphodiester bond at the inositol D1 carbon. Inositol phosphorylation occurs at the D3, D4, or D5 carbons. Specific kinase families are responsible for phosphorylation at each of these sites. Phosphatidylinositol-3 kinases (PI3K), phosphatidylinositol-4 kinases (PI4K), and phosphatidylinositol-5 kinases (PI5K) phosphorylate the D3, D4, and D5 inositol carbons respectively (15-17).

PIK-A49 showed *in vitro* translation elongation factor activity and an ability to activate *in vitro* PI4K lipid kinase activity (13,14). However, PIK-A49 does not have complete amino acid sequence identity with wild-type carrot eEF1A and has yet to be cloned as a full-length cDNA. It is therefore unclear whether PIK-A49 is a bonafide eEF1A protein. Neither is it known whether wild-type carrot eEF1A, or eEF1A proteins from non-plant species, participate in PI4K activation. In addition, there are three identified sub-families of PI4K proteins, PI4KIIIα, PI4KIIIβ and PI4KII (19,20), and it is unclear which PI4K isoform(s) are activated by PIK-A49 or other eEF1A proteins. Moreover, *in vitro* PI4K activation by PIK-A49/eEF1A has unknown physiological significance.

Here we report that human eEF1A2 can directly bind and activate PI4KIIIβ. Ectopic expression of eEF1A2 in rodent and human cells increases overall PI4K activity and cellular PI4P generation. Furthermore,

eEF1A2 ablation reduces endogenous PI4K activity. This suggests that eEF1A2 is a physiological regulator of PI4KIIIβ.

EXPERIMENTAL PROCEDURES

Cell lines. MCF7, BT549, and Rat2 cells were purchased from the American Type Culture Collection (ATCC) and grown according to ATCC instructions.

Adenoviral vectors. eEF1A2 was subcloned into the pShuttle-IRES plasmid (*EcoRV/XhoI*) with a Flag epitope tag. eEF1A2 and GFP virus were manufactured by the Adenoviral Core Facility of the University of Ottawa. For viral transduction, BT549 and Rat2 cells were infected with Ad-eEF1A2 or Ad-GFP at a multiplicity of infection (MOI) of 200 (BT549) or 500 (Rat2) in complete media. Cells were incubated with virus for a minimum of 24 hours.

Antibodies. Antibodies used for experiments are as follows: human PI4KIIIβ (Upstate Cell Signaling Solutions), β-actin (Sigma), HRP-conjugated goat anti-mouse IgG (Upstate Cell Signaling Solutions), HRP-conjugated anti-rabbit IgG, (Cell Signaling Technology), Golgin-97 (Molecular Probes). The generation of the rabbit polyclonal eEF1A2 antibody and its validation in western blotting, immunoprecipitation, and immuno-histochemistry is described elsewhere (10).

GST fusion proteins. eEF1A2 cDNA was cloned into the *EcoRI/NotI* site of pGEX-4T2 (Pharmacia). GST-eEF1A2 was transformed into *E coli* BL21DE3 and grown in LBA to $A_{600.}$ ~0.7. 0.5mM IPTG was added for 2 hours at 25°C. Bacteria were lysed in 25mM HEPES; pH7.9, 100mM KCl, 2 mM EDTA, 20% glycerol, 2mM DTT, and 1X protease inhibitor

cocktail (Roche). Glutathione Sepharose 4B beads (Amersham Bioscience) were equilibrated in lysis buffer and mixed with sonicated suspensions. PI4KIIIβ in pGEX-6P-3 was a gift of T. Balla (21,22). The GST-PI4KIIIβ fusion protein was purified as described (22). GST-C/EBPβ was a kind gift from N. Wiper-Bergeron (University of Ottawa). To remove the GST moiety, 100µg of GST-eEF1A2 was incubated overnight with 1U of Thrombin (Amersham) in 1x PBS at room temperature. PI4KIIIβ was generated by cleaving 100µg of GST-PI4KIIIβ with 1U of PreScission Protease (Amersham Biosciences) in 50 mM Tris-HCl, 150 mM NaCl, 1 mM EDTA, 1 mM DTT, pH 7.0 at 4°C.

Lipid kinase assay. 10 ul of recombinant protein in PBS, at concentrations indicated in the figure legends, was added to 35µl of kinase buffer (1mM EDTA, 30mM Hepes; pH 7.4, 100mM NaCl, 2mM $MgCl_2$, and 0.2% Triton X-100), 3mM PI (or as indicated in the figure legend) and 5µl of 10mM ATP containing 10µCi of ^{32}P-ATP, and incubated for 60 minutes. The reaction was stopped by the addition of 60µl of 1N HCl. Phospholipids were extracted by adding 160µl of $CHCl_3$:MeOH (1:1, v/v). After a brief vortex, samples were centrifuged for 10 minutes at 10000 x *g*. Aliquots of the organic phase (10-20µl) were spotted onto TLC plates (Sigma) and placed in a pre-equilibrated tank containing $CHCl_3$:acetone:MeOH:HOAc:water (46:17:15:14:8, v/v). Prior to use, TLC plates were precoated with 1% potassium oxalate, 3mM EDTA in methanol:water (2:3, v/v) for one hour and allowed to air dry overnight. Plates were activated by baking for 1 hour at 110 °C. Phosphatidylinositol standards were purchased from Avanti Polar Lipids, Inc.. PI4P spots were scraped and dissolved in 1-2 ml of water. Aliquots were

then diluted in BetaMax scintillation fluid (ICN Biomedicals) and scintillation counts were taken using the Wallac 1414 Liquid Scintillation Counter (Fisher Scientific Limited). Values of K_m, V_{max}, and K_{cat} were determined using the GraphPad Prism software (San Diego, California, USA). For assays involving cell lysates, recombinant eEF1A2 and the cell lysate was added in a total volume of 10 ul.

Crosslinking studies. Purified eEF1A2 and/or PI4KIIIβ (without GST) were incubated in PBS and crosslinked with 30mM dimethyl pimelimidate (DMP; Pierce) in 0.2M ethanolamine, pH 8.0 at room temperature. Reactions were stopped by addition of glacial acetic acid at a 1:4 (v/v) to the sample. Proteins were concentrated to a final volume of 50µl with Microcon Centrifugal Filter Devices (Millipore and loaded onto a 5% phosphate non-denaturing polyacrylamide gel and detected by coomassie staining.

Cell Lysis and Co-immunoprecipitation. For co-immunoprecipitation, cells were grown to 80-95% confluence in 100mm cell culture plates. Cells were lysed by sonication on ice in detergent-free buffer (137mM NaCl, 8mM KH_2PO_4 (pH 7.5), 2.7mM KCl, 2.5mM EDTA, and 1% Aprotonin, 1mg/ml leupeptin, 50mM NaF, 1mM Na_3VO_4, 10µg/ml pepstatin, 1mM PMSF). Protein levels were quantified using a Bradford assay (BioRad) according to the manufacturer's instructions and 100 µg of total protein was pre-cleared with protein G sepharose (Amersham Biosciences) for one hour at 4°C. Following this, 2-4µg of PI4KIIIβ, Flag, or eEF1A2 antibody coupled to beads were added and incubated overnight at 4°C. Beads were washed 3X in PBS, centrifuged, boiled for 5 minutes in Sample Buffer, and the supernatant subjected to SDS-PAGE. The covalent

coupling of the eEF1A2 antibody to protein A agarose beads was performed using a previously described protocol (23). Western blot detection was according to manufacturers' instructions or as described for the eEF1A2 antibody (10).

For Western blotting, cells were lysed in RIPA buffer (50mM Tris–Cl; pH 7.4, 1% Triton X-100, 1% sodium deoxycholate, 0.1% SDS, 1mM EDTA; pH 7.0, 150mM NaCl and 1% Aprotonin, 1mg/ml leupeptin, 50mM NaF, 1mM Na$_3$VO$_4$, 10μg/ml pepstatin in ethanol, and 1mM PMSF in DMSO).

siRNA transfections. Sequences of the eEF1A2 siRNAs are 5'-UGGUCC-UUUUGUCAAUACCtc-3' (siRNA #1) and 5'–UCGAACUUCUCAAUGGUCCtt-3' (siRNA #2). The negative control (NC) siRNA was purchased from Ambion (Cat. # 4611). siRNA transfections were performed using siPORT Lipid (Ambion) according to manufacturer's instructions.

Immunofluorescence. For the colocalization studies, MCF7 cells were fixed in 3.7% formaldehyde for 20 minutes at room temperature, washed 3X in PBS and permeabilized with 0.5% Triton X-100 in PBS for 15 minutes at room temperature. Following a one hour blocking period (5% fetal bovine serum in PBS) eEF1A2 was detected with the eEF1A2 antibody (1:100 in PBS, overnight) followed by an AlexaFluor 549 goat anti-rabbit IgG (1 in 450 in PBS, 1 hour; Molecular Probes). P I4KIIIβ was detected with a mouse IgG2a PI4KIIIβ antibody (1 in 500, overnight; BD Transduction Laboratories) followed by an AlexaFluor 488 goat anti-mouse IgG (1:450 in PBS, 1 hour; Molecular Probes). Golgi were detected with anti-human Golgin-97 (1:1000 in PBS, overnight, Molecular Probes) and an

AlexaFluor 488 goat anti-mouse IgG (1:450 in PBS, 1 hour; Molecular Probes). Cell nuclei were stained with Hoescht 33258 (20μg/ml; Sigma) for 10 minutes at room temperature. Slides were sealed with mounting media and viewed with an Olympus Fluoview FV1000 Laser Scanning Confocal Microscope. Fluorescence and colocalization was quantified using Olympus software (FV1000 Ver.01.04a).

To detect PI4P levels, Rat2 and BT549 cells were transfected with either eEF1A2-pcDNA3.1 (9) or GFP-pcDNA3.1 using Lipofectamine2000 (Invitrogen) according to manufacturer's instructions Five hours post-transfection, transfection media was removed and complete media added. The next day, cells were fixed and permeabilized as above. Cells were then blocked with 10% goat serum / PBS for 30 minutes at 37°C and anti-PI4P IgM antibody added (1:100 in PBS, overnight; Echelon Biosciences Inc.). Goat anti-mouse IgM, R-phycoerythrin (Caltag Laboratories) was then added at 1:100 in PBS for 30 minutes. eEF1A2 was detected with a monoclonal anti-V5 antibody (1:500 in PBS, 1 hour; Sigma) followed by an AlexaFluor 488 goat anti-mouse IgG (1:450 in PBS, 1 hour; Molecular Probes). Cell nuclei were stained with Hoescht 33258 (20μg/ml; Sigma) for 10 minutes at room temperature. Slides were viewed with either a Leica DM-1L Fluorescence microscope and deconvolved using Improvision 3.1 software or a Olympus FluoView FV1000 Laser Scanning Confocal microscope. Fluorescence was quantified with the confocal microscope using Olympus software (FV1000 Ver.01.04a).

RESULTS

eEF1A2 increases PI4KIIIβ lipid kinase activity. To determine whether eEF1A2

could activate PI4KIIIβ, we purified recombinant GST-eEF1A2 and GST-PI4KIIIβ. The proteins were isolated both with and without their GST moiety. A coomassie-stained gel of the purified proteins is shown in Fig. 1*A*. The predicted molecular weight of full-length, wild-type eEF1A2 is ~54 kDa and that of PI4KIIIβ is ~100 kDa.

We first determined whether eEF1A2 could increase PI4K activity in cell lysates. As shown in Fig. 1*B*, addition of GST-eEF1A2 to a cell lysate of BT549 breast carcinoma cells reproducibly doubled *in vitro* phosphatidylinositol-4 phosphate (PI4P) generation compared to the addition of GST alone or GST-coupled to the C/EBPβ transcription factor. A representative TLC plate is also shown in the right panel of Fig. 1*B*.

Bacterially expressed PI4KIIIβ has previously been reported to be active in *in vitro* lipid kinase assays (21,22). As shown in Fig. 1*C*, our GST-PI4KIIIβ is active *in vitro* and its kinase activity is inhibitable by 0.2μM Wortmannin. Wortmannin inhibition indicates that we are measuring the lipid kinase activity of a type III PI4 kinase, the family of PI4 kinases to which PI4KIIIβ belongs. To investigate whether purified eEF1A2 could directly activate PI4KIIIβ, we next added recombinant eEF1A2 (without GST) to purified PI4KIIIβ (without GST). As shown in Fig. 1*D*, eEF1A2 increased PI4KIIIβ lipid kinase activity in a dose-dependent manner. PI4KIIIβ activity was increased approximately two-fold. 100-200nM eEF1A2 is required to maximally activate a 100nM solution of PI4KIIIβ. No enhancement of PI4KIIIβ activity was observed in the presence of bovine albumin (BSA).

In order to further determine how eEF1A2 affected PI4KIIIβ activity, we experimentally determined the PI4KIIIβ K_m, V_{max}, and K_{cat} for phosphatidylinositol with and without eEF1A2. Bovine albumin served as the control. As shown in Fig. 1*E*, eEF1A2 (without GST) reproducibly increased the V_{max} of PI4KIIIβ (without GST) from 0.62 to 1.11 μmole/min/mg. This doubling of V_{max} was also mirrored in the increase of K_{cat} from 0.82 to 1.48 sec^{-1}. The PI4KIIIβ K_m was unchanged.

eEF1A2 binds PI4KIIIβ. We next tested whether eEF1A2 could directly interact with PI4KIIIβ in a cell-free system. As shown in Fig. 2*A*, purified PI4KIIIβ (without GST) was immunoprecipitated by GST-eEF1A2 and eEF1A2 (without GST) was immunoprecipitated by GST-PI4KIIIβ. Neither PI4KIIIβ nor eEF1A2 immunoprecipitated with GST alone. We next investigated the stoichiometry of eEF1A2 / PI4KIIIβ interaction. We incubated recombinant eEF1A2 and PI4KIIIβ (both without GST) and chemically crosslinked the resulting complex. As seen in Fig. *2B*, after an hour of incubation, most of the added PI4KIIIβ and eEF1A2 are found in a complex with an apparent molecular weight (MW) of 165kDa. The formation of the complex is time-dependent and a greater amount of complex is detected at 60 minutes of incubation relative to the 30 minute time point. eEF1A2 has an apparent MW of ~60kDa and that of PI4KIIIβ is ~100kDa. The ~165kDa MW of the complex indicates that eEF1A2 and PI4KIIIβ associate with a 1:1 stoichiometry. Neither eEF1A2 nor PI4KIIIβ form detectable multimers on their own. We were unable to detect protein complexes with a MW greater than 165 kDa, indicating that multimers containing more

than one molecule each of eEF1A2 or PI4KIIIβ do not form.

eEF1A2 interacts with PI4KIIIβ in mammalian cell lines. To determine whether eEF1A2 and PI4KIIIβ associate in cells, we first identified mammalian cells that express eEF1A2. In rodents and humans, eEF1A2 shows detectable mRNA and protein expression only in the tissues of the heart, brain and skeletal muscle (6-8). We have also observed eEF1A2 expression in many breast cancer cell lines (10). As shown in Fig. 3*A*, we detect eEF1A2 protein expression in the MCF7 human breast carcinoma cell line but not in BT549 breast carcinoma cells nor in the non-transformed Rat2 rat fibroblast cell line.

We then used co-immunoprecipitation to determine whether wild-type eEF1A2 and PI4KIIIβ associate in MCF7 cells. We use detergent-free cell lysis for these experiments. As shown in Fig. 3*B*, eEF1A2 detectably immunoprecipitates with PI4KIIIβ and PI4KIIIβ reciprocally immunoprecipitates with eEF1A2. Neither protein binds to the Flag antibody control. While immunoprecipitation is only semi-quantitative, we estimate that approximately ~10% of endogenous PI4KIIIβ associates with eEF1A2 under detergent-free lysis conditions. A similar ratio of eEF1A2 is associated with PI4KIIIβ.

eEF1A2 co-localizes with PI4KIIIβ in mammalian cell lines. To extend the co-immunoprecipitation data, we used confocal microscopy to visualize the cellular localization of eEF1A2 and PI4K in intact MCF7 cells. As shown in Fig. 4, and consistent with previous observations, PI4KIIIβ is found predominantly in the cytoplasm with substantial presence in the Golgi apparatus (19,20). eEF1A2 is found in the cytoplasm, nuclear membrane and to a limited extent in the nucleus. Superimposing the eEF1A2 and PI4KIIIβ images reveals some co-localization of the two proteins. Co-localizing eEF1A2/PI4KIIIβ proteins are found in the cytoplasm without dramatic concentration at either the plasma or nuclear membranes. Golgi PI4KIIIβ appears not to be co-localized with eEF1A2 and nuclear membrane eEF1A2 does not appear to co-localize with PI4KIIIβ. To further confirm that eEF1A2 is not found in the Golgi, we used confocal microscopy to determine that eEF1A2 does not co-localize with Golgin, a Golgi marker (Supplementary Figure 1). Thus, eEF1A2 and PI4KIIIβ co-localize in intact human cells, but this co-localization is restricted to the non-Golgi cytoplasm.

eEF1A2 is sufficient to increase cellular PI4K activity. To determine whether eEF1A2 expression was sufficient to increase PI4K activity in mammalian cells, we used an adenovirus to express eEF1A2 in BT549 and Rat2 cells. Neither cell line detectably expresses eEF1A2 without transduction (Fig. 3*A*). At a low multiplicity of infection (MOI) of 20 virus particles per cell, infection had little effect on PI4K activity; lipid phosphorylation was similar between eEF1A2-infected cells and those infected with GFP (Fig. 5*A*). However, increasing the MOI to 200 reproducibly doubled cellular PI4K activity in eEF1A2-infected cells relative to those infected with GFP (Fig. 5*A*). Similarly, infection of Rat2 cells with the eEF1A2 adenovirus doubled PI4K activity relative to GFP controls (Fig. 5*B*). Adenoviral infection by eEF1A2 does not detectably alter total PI4KIIIβ protein levels (Fig. 5*C*). Thus, eEF1A2 expression can increase PI4K activity in these mammalian cell lines.

eEF1A2 is a physiological PI4K regulator. To determine whether eEF1A2 had a physiological role in regulating PI4K activity, we reduced eEF1A2 protein levels in MCF7 cells. MCF7 cells express abundant eEF1A2 (Fig. 3*A*). For this purpose, we designed two eEF1A2-specific siRNAs. As shown in Fig. 6, both siRNAs substantially reduce eEF1A2 protein levels compared to those cells treated with a control siRNA or untreated cells. Some residual eEF1A2 remains, however. The siRNA-mediated decrease in eEF1A2 protein levels leads to a concomitant two-fold decrease in PI4K activity relative to controls.

eEF1A2 increases cellular PI4P generation. We next determined whether eEF1A2 could increase intracellular PI4P abundance. To this end, we transiently transfected Rat2 and BT549 cells with an eEF1A2 plasmid and stained these cells with an antibody specific for PI4P. As shown in Fig. 7*A*, BT549 and Rat2 cells transiently expressing eEF1A2 show PI4P staining that is visibly brighter than in untransfected cells, indicating greater abundance of PI4P upon eEF1A2 expression. The increase in PI4P occurs throughout the cytosol (Fig. 7*A*). Transfection with GFP had no visible effect on PI4P levels (Fig. 7*B*). To quantitate the eEF1A2-dependent increase in PI4P generation, we divided each transfectant pool into groups based on expression of the transfected protein and quantified PI4P fluorescence in individual cells from each group. As shown in Fig. 7*C*, cells expressing moderate or high levels of eEF1A2 each have a significantly higher level of PI4P than those that express no/low eEF1A2 ($p < 0.001$, Mann-Whitney). This increase of PI4P generation occurred in both Rat2 and BT549 cells transfected with eEF1A2. GFP had no effect on PI4P

generation. Thus, eEF1A2 expression increases intracellular PI4P abundance.

DISCUSSION

Phosphatidylinositol lipids are well-documented participants in pathways that regulate organelle biogenesis, cell morphology, proliferation and oncogenesis (24). In this report, we show that eEF1A2 binds phosphatidylinositol-4 kinase III beta (PI4KIIIβ), increases its *in vitro* lipid kinase activity and can increase intracellular PI4P generation in rat and human cells.

We find that purified eEF1A2 can increase recombinant PI4KIIIβ activity *in vitro*. Two other direct PI4KIIIβ activators have been previously identified: ADP Ribosylation Factor (ARF) and Neuronal Calcium Sensor-1 (NCS-1)(25,26). ARF, a small GTPase, regulates Golgi function through PI4KIIIβ activation (26). NCS-1 controls IgE-mediated exocytosis in mast cells through PI4KIIIβ(27). Since we find that eEF1A2-directed siRNA reduces PI4K activity and that ectopic eEF1A2 expression increases this activity, it is likely that eEF1A2 is a novel and physiological PI4KIIIβ activator.

In human cells, the majority of PI4K activity is associated with the plasma membrane and the membranes of the nucleus, lysosome, Golgi, and endoplasmic reticulum (20,28-31). PI4Ks are also known to localize and be active in several specialized organelles and secretory vesicles (31). The yeast homolog of mammalian PI4KIIIβ, *PIK1*, has been studied in great detail (32-37). Pik1p, the protein encoded by *PIK1*, is essential for normal secretion, Golgi and vacuole membrane dynamics, and endocytosis (32-37). Pik1p localizes to the nucleus and the *trans*-Golgi (33,37). *Pik1^{ts}*

cells exhibit a defect in secretion of Golgi-modified secretory pathway cargos (35). Mammalian PI4KIIIβ is heavily concentrated in the Golgi apparatus(38,39), although we find detectable protein in the non-Golgi cytoplasm. However, we do not see appreciable eEF1A2 protein in the Golgi and there is therefore little co-localization between Golgi PI4KIIIβ and eEF1A2. The co-localization we observe between PI4KIIIβ and eEF1A2 cells is in the non-Golgi cytoplasm. We have observed no consistent Golgi defects in eEF1A2-expressing cells (not shown), suggesting that eEF1A2's capacity to increase PI4P formation is regulating some non-Golgi aspect of cell physiology. Active PI4K is observed in the non-Golgi cytosol (40) and we find that eEF1A2 expression increases PI4P generation throughout the cell.

The molecular mechanism by which eEF1A2 activates PI4KIIIβ is currently unknown. eEF1A proteins bind and hydrolyze GTP, and bind tRNA. They have not been shown to have phospho-transferase activity or other capacity to covalently modify proteins. Thus it is unlikely that eEF1A2 affects PI4KIIIβ activity by post-translationally modifying it. Because eEF1A2 expression does not increase steady-state PI4KIIIβ protein levels (Fig. 5C), it is unlikely that eEF1A2 expression increase cellular PI4P generation by increasing the amount of PI4KIIIβ message being translated. We propose that direct interaction between eEF1A2 and PI4KIIIβ leads to a conformational change in PI4KIIIβ that increases its catalytic activity. This hypothesis is consistent with our observations that eEF1A2 increases the overall PI4KIIIβ catalytic rate (K_{cat}) and makes PI4KIIIβ a more efficient kinase (V_{max}/K_m). While the possibility of this conformational change remains an open one,

we do not believe that eEF1A2 is a general phosphatidylinositol kinase activator. We have been unable to detect physical interaction between eEF1A2 and PI3K nor have we observed activation of this kinase by eEF1A2 (data not shown).

Our *in vitro* results suggest that eEF1A2 and PI4KIIIβ bind in a 1:1 stoichiometry and the majority of recombinant eEF1A2 and PI4KIIIβ are competent to physically interact with each other. However, up to a two-fold molar excess of recombinant eEF1A2 is required to maximally increase *in vitro* PI4KIIIβ activity. Thus, it is possible that some post-translational modification of eEF1A2 may enhance its ability to activate PI4KIIIβ. Yang and colleagues showed that dephosphorylation of PIK-A49 prevented it from activating PI4KIIIβ,and that activation could be restored by *in vitro* phosphorylation of PIK-A49 by a calcium-dependent protein kinase (14). The possibility of post-translational modification of eEF1A2 enhancing PI4KIIIβ activity is intriguing. However, no post-translational modifications of eEF1A2 have yet been identified and our results indicate that post-translational modification of eEF1A2 is not obligatory for PI4KIIIβ activation.

eEF1A2 is highly expressed in a 30-60% fraction of breast, ovary and lung tumors (9-12). We have previously reported that eEF1A2 has transforming properties (9) and that its inactivation in mice increases lymphoid apoptosis (41). This identifies eEF1A2 as an important human oncogene. We hypothesize that eEF1A2 activates oncogenesis through PI4K activation and PI4P generation. Our observation that eEF1A2 expression is sufficient to increase both PI4K activity and PI4P levels indicates that high eEF1A2 expression in human

tumors likely leads to an overall increase in cellular PI4P production. We propose that increased production of PI4P could increase the abundance of PI(4,5)P$_2$ and PI(3,4,5)P$_3$. Both these phospholipids are second messengers that regulate actin cytoskeletal organization, intracellular vesicular trafficking and proliferation (15,20,42-46). Of particular importance to oncogenesis would be PI(3,4,5)P$_3$, the abundance of which controls cell growth, apoptosis and cell invasiveness. While PI3K activity has long thought to be the rate-limiting step in the production of PI(3,4,5)P$_3$, this may not be the case in tumors that have high PI3K activity through oncogenic mutation of the kinase or have inactivating mutations in the PTEN lipid phosphatase (47). In those tumors with constitutively active PI3K or inactive PTEN, increased PI4K activity would be predicted to increase overall PI(3,4,5)P$_3$ abundance and activate PI(3,4,5)P$_3$-dependent signaling. This idea is consistent with a recent report by Pendaires and colleagues who show that the phosphatidylinositol-5 phosphate produced by the *Shigella* pathogen is sufficient to activate Akt (48), a serine threonine kinase whose activity is dependent on PI(3,4,5)P$_3$ abundance (49). No PI4K has been reported to activate PI(3,4,5)P$_3$ production, nor have PI4K genes been reported to be transforming or to be highly expressed during oncogenesis. However, this idea has not been fully explored.

eEF1A proteins have a well characterized ability to bind and bundle F-actin (2,3). It has been proposed that eEF1A2 couples the protein translation machinery to actin cytoskeleton assembly. Because we find that eEF1A2 directly binds PI4KIIIβ, it is probable that eEF1A2 links protein translation to phosphatidylinositol generation and the actin cytoskeleton.

In summary, we have identified eEF1A2 as a direct activator of PI4KIIIβ. Ectopic expression of eEF1A2 increases cellular PI4K activity and increases cellular PI4P abundance. Furthermore siRNA-mediated eEF1A2 inactivation decreases PI4K activity. This is consistent with the idea that eEF1A2 functionally and physiologically regulates PI4K function. We propose that PI4KIIIβ activation has an important role in eEF1A2-mediated tumorigenesis and transformation.

FOOTNOTES

The abbreviations used are: eEF1A2, eukaryotic elongation factor 1 alpha 2; PI. phosphatidylinositol; PI4K, phosphatidylinositol-4 kinase; PI4P, phosphatidylinositol-4

phosphate; siRNA, short-interfering RNA; GFP, green fluorescent protein; C/EBPβ,CAAT/enhancer binding protein β; GST, glutathione-S-transferase; DMP, dimethyl pimelimidate; CHCl₃, chloroform; MeOH, methanol; HOAC, acetic acid; TLC, thin-layer chromatography; MOI, multiplicity of infection; ARF, ADP-ribosylation factor; NCS-1, neuronal calcium sensor-1.

REFERENCES

1.   Hershey, J. W. (1991) *Annu Rev Biochem* **60**, 717-755
2.   Condeelis, J. (1995) *Trends Biochem Sci* **20**, 169-170
3.   Shiina, N., Gotoh, Y., Kubomura, N., Iwamatsu, A., and Nishida, E. (1994) *Science* **266**, 282-285
4.   Shultz, L. D., Sweet, H. O., Davisson, M. T., and Coman, D. R. (1982) *Nature* **297**, 402-404
5.   Chambers, D. M., Peters, J., and Abbott, C. M. (1998) *Proc Natl Acad Sci U S A* **95**, 4463-4468
6.   Knudsen, S. M., Frydenberg, J., Clark, B. F., and Leffers, H. (1993) *Eur J Biochem* **215**, 549-554
7.   Lee, S., Wolfraim, L. A., and Wang, E. (1993) *J Biol Chem* **268**, 24453-24459
8.   Kahns, S., Lund, A., Kristensen, P., Knudsen, C. R., Clark, B. F., Cavallius, J., and Merrick, W. C. (1998) *Nucleic Acids Res* **26**, 1884-1890
9.   Anand, N., Murthy, S., Amann, G., Wernick, M., Porter, L. A., Cukier, I. H., Collins, C., Gray, J. W., Diebold, J., Demetrick, D. J., and Lee, J. M. (2002) *Nat Genet* **31**, 301-305
10.   Kulkarni, G., Turbin, D. A., Amiri, A., Jeganathan, S., Andrade-Navarro, M. A., Wu, T. D., Huntsman, D. G., and Lee, J. M. (2006) *Breast Cancer Res Treat*
11.   Li, R., Wang, H., Bekele, B. N., Yin, Z., Caraway, N. P., Katz, R. L., Stass, S. A., and Jiang, F. (2005) *Oncogene*
12.   Tomlinson, V. A., Newbery, H. J., Wray, N. R., Jackson, J., Larionov, A., Miller, W. R., Dixon, J. M., and Abbott, C. M. (2005) *BMC Cancer* **5**, 113
13.   Yang, W., Burkhart, W., Cavallius, J., Merrick, W. C., and Boss, W. F. (1993) *J Biol Chem* **268**, 392-398
14.   Yang, W., and Boss, W. F. (1994) *J Biol Chem* **269**, 3852-3857
15.   Carpenter, C. L., and Cantley, L. C. (1990) *Biochemistry* **29**, 11147-11156
16.   Fruman, D. A., Meyers, R. E., and Cantley, L. C. (1998) *Annu Rev Biochem* **67**, 481-507
17.   Meijer, H. J., and Munnik, T. (2003) *Annu Rev Plant Biol* **54**, 265-306
18.   Overduin, M., Cheever, M. L., and Kutateladze, T. G. (2001) *Mol Interv* **1**, 150-159
19.   Balla, A., and Balla, T. (2006) *Trends Cell Biol* **16**, 351-361
20.   Heilmeyer, L. M., Jr., Vereb, G., Jr., Vereb, G., Kakuk, A., and Szivak, I. (2003) *IUBMB Life* **55**, 59-65
21.   Balla, A., Vereb, G., Gulkan, H., Gehrmann, T., Gergely, P., Heilmeyer, L. M., Jr., and Antal, M. (2000) *Exp Brain Res* **134**, 279-288
22.   Zhao, X. H., Bondeva, T., and Balla, T. (2000) *J Biol Chem* **275**, 14642-14648
23.   Harlow, E., and Lane, D. (1999) in *Using Antibodies: A Laboratory Manual*, pp. 522-523, Cold Spring Harbor Laboratory Press
24.   Pendaries, C., Tronchere, H., Plantavid, M., and Payrastre, B. (2003) *FEBS Lett* **546**, 25-31

25.	Zhao, X., Varnai, P., Tuymetova, G., Balla, A., Toth, Z. E., Oker-Blom, C., Roder, J., Jeromin, A., and Balla, T. (2001) *J Biol Chem* **276**, 40183-40189

26.	Godi, A., Pertile, P., Meyers, R., Marra, P., Di Tullio, G., Iurisci, C., Luini, A., Corda, D., and De Matteis, M. A. (1999) *Nat Cell Biol* **1**, 280-287

27.	Kapp-Barnea, Y., Melnikov, S., Shefler, I., Jeromin, A., and Sagi-Eisenberg, R. (2003) *J Immunol* **171**, 5320-5327

28.	Liu, G., Loraine, A. E., Shigeta, R., Cline, M., Cheng, J., Valmeekam, V., Sun, S., Kulp, D., and Siani-Rose, M. A. (2003) *Nucleic Acids Res* **31**, 82-86

29.	Larijani, B., Barona, T. M., and Poccia, D. L. (2001) *Biochem J* **356**, 495-501

30.	Raben, D. M., and Baldassare, J. J. (2000) *Eur J Histochem* **44**, 67-80

31.	Guo, J., Wenk, M. R., Pellegrini, L., Onofri, F., Benfenati, F., and De Camilli, P. (2003) *Proc Natl Acad Sci U S A* **100**, 3995-4000

32.	Audhya, A., Foti, M., and Emr, S. D. (2000) *Mol Biol Cell* **11**, 2673-2689

33.	Garcia-Bustos, J. F., Marini, F., Stevenson, I., Frei, C., and Hall, M. N. (1994) *Embo J* **13**, 2352-2361

34.	Hama, H., Schnieders, E. A., Thorner, J., Takemoto, J. Y., and DeWald, D. B. (1999) *J Biol Chem* **274**, 34294-34300

35.	Nguyen, P. H., Hasek, J., Kohlwein, S. D., Romero, C., Choi, J. H., and Vancura, A. (2005) *FEMS Yeast Res* **5**, 363-371

36.	Sciorra, V. A., Audhya, A., Parsons, A. B., Segev, N., Boone, C., and Emr, S. D. (2005) *Mol Biol Cell* **16**, 776-793

37.	Walch-Solimena, C., and Novick, P. (1999) *Nat Cell Biol* **1**, 523-525

38.	Weisz, O. A., Gibson, G. A., Leung, S.-M., Roder, J., and Jeromin, A. (2000) *J. Biol. Chem.* **275**, 24341-24347

39.	Bruns, J. R., Ellis, M. A., Jeromin, A., and Weisz, O. A. (2002) *J Biol Chem* **277**, 2012-2018

40.	Drobak, B. K., Dewey, R. E., and Boss, W. F. (1999) *Int Rev Cytol* **189**, 95-130

41.	Potter, M., Bernstein, A., and Lee, J. M. (1998) *Cell Immunol* **188**, 111-117

42.	Balla, T. (1998) *Biochim Biophys Acta* **1436**, 69-85

43.	Gehrmann, T., and Heilmeyer, L. M., Jr. (1998) *Eur J Biochem* **253**, 357-370

44.	Huijbregts, R. P., Topalof, L., and Bankaitis, V. A. (2000) *Traffic* **1**, 195-202

45.	Maruta, H., He, H., Tikoo, A., Vuong, T., and Nur, E. K. M. (1999) *Microsc Res Tech* **47**, 61-66

46.	Insall, R. H., and Weiner, O. D. (2001) *Dev Cell* **1**, 743-747

47.	Wymann, M. P., and Marone, R. (2005) *Curr Opin Cell Biol* **17**, 141-149

48.	Pendaries, C., Tronchere, H., Arbibe, L., Mounier, J., Gozani, O., Cantley, L., Fry, M. J., Gaits-Iacovoni, F., Sansonetti, P. J., and Payrastre, B. (2006) *Embo J* **25**, 1024-1034

49.	Downward, J. (2004) *Semin Cell Dev Biol* **15**, 177-182

FIGURE LEGENDS

Figure 1. eEF1A2 activates PI4KIIIβ lipid kinase activity. *A*. Coomassie stain of purified recombinant eEF1A2 and PI4KIIIβ proteins, with and without their GST moiety. 30μg of each sample were loaded on a 10% SDS-PAGE gel. *B*. *Left Panel*. Addition of 10 uM GST-eEF1A2 to a protein lysate from BT549 cells increases total PI4K lipid kinase activity relative to the addition of GST alone or GST-C/EBPβ. Activation is calculated relative to the GST alone control and is the mean and standard deviation of three independent experiments with triplicate scintillation counts. Significant activation (p<0.05, Student's *t*-test) is indicated by (*). *Right Panel*. A representative TLC plate from one of the kinase assays. *C*. Purified recombinant GST- PI4KIIIβ protein has lipid kinase activity (open circles) that is inhibited by 0.2μM Wortmanin (closed circles). Fold increase is calculated relative to no protein control. Reaction contains 20 nM PI. *D*. PI4KIIIβ (GST-free) activity is increased by eEF1A2 (GST-free) addition (open circles) but not by bovine albumin (closed circles). Lipid kinase assays are the mean and standard deviation of triplicate experiments with 3mM phosphatidylinositol and 100nM PI4KIIIβ (GST-free). *E*. eEF1A2 increases the V_{max} of the reaction but not the K_m. *Top Panel*. A representative kinase assay using 100nM PI4KIIIβ (GST free) and either 2.5μM eEF1A2 (GST free) or 2.5μM bovine albumin. *Bottom Panel*. Summary of PI4KIIIβ kinetic parameters. Values are the means and standard deviations from three independent experiments. eEF1A2 significantly increases the V_{max} and K_{cat} values (* and ‡, respectively; p<0.0005, unpaired *t*-test with Welch correction) but not the K_m.

Figure 2. eEF1A2 and PI4KIIIβ interact in a cell-free system. *A*. 30μg of purified eEF1A2 or PI4KIIIβ, both GST free, were incubated with 30μg GST, GST-PI4KIIIβ, or GST-eEF1A2. Precipitated proteins were then detected by Western blotting (WB) with PI4KIIIβ or eEF1A2 antibodies (indicated). *B*.   The eEF1A2-PI4KIIIβ complex consists of a 1:1 molar ratio of eEF1A2 and PI4KIIIβ.   10 μM each of eEF1A2 or PI4KIIIβ (both without GST) were incubated for the indicated times and crosslinked with DMP. Purified eEF1A2 and PI4KIIIβ have apparent molecular weights of 60kDa and 100kDa, respectively.   Incubating a mixture of eEF1A2 and PI4KIIIβ results in a complex with an apparent molecular weight of ~165kDa.

Figure 3. eEF1A2 and PI4KIIIβ interact in human cells. *A*. eEF1A2 protein expression is detected in MCF7 cells but not in BT549 or Rat2 cells. Actin is the loading control. *B*. Antibodies for either eEF1A2 or PI4KIIIβ were used for immunoprecipitation (IP) in detergent-free whole cell lysates (WCL) of MCF7 cells. An anti-Flag antibody is used as a specificity control. Co-immunoprecipitating proteins were detected by Western blotting (WB) using eEF1A2 and PI4KIIIβ antibodies. The WCL lane contains 25 μg of total cellular protein and each immunoprecipitation was performed using 25 μg of protein lysate.

Figure 4. eEF1A2 and PI4KIIIβ co-localize in human cells. Confocal microscopy showing eEF1A2 and PI4KIIIβ protein localization in MCF7 cells. The left panels show cells stained for DNA (blue), PI4KIIIβ (green), or eEF1A2 (red). The Merge panel is DNA, PI4KIIIβ and eEF1A2 with pixels of co-localization shown in white. The DNA + colocalization panel shows only co-localized pixels and DNA. Right panels are a magnification of the field indicated by the

yellow boxes of the left panels. Golgi apparatus is indicated by arrows. Scale bars in the left and right panels are 40 and 12 um respectively.

Figure 5. eEF1A2 expression increases overall cellular PI4K activity. *A. Left Panel*. BT549 cells were transduced with Ad-eEF1A2 or Ad-GFP at a multiplicity of infection (MOI) of either 20 or 200 plaque forming units per cell. At a MOI of 20, there is no significant change in PI4P generation. At a MOI of 200, there is a significant increase in PI4K activity in eEF1A2 transduced cells relative to GFP transduced ones ($p<0.05$; Student's *t*-test). Fold activation is calculated relative to untransduced cells and is the mean and standard deviation of three independent experiments. *Right Panel*. A representative TLC plate. *B*. Transduction of Rat2 cells with Ad-eEF1A2 at a MOI of 500 similarly increases PI4K activity ($p<0.05$; Student's *t*-test). Protein levels of eEF1A2 and actin are shown. Control cells are untranduced. *C,* BT549 cells transduced with Ad-eEF1A2 do not show an increase in steady-state PI4KIIIβ protein levels as seen by Western blotting. Actin was used as a loading control and cells were transduced as figure 5A at an MOI of 200.

Figure 6. siRNA-mediated eEF1A2 downregulation decreases overall cellular PI4K activity in MCF7 cells. Two siRNAs directed against eEF1A2 decrease its steady state protein level in MCF7 cells (bottom panel; Western blot) relative to untreated cells or those treated with a negative control (NC) siRNA. Downregulation of eEF1A2 significantly decreased overall PI4K activity ($p<0.05$; Student's *t*-test). Fold activation is calculated relative to untreated cells and is the mean and standard deviation of three independent experiments.

Figure 7. Ectopic expression of eEF1A2 increases cellular PI4P abundance. *A*. Rat2 and BT549 cells were transiently transfected with an eEF1A2 expression plasmid and stained for DNA (blue), eEF1A2 (green) and PI4P (red). A higher magnification view of an eEF1A2-expressing cell (yellow box) is shown in the far right panels. *B*. Rat2 and BT549 cells were transiently transfected with a GFP expression plasmid and stained for DNA (blue) and PI4P (red). A GFP-expressing cell is marked by a yellow box. *C*. Quantification of eEF1A2-mediated increase in cellular PI4P levels. *Top Panel*. PI4P levels in eEF1A2-transfected Rat2 and BT549 cells expressing no/low, moderate, or high levels of eEF1A2. Cells expressing moderate or high levels of eEF1A2 each show significantly higher PI4P staining (both $p<0.0001$, Mann-Whitney test, *) than those expressing no/low eEF1A2. *Bottom Panel*. Quantification of PI4P staining in GFP-transfected Rat2 and BT549 cells expressing no/low, moderate and high levels of GFP. eEF1A2 staining was categorized as negative/low when the eEF1A2 fluorescence/unit area ratio was <1400, as moderate when this ration was between 1400-3500 for Rat2 or between 1400-2500 for BT549, and as high when the ratio exceeded 3500 or 2500 for Rat2 and BT549 respectively.

Supplementary Figure 1. eEF1A2 is not present in the Golgi. MCF7 cells were stained for DNA (blue), endogenous eEF1A2 (red) and the Golgi marker Golgin (green) and visualized by confocal microscopy. The eEF1A2 and Golgin merge shows no substantial colocalization. Scale bars are 40 um in length.
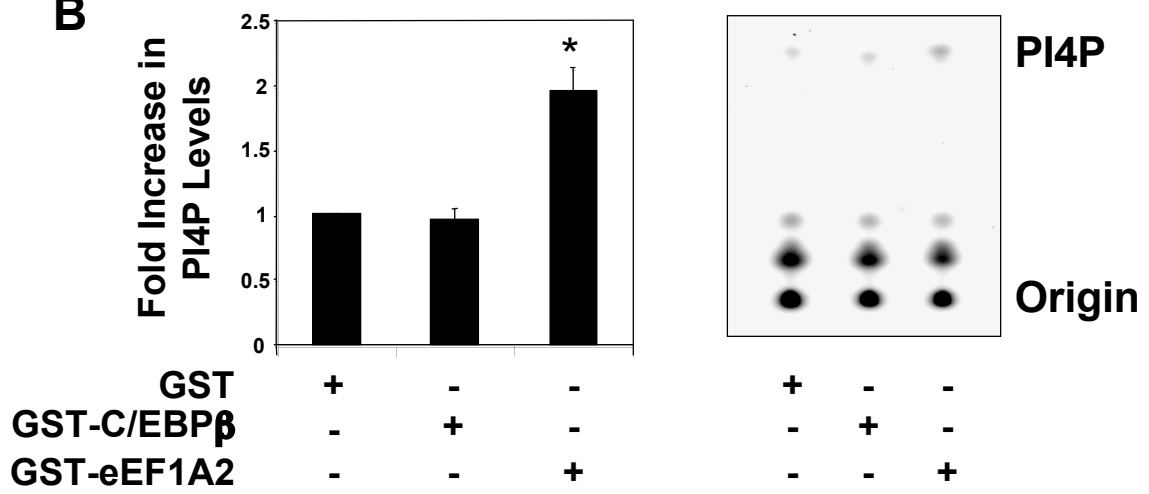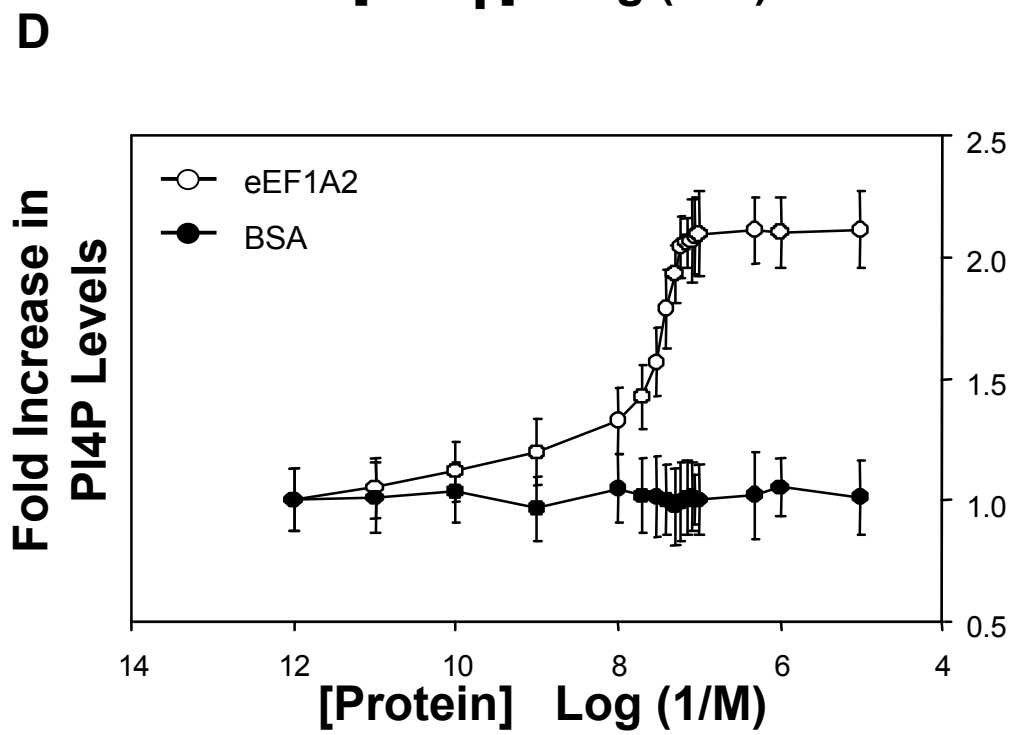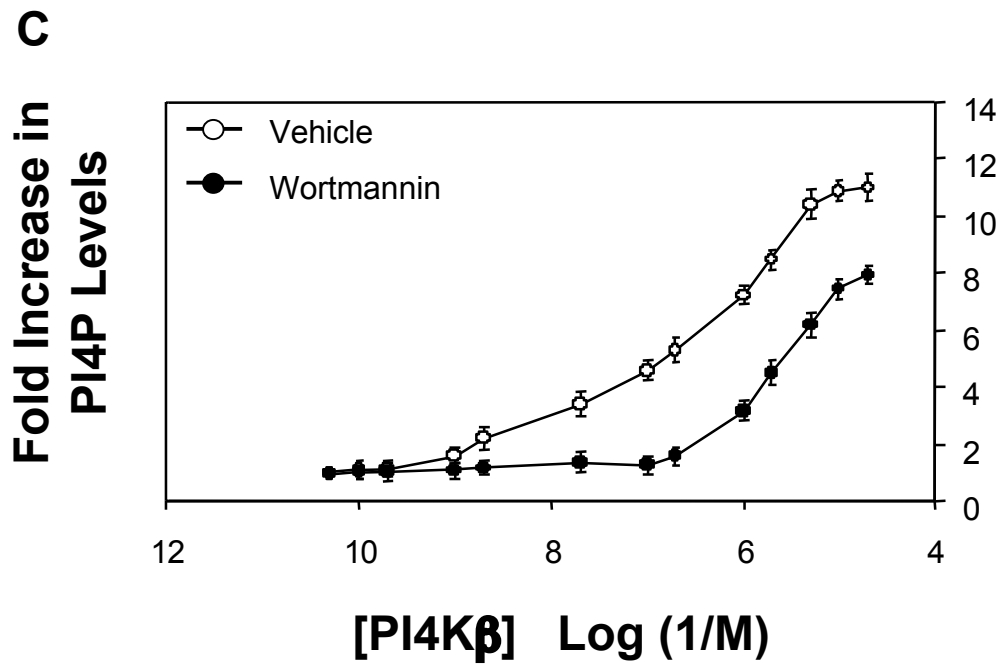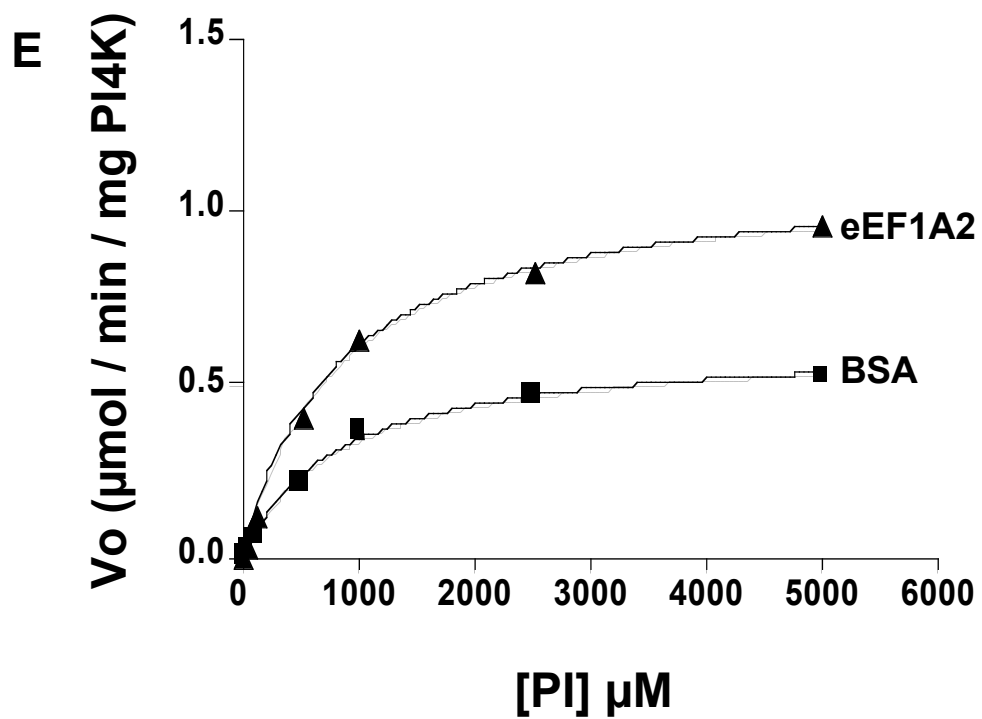
FIGURE 1

A

B

GST	+	-	-
GST-C/EBPβ	-	+	-
GST-eEF1A2	-	-	+

FIGURE 1

C

D
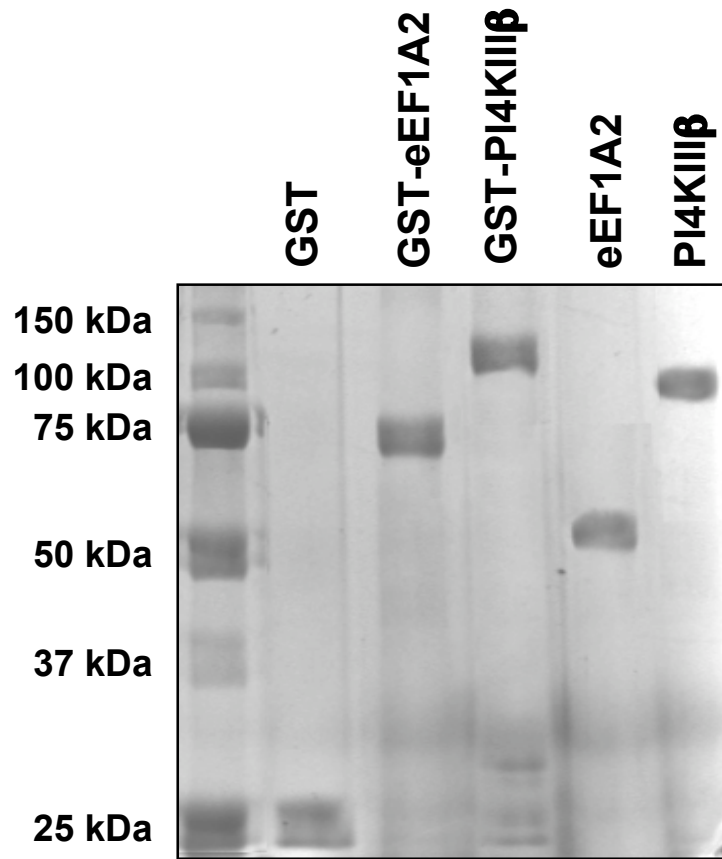
FIGURE 1

	BSA	eEF1A2
Km (µM)	836 ± 96	839± 64
Vmax (µmole / min / mg PI4K)	0.618 ± 0.02*	1.11 ± 0.03*
Kcat (1 / sec)	0.824 ± 0.03 ‡	1.48 ± 0.03 ‡

FIGURE 2

A

100 kDa				PI4KIIIβ
50 kDa				eEF1A2

+	+	−	−	GST
+	−	−	+	eEF1A2
−	+	+	−	PI4KIIIβ
−	−	+	−	GST-eEF1A2
−	−	−	+	GST-PI4KIIIβ

B

Time (min)

0	60	0	60	0	30	60

250 kDa
150 kDa
100 kDa
75 kDa
50 kDa

eEF1A2	+	+	−	−	+	+	+
PI4KIIIβ	−	−	+	+	+	+	+

FIGURE 3

A

BT549   Rat2   MCF7

eEF1A2

Actin
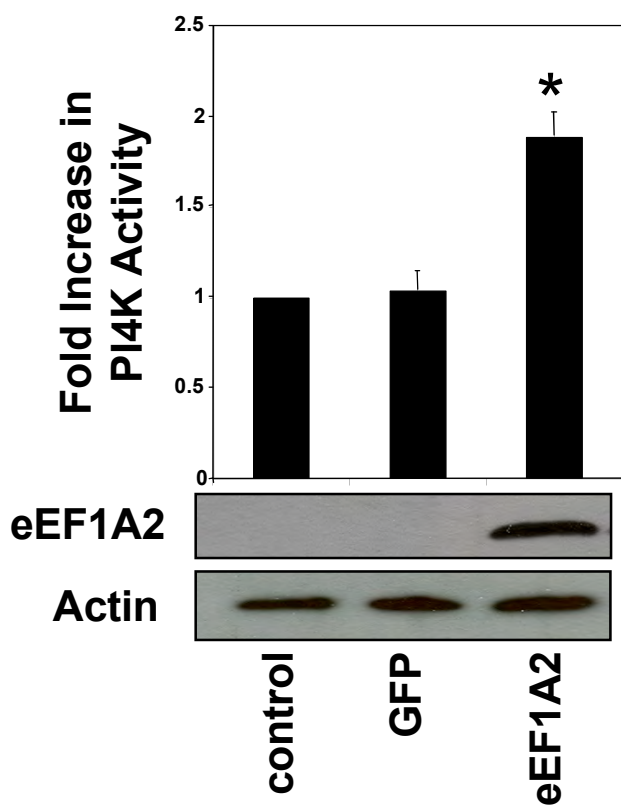
B

IP

WB

WCL   PI4KIIIβ   eEF1A2   Flag

PI4KIIIβ

eEF1A2

FIGURE 4

FIGURE 5

FIGURE 6

FIGURE 7

A

| eEF1A2 and DNA | PI4P | PI4P |

Rat2

BT549

B

| GFP and DNA | PI4P |

Rat2

BT549

FIGURE 7

C

Rat2

BT549

PI4P Expression / Unit Area (Arbitrary Units)

1053 ± 120   N = 59
1799 ± 475 *   N = 98
3276 ± 1003 *   N = 86

1516 ± 232   N = 51
2272 ± 406 *   N = 75
2868 ± 929 *   N = 76

Negative/Low   Moderate   High

eEF1A2 Expression (Arbitrary Units)

Rat2

BT549

PI4P Expression / Unit Area (Arbitrary Units)

N = 52   N = 92   N = 58

N = 46   N = 68   N = 88

Negative/Low   Moderate   High

GFP Expression (Arbitrary Units)